UNIVERSITY OF CAPE TOWN

DEPARTMENT OF MATERIALS ENGINEERING

THE EFFECT OF ALLOY CHEMISTRY AND STRAIN RATE ON THE M_{d30} TEMPERATURE OF METASTABLE AUSTENITIC STAINLESS STEELS

AUTHOR: JONES MALESELA PAPO

A THESIS SUBMITTED FOR THE FULFILLMENT OF REQUIREMENTS OF THE DEGREE OF M.Sc (APPLIED SCIENCE IN MATERIALS ENGINEERING)

JUNE 1994

ABSTRACT

The work covered in this thesis provides a comprehensive discussion of the transformation behaviour of Type 304 metastable stainless steels with small variations in alloy composition. The study focuses mainly on the austenite stability with respect to alloy composition, rate of deformation and temperature. To achieve these objectives, uniaxial tensile tests at 0.3 true strain were performed at low and high strain rates ($10^{-3}s^{-1}$ and 3 x $10^{-2}s^{-1}$ respectively), in the temperature range of -60 to 55°C under isothermal testing conditions. The amount of martensite formed (i.e. the transformation product) as a function of strain was obtained by monitoring the progress of transformation with a magnetic detection device. Austenite stability against spontaneous martensite transformation was determined by carrying out qualitative Ms (martensite start) temperature tests by refrigerating the alloys to -196°C in liquid nitrogen.

It was found that the highly alloyed materials have increased austenite stabilities when compared with their less highly alloyed counterparts. The difference in the extent of transformation between different alloys was found to be more pronounced at test temperatures where transformation is highly temperature sensitive (-40 to 0°C). Furthermore, at this temperature range, martensite transformation was found to be highly dependent on strain rate. Low strain rate tests gave higher amounts of martensite than high strain rate tests. At very low and high temperatures (≈-60°C and 23°C respectively) however, transformation was found to be less dependent on strain rate. The quantitative measure of austenite stability termed the M_{d30} temperature, which is defined as the temperature at which 50% martensite will form after a true strain of 0.3; was found to vary with both alloy composition and strain rate. The highly alloyed steels at both low and high strain rates gave lower M_{d30} temperatures compared with the less highly alloyed steels which gave higher M_{d30} values. For any particular alloy, the M_{d30} value observed at the low strain rate was higher than the value observed at the high strain rate.

All alloys resisted spontaneous martensite transformation even when unstabilised by solution treatment at lower temperatures of 900 and 950°C.

It was concluded that the $\gamma \rightarrow \alpha'$ transformation is highly dependent on strain rate in the temperature range where transformation is very sensitive to temperature. In this temperature range the M_{d30} temperature varies with both alloy composition and strain rate. However, the observed M_{d30} temperature values were found to be significantly lower than those calculated from the existing empirical M_{d30} relationships. This high austenite stability against transformation was further evidenced by the resistance of alloys against spontaneous martensite transformation.

ACKNOWLEDGEMENTS

* I wish to express my sincere thanks to *COLUMBUS STAINLESS (PTY) LTD* and their Research and Development personnel, particularly Messrs. J. Hewitt and L. Matthews and my bursars *DE BEERS RESEARCH LABORATORIES (PTY) LTD*, for their financial support and constructive advice during the course of this project.

* The technical advice and assistance of Mr. Potgieter and Dr. M. Cortie of Mintek, Mr. G. Doyle of Geology Department at U.C.T. and Miss. T. Biggs, former office partner, on the XRD is highly appreciated.

* To my supervisor Dr. R.D. Knutsen, thank you for your ever constructive criticism and advice and your quest for perfection and excellence. The qualities I'll forever be grateful for.

* To my lecturers and professors, many thanks for the knowledge and expertise you imparted on me. The zeal and vigour you potrayed in your lectures during all these years will always be an inspiration.

* To Messrs. B. Greeves and J. Petersen (on photography), G. Newins, R. Hendricks and N. Dreze (workshop staff) and D. Dean (for your electronic expertise), your expertise and patience will always be fondly remembered.

* To the Materials Engineering "family" (students and staff, past and present), many thanks for providing an environment conducive for both personal and intellectual fulfillment. The good memories and valuable companionship you provided left an indelible impression on me.

* To my loving parents, siblings and friends (Norman Gwebu, Innocent Shabalala and Dumile Nomkhosi Zungu), your encouragement and moral support will always be lauded.

To all of you, may the days of tomorrow herald moments of bliss and prosperity and may peace and harmony prevail amongst all South Africans.
Dedicated to the memory of my grandparents.

LIST OF SYMBOLS

C_γ, $C\alpha'$ - Volume fraction of austenite and martensite respectively

G, GSN - ASTM grain size number

FCC - Face centred cubic

F-ratio - Test statistic for significance test of coefficients

$I\alpha'$, I_γ - Measured integrated intensities of martensite and austenite respectively

L_3 - Mean lineal intercept

L_T- Total length of line for the lineal intercept method for grain size measurement

M - Magnification

M - Martensite

Md - Temperature above which no martensite transformation occurs during deformation

M_{d30} - Temperature at which 50% martensite will form after a true plastic strain of 0.30

M.E.T. - Maximum elongation temperature

MoKα - Molybdenum radiation

Ms - Martensite start temperature

M_T- Martensite content limiting value

n_γ, $n\alpha'$ - Number of austenite and martensite reflections respectively

P - Number of grains intercepted

R - Linear correlation coefficient

R - Multiple correlation coefficient

R_γ, Rα - R factors of austenite and martensite respectively

S - Engineering stress

T - Temperature

T_E- Thermodynamic equilibrium temperature

V - Voltage

α' - martensite

δ - ferrite - Delta ferrite

σ - True stress

e - Engineering strain

γ- Austenite

ε- True strain

σ- Magnetization value

θ - Bragg angle

CONTENTS

PAGE No.

Abstract

Acknowledgements

List of symbols

CHAPTER 1 INTRODUCTION

1.1 General 1

1.2 Aim of research 2

1.3 Research approach 2

CHAPTER 2 LITERATURE REVIEW

2.1 General 4

2.2 Deformation-induced martensite in metastable austenitic stainless steels

2.2.1 Thermodynamics of deformation-induced martensite 6

2.2.2 Stress-assisted and strain-induced martensite transformation 8

2.3 Factors affecting transformation to martensite during plastic deformation

2.3.1 The effect of temperature on transformation to martensite on plastic deformation 10

2.3.2 The influence of strain rate on deformation-induced martensite transformation 16

(a) The effect of strain rate as a function of testing environment

(i) Non-isothermal testing environment 16

(ii) Isothermal testing environment 19

2.3.3 The effect of alloy chemistry on deformation-induced transformation 23

(a) Existing Md empirical equations as a measure of alloy stability 25

(b) Comparison of the existing Md equations 27

2.4 Importance of M_{d30} temperature in engineering applications 30
2.4.1 Problems due to inaccurate control of the M_{d30} temperature 32
2.4.2 Limitations of the existing M_{d30} empirical equations 33
2.5 Martensite start temperature as a criterion of austenite stability 34

CHAPTER 3 EXPERIMENTAL PROCEDURE

3.1 Materials and preparation 38
3.1.1 Heat treatment 39
3.1.2 Metallography and grain size measurement 39
3.2 Tensile testing 41
3.2.1 Specimen geometry 41
3.2.2 Test apparatus 42
3.3 Measurement of deformation-induced martensite
3.3.1 Magnetic detection device
(a) Introduction 43
(b) Development of magnetic detection device 45
(c) Operation of the magnetic detection device 47
(d) Calibration of the magnetic detection device 47
(e) Appraisal of the reliability of the magnetic detection device
(i) Graphs of voltage against time 50
(ii) Calibration of the voltage values to volume fraction martensite
(1) Effect of temperature on voltage values 56
(2) Influence of areal reduction on voltage readings 58
(3) Regression equations relating voltage to volume fraction of martensite 59
3.3.2 X-ray diffractometry
(a) Sample preparation for X-ray diffraction 61
(b) X-ray equipment and procedure 61

(c) Data analysis 61

3.4 Clarification of the discrepancy between existing M_{d30} relationships and measured M_{d30} values 64

3.4.1 Test statistics for analysis of regression results

(a) Multiple regression analysis 65

(b) Linear regression analysis 66

3.5 Martensite start temperature (Ms) qualitative tests 67

CHAPTER 4 EXPERIMENTAL RESULTS

4.1 Microstructural analysis

4.1.1 Phase compositions 69

4.1.2 Grain size measurement 71

4.2 Alloy stability with respect to temperature and strain rate

4.2.1 Qualitative assessment of influence of temperature and strain rate towards martensite formation

(a) Influence of temperature on martensite formation 72

(b) Influence of strain rate on martensite formation 78

4.2.2 Quantitative assessment of influence of temperature and strain rate on transformation to martensite

(a) Martensite transformation during deformation 78

(b) Martensite transformation as function of temperature 82

(c) Temperature sensitivity of martensite formation against temperature 84

(d) Determination of M_{d30} temperatures 87

(i) Formulation of M_{d30} equations 88

1 M_{d30} equations according to elements considered in Angel and Pickering's equations 89

2 M_{d30} equations according to elements considered in Nohara et al's equation 90

(c) Relationship between observed M_{d30} values alloying elements 92

4.3 Alloy stability on refrigeration 99

CHAPTER 5 DISCUSSION

5.1 Temperature and strain rate influence towards martensite formation

5.1.1 Martensite transformation during deformation 102

5.1.2 Martensite transformation as a function of temperature 104

5.2 The effect of strain rate on the M_{d30} temperature 108

5.3 The effect of alloy chemistry on the M_{d30} temperature

5.3.1 Qualitative effect of alloy chemistry on the M_{d30} temperature 110

5.3.2 Quantitative effect of alloy chemistry on the M_{d30} temperature 111

5.3.3 Austenite stabilising effect of elements in the M_{d30} equations 114

5.4 Assessment of the formulated M_{d30} equations 116

5.5 Austenite stability on spontaneous transformation to martensite 117

CHAPTER 6 CONCLUSIONS

6.1 Introduction 120

6.2 List of conclusions 120

6.3 Recommendations

6.3.1 Magnetic detection device 122

6.3.2 Limitations of the formulated M_{d30} empirical equations 123

REFERENCES

124

APPENDICES

1 INTRODUCTION

1.1 General

A standard grade of austenitic stainless steel sheet used for pressforming of many articles, such as sink bowls and wash troughs is A.I.S.I type 304 [28]. The production techniques subject the sheet metal to great amount of stretching, so that selection of steel composition to maximise formability in stretch forming operations is required. It has been shown that composition of austenitic stainless steel sheet can be modified to improve the productivity of pressforming operations, at varying forming speed and temperature.

The forming of austenitic stainless steels is further complicated by the transformation of austenite to martensite. This transformation may play an important role in the mechanical working of these steels if carefully controlled. The effect of forming on austenitic stainless steels is great, and since this effect is related to the temperature dependence of martensite transformation, the optimum temperature region will be governed by the austenite stability of the material. Austenite stability is generally expressed as the M_{d30} temperature which is arbitrarily defined as the temperature at which a volume fraction of 50% martensite will form after a true plastic strain of 0.3. This characteristic temperature gives a quantitative data on the specific influence of the alloying elements on the stability of the austenite [12]. Empirical M_{d30} relationships have been formulated by various investigators, and are expressed as equations of the first order involving individual alloying elements. While the effects of composition on the M_{d30} temperature has been reported in the literature at some length [12,30], there is little quantitative information concerning the influence of strain rate on the M_{d30} temperature. The work reported in this thesis was initiated in order to obtain such information.

1.2 Aim of Research

The main purpose of this project is to review the existing M_{d30} empirical equations for type 304 stainless steel compositions with respect to strain rate. Whilst this is the main purpose of this study, various factors such as test temperature, usually come into play indirectly affecting martensite transformation. It is thus necessary to include these factors to establish an overall understanding of the transformation behaviour of these steels. Hence, the prime objectives of this study are:

(1) To qualitatively assess the influence of test temperature towards martensite transformation.

(2) To critically appraise the reliability of a simple magnetic device for critically assessing the propensity for an alloy to form martensite during deformation.

(3) To investigate the influence of strain rate on the M_{d30} value.

(4) To clarify the discrepancy between existing M_{d30} relationships and measured M_{d30} values for type 304 stainless steels.

(5) To determine the austenite stability of type 304 stainless steels on spontaneous transformation to martensite.

1.3 Research Approach

The first approach involves a comprehensive microstructural study of the experimental alloys after solution treatment. This involves the analysis of the phases and grain sizes constituting these alloys. The transformation behaviour of these alloys will then be compared as a function of test temperature under uniaxial tension at two nominal strain

rates of 10^{-3} (low strain rate) and 3 x $10^{-2}s^{-1}$ (high strain rate). The austenite stability of each alloy as a function of strain rate under this mode of deformation will be qualitatively compared using magnetic techniques. The use of the magnetic techniques with X-ray diffraction will allow quantitative appraisal of the deformation behaviour of these alloys. This will allow the experimental determination of M_{d30} values under different strain rates, which will provide adequate information for the formulation of M_{d30} empirical relationships using multiple regression analysis. Austenite stability against spontaneous transformation will be carried out by immersing the experimental alloys in liquid nitrogen at -196°C.

2 LITERATURE REVIEW

2.1 General

Austenitic (Fe-Cr-Ni) stainless steels exhibit a good combination of corrosion resistance and optimum mechanical properties, as compared to martensitic and ferritic (Fe-Cr) stainless steels. Although martensitic and ferritic steels are cheaper, as a result of low percentage nickel (0-1wt%), they generally have low formability and toughness compared to their austenitic counterparts (table 2.1).

STEEL	YIELD STRESS (MPa)	UTS (MPa)	ELONGATION %
MARTENSITIC e.g. 431	400-900	900-2000	10-20
FERRITIC e.g. 430	280-450	450-580	20-35
AUSTENITIC e.g. 301	300-500	800-1300	45-65

Table 2.1: Comparison of mechanical tensile properties ferritic, martensitic and austenitic stainless steels. (After Ref 43)

Consequently, austenitic stainless steels are mostly used in applications which require good corrosion resistance and formability. Because of their high work-hardening rates, austenitic stainless steels perform well in stretch-forming operations. The high work-hardening rate has two distinct effects. Firstly, the critical strain level for plastic instability is increased; secondly, strain concentrations in the pressing are reduced because work-hardening in heavily deformed areas raises the flow stress above that of surrounding regions, so that subsequent strain is spread into the lower strain areas, and higher overall strains can be tolerated before the forming limit is reached [28].

Of the family of austenitic stainless steels, the AISI 300 series is perhaps the most widely used. The alloy compositions of some AISI 300 stainless steels are given in table 2.2.

TYPE	C max	Si max	Mn max	Cr	Ni	Mo	Ti x %C min	Nb x %C min
301	0.15	1.00	2.00	16-18	6-8			
302	0.15	1.00	2.00	17-19	8-10			
304	0.08	1.00	2.00	18-20	8-12			
310	0.25	1.00	2.00	24-26	19-22			
316	0.08	1.00	2.00	16-18	10-14	2.0-3.0		
321	0.08	1.00	2.00	17-19	9-12		5	
347	0.08	1.00	2.00	17-19	9-13			10

Ti X %Cmin implies the composition of titanium allowed equals 5 times the minimum composition of carbon in wt%.

Table 2.2: Specific analysis (wt%) of the AISI 300 series austenitic stainless steels. (After Ref 40)

The austenitic stainless steels may be divided into three groups: (a) *The normal unstabilized compositions* such as types 301, 302, 304 and 310. These steels are annealed to ensure maximum corrosion resistance and to restore maximum softness and ductility. During annealing, carbides, which markedly decrease resistance to intergranular corrosion are dissolved.

(b) *The stabilised compositions*, principally types 321 and 347 which contain controlled amounts of Ti or of Nb-plus-Ta, which renders the steel nearly immune to intergranular precipitation of chromium carbide and its adverse effects on corrosion resistance.

(c) *The extra low carbon grades*, such as types 304L and 316L. These grades are intermediate in precipitation of chromium carbides to the stabilised and unstabilized

grades. The carbon content (0.03 wt% max) is low enough to reduce precipitation of intergranular carbides to a safe level.

Of the AISI 300 series austenitic stainless steels, AISI 304 is the most widely used [1]. Its forming properties are characterised, among other things, by the yielding and work hardening behaviour of the austenite lattice, its high carbon and nitrogen solubility and the associated almost complete freedom from precipitates. But, the metastability of the austenite is particularly important [1]. Given the target control of chemical composition and of temperature during the forming process, austenitic stainless steels can be subjected to forming operations to which no other ferrous material is amenable [1]. AISI 304 austenitic stainless steels may be divided into two groups: *(a) The normal unstabilized compositions and (b) The extra low carbon grades.*

The characteristic property of these types of austenitic stainless steels (AISI 304 and 304L) is that they cannot be hardened by heat treatment but will harden as a result of cold working. Cold working induces transformation of austenite to martensite, henceforth referred to as deformation-induced martensite. The effect of this metastability is that through the introduction of forming energy the austenite lattice undergoes martensitic transformation to a greater or lesser degree depending on forming temperature, thereby producing an additional work-hardening mechanism alongside that provided by dislocation reactions [1].

2.2 Deformation-Induced Martensite in Metastable Austenitic Stainless Steels

2.2.1 Thermodynamics of Deformation-Induced Martensite

Plastic deformation has a significant effect upon volume fraction martensite formed as a function of temperature such as shown in fig. 2.1.

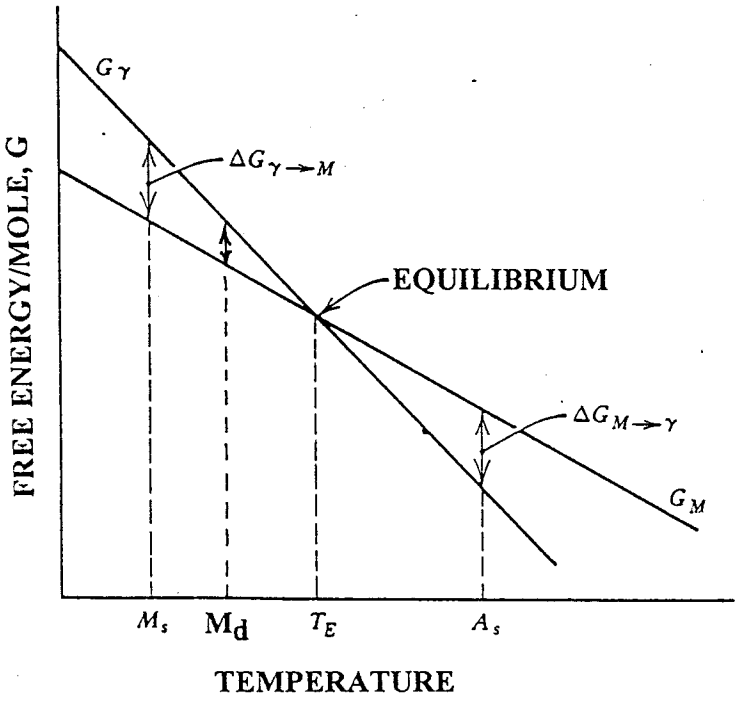

Fig 2.1: Schematic representation of the free energy development of the austenite and martensite phases with temperature. G_γ corresponds to the free energy of the austenite and G_M to the free energy of the martensite. (After Ref 5)

A transformation will occur if the total free energy of a system is reduced. The driving force for an austenite to martensite transformation is the difference in free energy between the austenite and martensite phases (fig 2.1). At a temperature T_E the driving force is equal to zero. The free energy change of the system must be large enough to enable the reaction to mount the activation barrier between the austenitic and martensitic states and also supply energy to be bound as surface energy, elastic and kinetic energy [12]. Because of these and other hindrances to the reaction, martensite does not form spontaneously at the thermodynamic equilibrium temperature T_E, but only after a certain amount of undercooling [12]. If undercooling occurs to some temperature M_D, the free energy of the martensite phase is lower than that of the austenite phase. But, without the action of applied stress martensite phase is inhibited from nucleating primarily because of the large

strain energy associated with shape change, which is produced when a martensite plate forms. The function of the applied stress producing deformation is to reduce the nucleation barrier that results from the shape change and, thereby, permit martensite to form at a lower driving force than it would form in the absence of the deformation. Hence, the M_D temperature is defined as the temperature above which no martensite will form even after severe plastic deformation [55].

Martensite transformation can also occur spontaneously when steels are quenched from high temperatures below a certain value called martensite start temperature Ms. At this temperature no plastic deformation is required to expedite transformation to martensite. Undercooling is sufficiently high to provide enough energy to overcome the martensite nucleation barrier.

2.2.2 Stress-Assisted and Strain-Induced Martensite Transformation

As the kinetics of martensitic transformations are nucleation controlled, two modes of deformation-induced transformation can be distinguished according to the origin of the nucleation sites which initiate transformation. Nucleation on the same initial nucleation sites which trigger the spontaneous transformation on cooling, but assisted thermodynamically by applied stress, is defined as stress-assisted nucleation; strain-induced nucleation arises from the production of new nucleation sites by plastic strain [58]. The condition under which each mode of transformation dominates can be indicated in a stress-temperature diagram (Fig. 2.2).

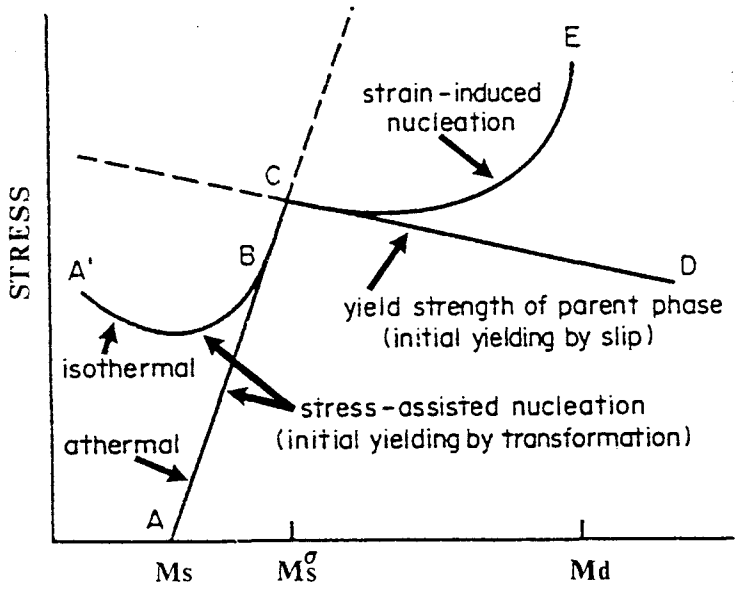

Fig 2.2: Schematic representation of the stress-assisted and strain-induced regimes for mechanically induced transformation. Initial yielding is controlled below Ms^σ by transformation plasticity, and above Ms^σ by slip in the parent phase. (After Ref 58)

For an alloy exhibiting apparently athermal transformation kinetics, no stress is required for transformation at the Ms temperature, represented by point A. At higher temperatures, the stress required for stress-assisted transformation on the same nucleation sites follows line ABC. At point C, this stress reaches the yield stress for slip in the parent phase, defining a temperature Ms^σ which can be regarded as the highest temperature for which transformation can be induced by elastic stress. Owing to the effect of transformation plasticity below Ms^σ, the observed macroscopic yield stress will follow the curve ABCD, such that the Ms^σ can be identified by a reversal of the temperature dependence of the yield stress [58].

Above Ms^σ, plastic flow occurs before the stress for stress-assisted nucleation is reached, and the production of new strain-induced nucleation sites contributes to the transformation kinetics. The stress at which the martensite is first detected then follows the curve CE. Owing to the potency of the strain-induced nucleation sites, this curve can at first follow

the curve CD for the initiation of parent phase slip. At point E, the amount of imposed deformation is limited by fracture, thus defining the Md, the highest temperature at which transformation can be mechanically induced [58]. Therefore, the condition for stress-induced formation of martensite is $\sigma_{\gamma\rightarrow\alpha'} < \sigma_{yield\gamma}$ (when martensite forms below the actual yield strength of the austenite). Strain-induced martensite forms when slip in the austenite precedes its formation. Hence, the condition of formation is $\sigma_{\gamma\rightarrow\alpha'} > \sigma_{yield\gamma}$ [26]. Austenitic stainless steels have been reported to undergo strain-induced martensitic transformation since transformation occurs only after some degree of plastic strain depending on test temperature [31].

2.3 Factors Affecting Transformation to Martensite during Plastic Deformation

Transformation to martensite by deformation has been extensively studied in the metastable austenitic stainless steels [28,53,12,30]. The most important factors influencing the stability of the austenite were found to be temperature, rate of deformation and chemical composition [12,28,53].

2.3.1 The Effect of Temperature on Transformation to Martensite on Plastic Deformation

Angel [12] discussed the influence of temperature in terms of the relationship between the martensitic and the slip mode of deformation. As the martensitic transformation is associated with a shear strain (of about 0.20) it may be regarded as a deformation process that competes with the usual slip process. With decreasing temperature the critical resolved shear stress for slip (i.e. the resistance to slip) increases, whereas the resistance to martensite formation decreases. Above a certain temperature the resistance to slip is less than the resistance to martensite formation and slip is therefore the dominating process of deformation [12]. To demonstrate this phenomenon Angel [12] related martensite content to true tensile plastic strain at various deformation temperatures as shown in fig 2.3.

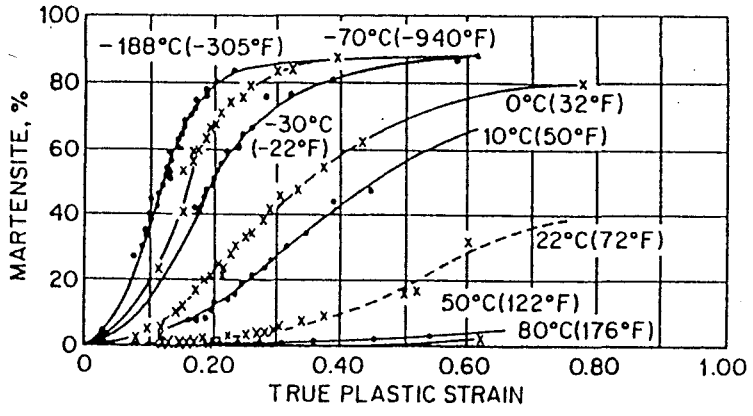

Fig 2.3: Formation of martensite by plastic tensile strain at various deformation temperatures. (After Ref 12)

The rate of reaction dM/dε (the slope of the curves in fig 2.3) was found to be zero at the beginning and gradually increases to a maximum after a considerable amount of strain. After this the rate gradually decreases until no further transformation occurs upon further straining, and a limiting value for the martensite content, M_T is reached [12]. The limiting value M_T is lower the higher the temperature, and becomes zero after a certain temperature which according to definition is the M_D temperature. The M_T value in no case exceeded about 90% of martensite. The decreasing reaction rate dM/dε can be regarded as depending either on a stabilising effect of deformation on the austenite, or on a decreasing amount of austenite available for transformation [12]. Ludwigson et al [32] on the other hand, attributes this to the partitioning effect which refers to the fact that existing martensite plates act as barriers and limit the growth of new martensite plates. Thus they effectively partition the remaining austenite into progressively smaller volumes.

Apart from relating martensite content to true plastic strain at various temperatures, fig 2.3 can be used to explain the effect of temperature on martensite transformation at a given plastic true strain. To illustrate this phenomenon, the approximate differences in the martensite content at a true plastic strain of 0.3 were determined with respect to decreasing temperature and are shown in table 2.3.

TEMPERATURE RANGE (°C)	ΔT(°C)	ΔM(% approximately)
50 to 80	30	0
22 to 50	28	4
10 to 22	12	23
0 to 10	10	14
-30 to 0	30	31
-70 to -30	40	9
-188 to -70	118	3

ΔT and ΔM are temperature and martensite differences associated with a particular temperature range.

Table 2.3 Variation of martensite content at 30% true strain as a function of temperature. (After Ref 12)

From table 2.3 it can be seen that at high and low temperature extremes (e.g. $50 \leq T \leq 80$°C and $-18 \leq T \leq -70$°C), a large variation in temperature results in very small variations in martensite content. However, at intermediate temperatures (e.g. $-30 \leq T \leq 10$°C), a radical change of stability of the austenite within a narrow temperature range is observed. This observation implies that the temperature sensitivity of martensite transformation will be low at high and low temperature extremes, and very high at intermediate temperatures. The concept of temperature sensitivity of martensite transformation as a function of temperature was illustrated by Rosen et al [13]. They illustrated this by measuring the slopes of appropriate curves of % martensite versus temperature, for alloys strained to fracture. The slope at any temperature indicates the temperature sensitivity of martensite formation. The results obtained by Rosen et al [13] are indicated in figs 2.4 and 2.5. Since the % martensite versus temperature curves have negative slopes, the parameter (-dM/dT) will give positive slopes and can still be used to determine temperature sensitivity of martensite formation at a particular temperature.

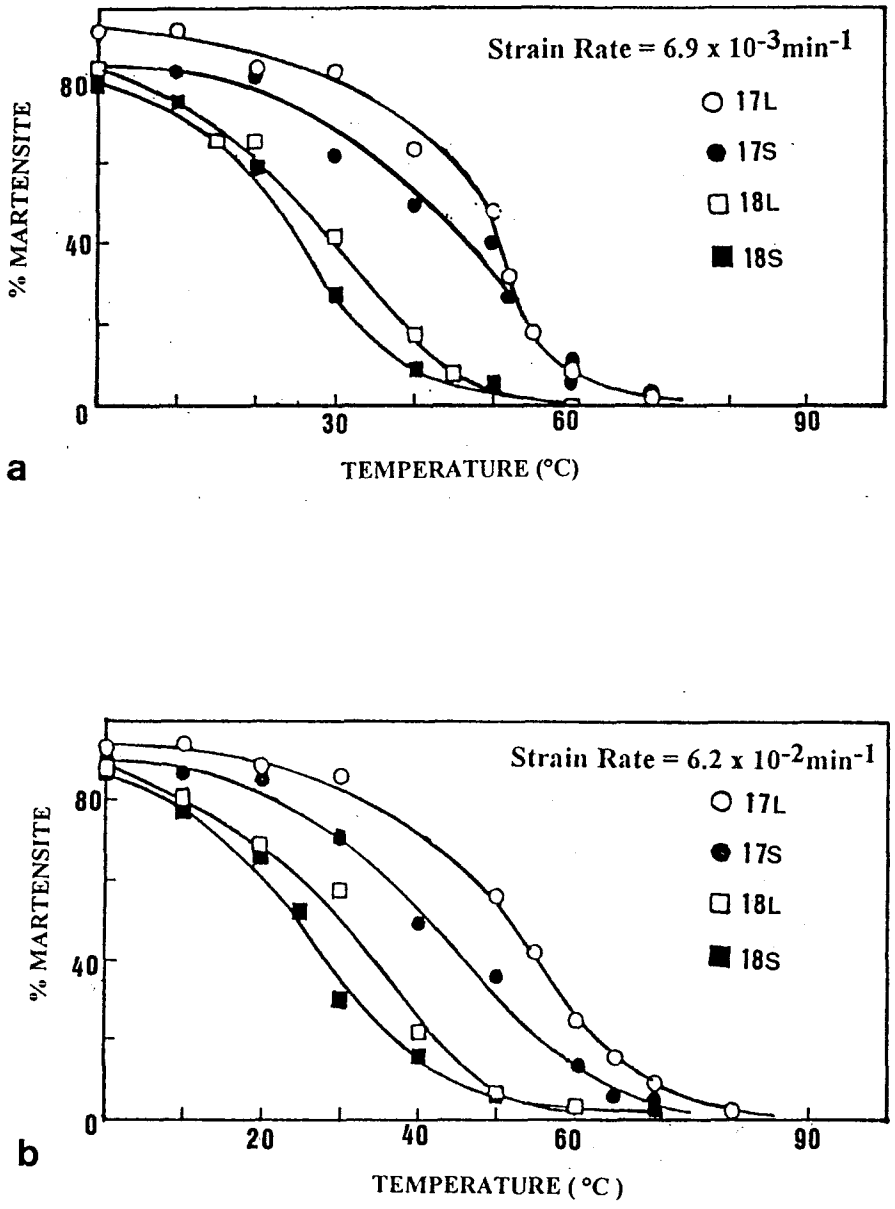

Fig 2.4: Martensite content of fractured specimens versus testing temperature for a strain rate of (a) 6.9 x $10^{-3}min^{-1}$; and (b) 6.2 x $10^{-2}min^{-1}$. The 17 type specimens are of 301 type whereas 18 type specimens are of 304 type. L and S refer to large and small grain size respectively. (After Ref 13)

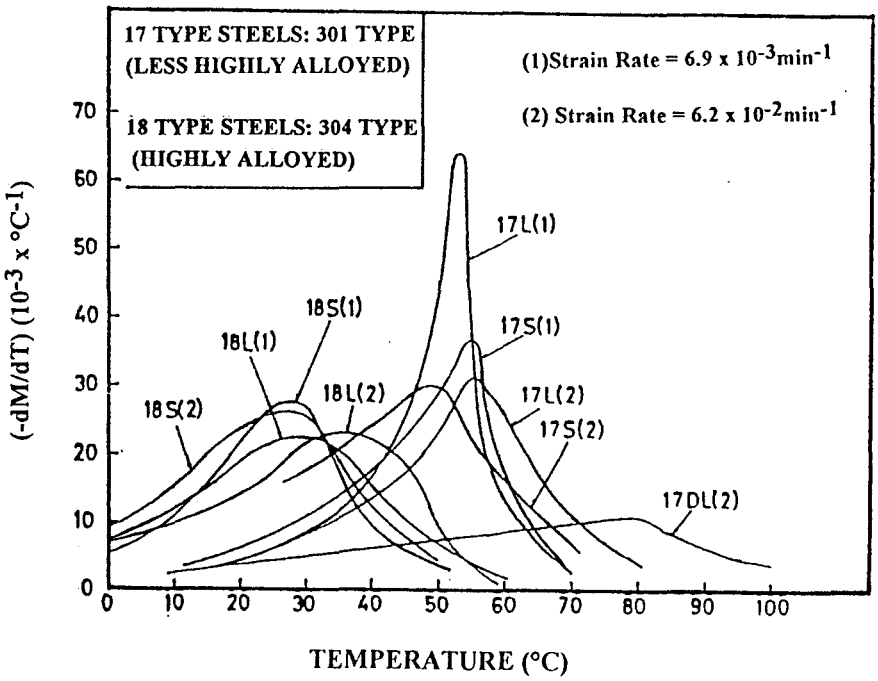

Fig 2.5:(-dM/dT) versus testing temperature for specimens studied in fig 2.4. The shifting of (-dM/dT) curves to higher temperatures for a particular alloy, corresponds to an increase in martensite content. (After Ref 13)

The peaks on the (-dM/dT) versus temperature curves coincide with regions of maximum slope on the % martensite versus temperature curves. At the temperatures of the maxima, the martensite transformation is highly dependent on temperature. Hence, at regions around the peaks on the (-dM/dT) versus temperature curves, martensite content will change drastically over a narrow temperature range.

Thus the influence of temperature on transformation to martensite can be summed up as follows:

(1) At a given temperature below the Md temperature, transformation increases with increasing plastic strain up to a limiting value M_T, above which no transformation occurs even after extensive plastic deformation. The M_T value is lower the higher the temperature (fig 2.3).

(2) At a given plastic strain, the amount of martensite increases with decreasing temperature as illustrated in fig 2.6.

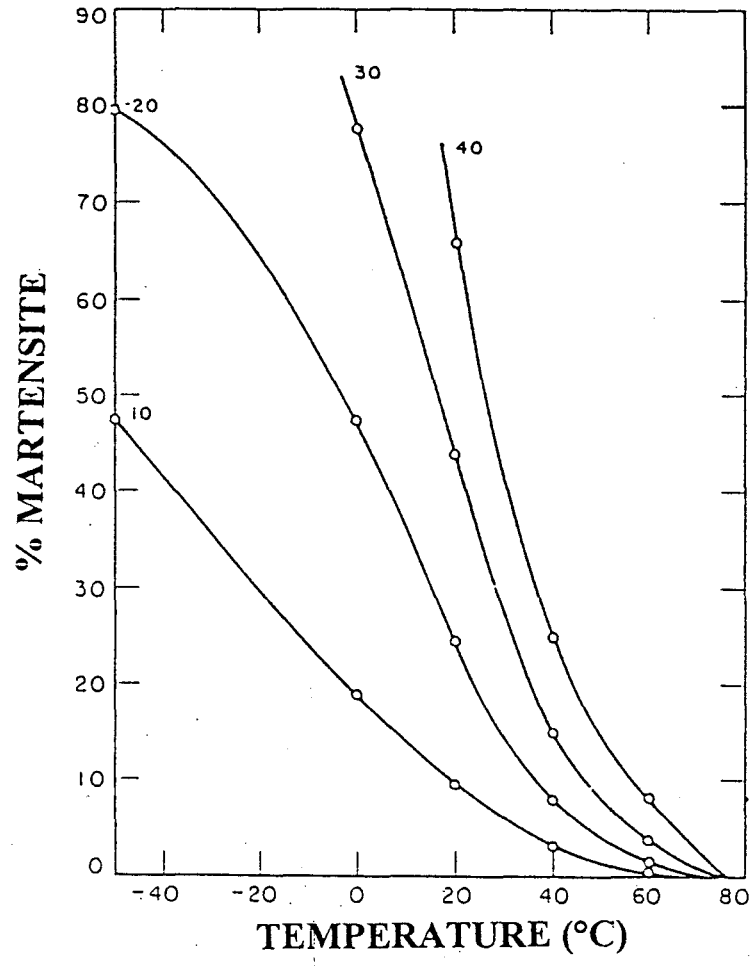

Fig 2.6: The amount of martensite produced during deformation of a 0.058% carbon alloy as a function of temperature for 10, 20, 30 and 40% tensile elongation. (After Ref 70)

2.3.2 The Influence of Strain Rate on Deformation-Induced Martensite Transformation

A number of investigators [53,28,34] have examined the effect of strain rate on deformation-induced martensite transformation. Bressanelli et al [53] found that strain rate indirectly affects the martensite reaction through its influence on specimen temperature. Besides the strain rate, the temperature of the specimen is also a function of the amount of strain [53]. The specimen temperature can be controlled by performing deformation tests in temperature controlled environments. The primary aim of these environments is to remove thermal gradients which develop during deformation. Various investigators [28,34,53] studied the effect of strain rate on $\gamma \rightarrow \alpha'$ transformation in specimens tested in uniaxial tension under isothermal and non-isothermal conditions.

(a) The Effect of Strain Rate as a Function of Testing Environment

(i) Non-Isothermal Testing Environment

A detailed study of thermal effects under non-isothermal conditions (in air) for various strain rates was performed by Ayres [34]. The results of this study are shown in fig 2.7.

For all the strain rates of approximately 10^{-3} to 10^{-1} s^{-1}, there is substantial heat transfer along the gauge length of the tensile specimen. The maximum temperature rise was found to occur at high plastic strains. Such temperature variations along the gauge length clearly indicates that martensite volume fraction will vary along the gauge length of the specimen, given the temperature dependence of $\gamma \rightarrow \alpha'$ already discussed in section 2.3.1. At low strain rates (about 10^{-3} s^{-1}) however, thermal gradients along the gauge length are very minimal. Hecker et al [33] and Kumar et al [35] both reported about 1°C rise in temperature near the end of the gauge length. Bressanelli et al [53] attributed this low amount of adiabatic heating at low strain rates to the fact that there is sufficient time for a large part of the heat of deformation to be dissipated by the specimen. Thus, the martensite content increases almost linearly with strain (fig 2.8).

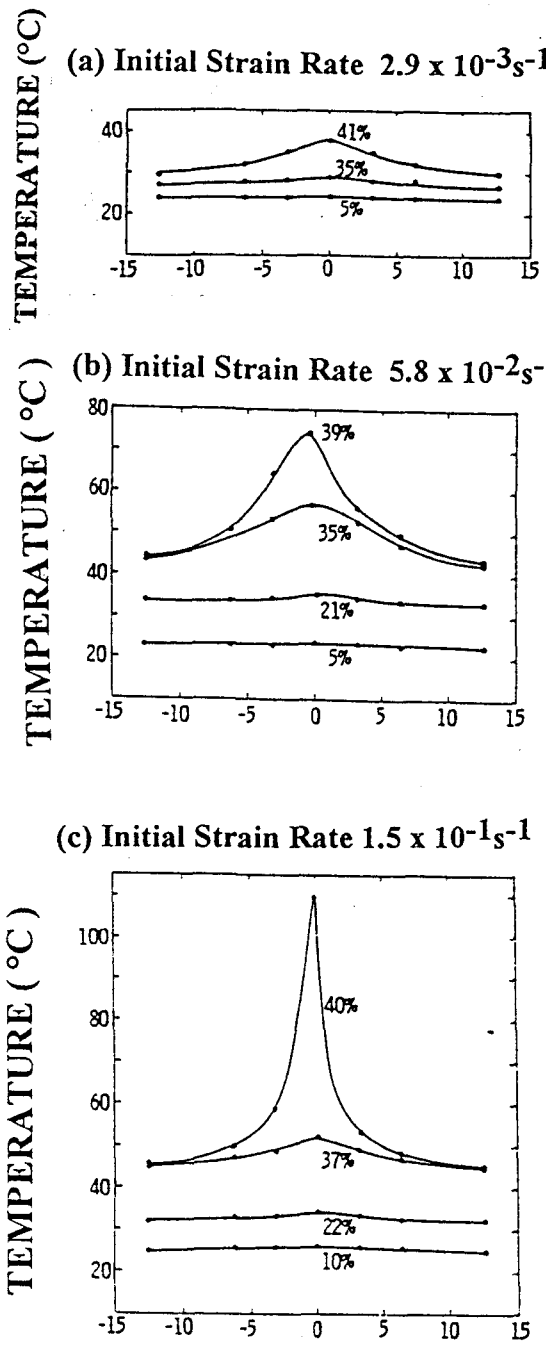

Fig 2.7: Thermal distributions at various amounts of engineering strain in specimens tested in air at initial strain rates of (a) 2.9 x 10^{-3} s^{-1}, (b) 5.8 x 10^{-2} s^{-1}, and (c) 1.5 x 10^{-1} s^{-1}. (After Ref 34)

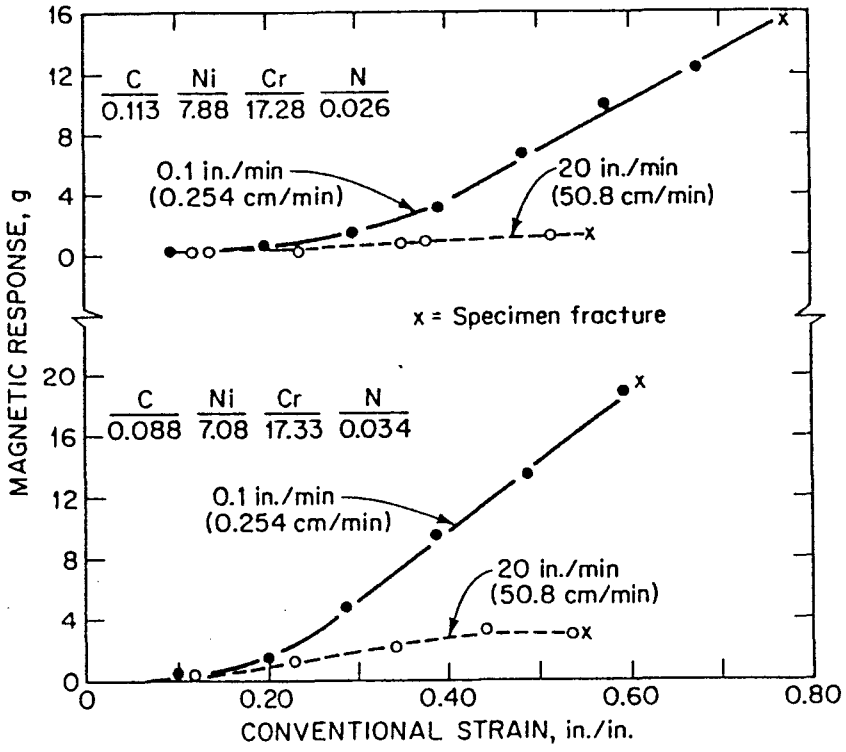

MAGNETIC RESPONSE (g)	% MARTENSITE
1	20
4	50
9	70
16	90

Fig 2.8: Effect of strain rate on martensite formation (magnetic response) in type 304 stainless steels deformed in air. (After Ref.53)

At high strain rates (about 10^{-1} s^{-1}) however, there is rapid development of thermal gradients during straining (fig 2.7(c)). The greatest temperature rise measured was about 110°C at 40% strain. This temperature increase resulting from adiabatic heating explains the sufficient suppression of austenite to martensite transformation at high strain rates in fig 2.8.

Bressanelli et al [53] attributed this phenomenon to the fact that at high strain rates there is considerably less time for the heat of deformation to be dissipated. Because of specimen

heating, the martensite content does not increase in the same rate as in the low strain rate case as indicated in fig 2.8 [53].

(ii) Isothermal Testing Environment

There is lack of agreement in the literature on the mechanistic effect of strain rate on transformation under isothermal testing conditions. Bressanelli et al [53] examined the effect of a wide range of strain rates on room temperature transformation of Type 301 steels, and concluded that strain rate had little direct effect on transformation, provided the effects of adiabatic heating were minimised. They illustrated this observation by comparing a series of uniaxial tensile tests in a water bath (isothermal environment) and air (non-isothermal environment) at 23°C (fig 2.9).

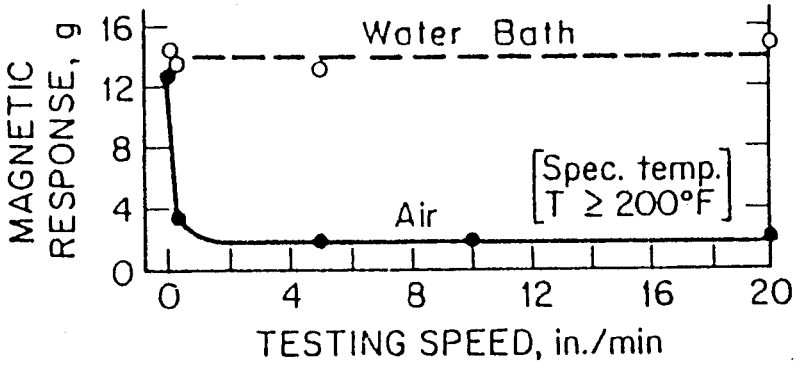

Fig 2.9: Effect of test medium and resultant temperature on martensite formation in type 301 deformed in ambient temperature bath and air. (After Ref. 53)

Contrary to the above assertion, Livitsanos et al [5] reported a decrease in the amount of martensite as strain rate is increased for tests carried out on Type 301 steel at a temperature range of 40-100°C under isothermal conditions (fig. 2.10). An important observation from fig 2.10 is that, particularly at lower temperatures, there seems to be a limiting strain rate below which transformation is independent of strain rate. Livitsanos et al [5] concluded that at very low test temperatures (≈ 40°C) transformation is relatively

independent of strain rate. Livitsanos et al's [5] results are corroborated by results obtained from a set of tests carried out by Bressanelli et al [53] on a type 301 steel at a temperature range of -73 to 93°C under isothermal conditions. Contrary to prior observation illustrated in fig 2.9, they [53] reported less martensite for specimens tested at the high strain rate compared to specimens tested at the low strain rate (fig 2.11).

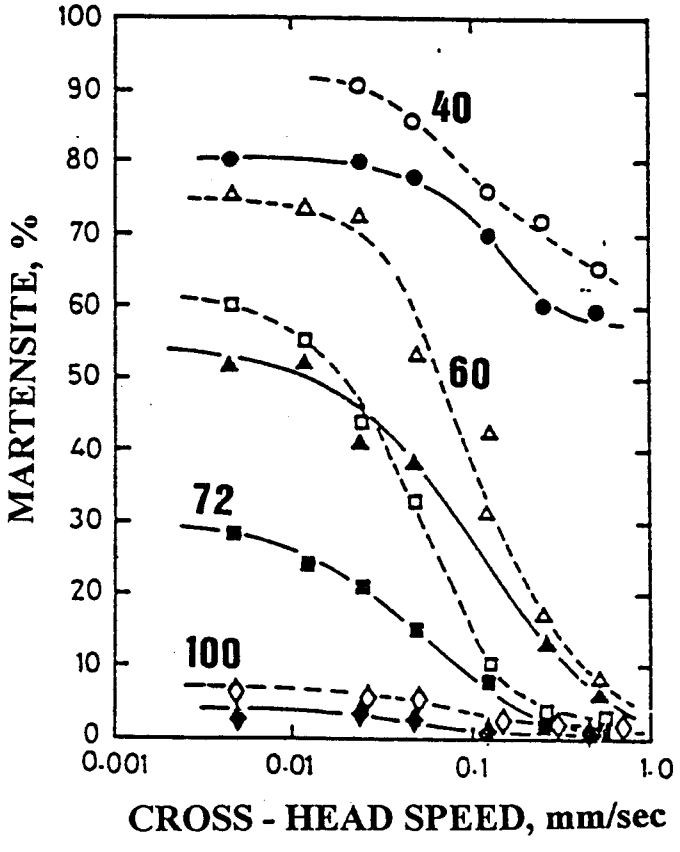

Fig 2.10: The effect of test temperature and crosshead speed on formation of martensite under isothermal conditions in the neck and in the uniformly-deformed zone of Type 301 18/8 stainless steel. Open symbols refer to the necked region and closed symbols refer to the uniformly-deformed zone. Test temperature at 40, 60, 72 and 100°C. (After Ref 5)

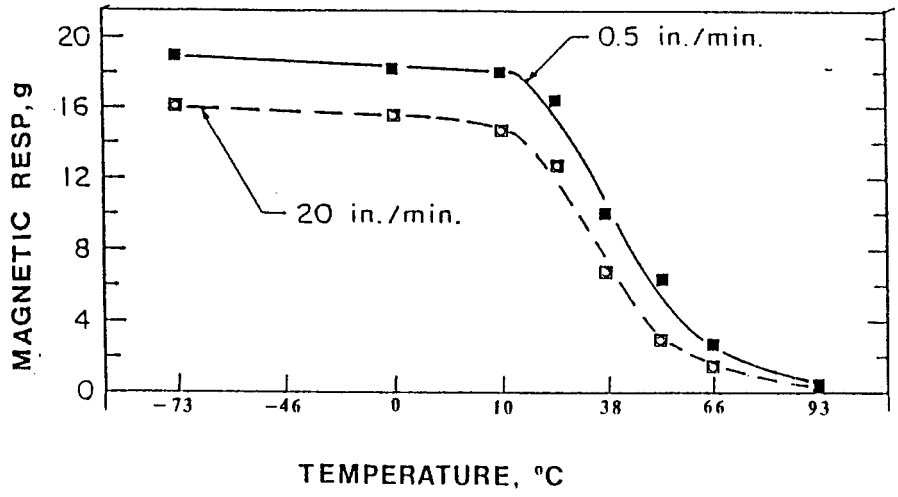

Fig 2.11: Effect of test temperature and test speed (strain rate) on martensite content (magnetic response, g) of Type 301 stainless steel for tests performed under isothermal conditions. (After Ref 53)

The difference in martensite content was greatest at the low temperature range of 10 to -73°C. Bressanelli et al [53] concluded that at lowest temperatures the large amount of heat generated by the martensite reaction was not thoroughly removed from specimens tested at high strain rates. Furthermore, because less martensite was formed at higher temperatures, less heat was produced during deformation and the liquid baths more closely served their intended purposes [53]. The decrease in the amount of martensite at constant temperature as strain rate is increased was also reported by Form et al [38] on isothermal tests performed on an AISI 303 steel (C = 0.045 wt%).

Contrary to the findings of Livitsanos et al [5] and Form et al [38], Huang et al [31] reported an increase in the amount of martensite as strain rate was increased for a type 304 stainless steel (fig 2.12).

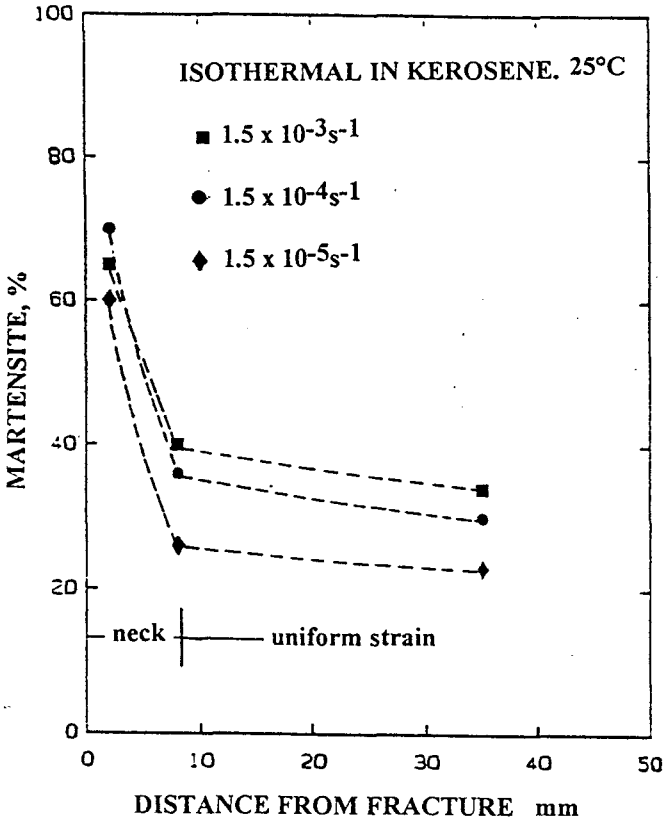

Fig 2.12: The effect of strain rate on the extent of deformation-induced martensite on type 304 stainless steel. (After Ref 31)

Huang et al's results are supported by the findings of Rosen et al [13], for tests performed on type 301 and 304 alloys (see fig 2.4 in section 2.3.1) under isothermal conditions. They found that a reduction in strain rate causes a shift of % martensite versus temperature curves along the temperature axis, towards lower temperatures. This observation was accompanied by the shifting of the low strain rate (6.9×10^{-3} min^{-1}) peaks on the (-dM/dT) versus temperature curves towards lower temperatures, compared to the high strain rate (6.2×10^{-2} min^{-1}) peaks (fig 2.5 in section 2.3.1). The shifting of the low strain rate curves towards lower temperatures, implies a reduction in martensite content at a particular temperature [13].

Due to contradictions concerning the effect of strain rate on $\gamma \rightarrow \alpha'$ transformation under isothermal testing environment, it becomes difficult to predict which trend a particular alloy is most likely to follow when tests are performed under isothermal conditions.

2.3.3 The Effect of Alloy Chemistry on Deformation-Induced Transformation

In a metastable stainless steel transformation may take place on cooling alone or, more readily, by application of a combination of cooling and plastic deformation. As already explained in section 2.2, Ms temperature is defined as the temperature at which transformation first commences on cooling, while Md, considerably higher than Ms temperature, is defined as the temperature above which no martensite is produced in the steel even after considerable plastic deformation. The susceptibility of a steel to transform in this manner is an extremely sensitive function of its chemical composition such that different batches of similar types are frequently observed to have vastly different stabilities (fig 2.13) [30].

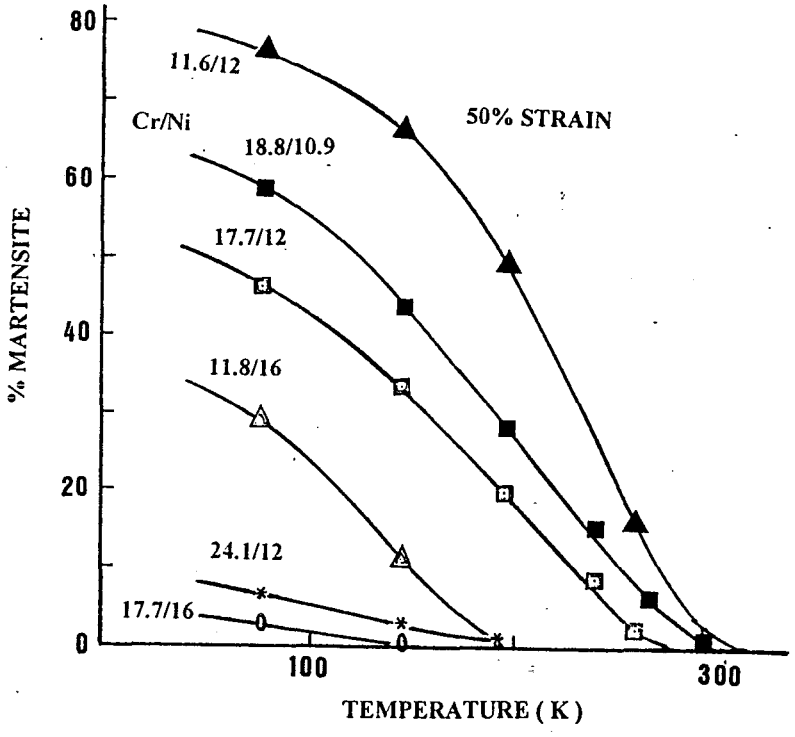

Fig 2.13: Martensite produced in different steels as a function of temperature for 50% strain. (After Ref 30)

Provided their compositions are known, the Ms temperature of steels in AISI 300 series can be estimated rather satisfactorily by means of the following empirical equations [9,52]:

$$Ms(°C) = 1305 - 61.1(Ni) - 41.7(Cr) - 33.3(Mn) - 27.8(Si) - 1667(C+N) \quad \text{.....(1)}$$

$$Ms(°C) = 502 - 810(C) - 1230(N) - 13(Mn) - 30(Ni) - 12(Cr) - 54(Cu) - 46(Mo) \quad \text{....(2)}$$

where ( ) denote weight percent of the corresponding element.

Williams et al [30] reported that Ms temperatures are very sensitive to composition; and are reduced by most alloying elements, including Cr, Ni, Mn and N_2 [11]. Furthermore, the Ms temperature-composition relationships differ widely and in general are valid only for the composition range for which they were derived [11]. Their sensitivity to compositional changes is further highlighted by the fact that residual elements in the stainless steel composition may reduce the Ms temperature by around 50°C [11]. The above-mentioned discussion probably explains the significant difference between equations (1) and (2). On closer comparison of the coefficients for the elements considered in these equations, it can be inferred that they will give significantly different Ms temperature predictions. The quantitative comparison between these two equations will be illustrated later in chapter 3.

The stability of austenite against martensite transformation is usually measured by the Ms and Md temperature. However, Ms temperature is hardly an adequate criterion of stability on its own for engineering applications, bearing in mind the powerful influence of plastic deformation in promoting transformation to martensite [30]. A particular material could, for example, have an Ms less than absolute zero, indicating complete stability against transformation, but an Md higher than room temperature, in which case mishandling could result in the formation of martensite [30]. Different researchers [12,30,57] have adopted a variety of arbitrary definitions of Md incorporating different strain and martensite levels.

This kind of expression of the Md temperature is preferred because it is easier to identify the temperature corresponding to a finite rather than zero martensite levels [30].

(a) Existing Md Empirical Equations as a Measure of Alloy Stability

Various authors [12,52,30] have adopted different expressions for the Md temperature to illustrate the effect of composition on austenite stability in regard to martensite formation. They are similar in that they were all evaluated statistically and are expressed as equations of the first order concerning individual alloying elements. The effect of composition on austenite stability in this case, is used differently from the usual concept of stability. In the usual sense, stability of the austenite is used to denote stability of the austenite in regard to formation of δ-ferrite (delta-ferrite) at high temperatures [12]. In this sense Si, Cr, Mo are said to be ferrite forming elements, whereas C, Mn, Ni and N_2 are austenite stabilising elements [12].

On the contrary, with regard to the formation of martensite at considerably lower temperatures, either spontaneously or by deformation, behaviour of the elements is quite different. In this case, with some possible exceptions (such as cobalt) [26], they all tend to stabilise the austenite independent of whether or not the added element has an fcc lattice structure. A strong δ-ferrite former such as Cr acts as a strong austenite stabiliser in the similar way to Ni [12].

To obtain quantitative data on the specific influence of the alloying elements on austenite stability, a number of steels covering the AISI 300 series were chosen and the Md temperatures were determined isothermally for each as a characteristic measure of austenite stability [12,30]. In choosing these steels no attempt was made to vary one element at a time and to keep others constant. All were allowed to vary simultaneously from one steel to another, and the values were treated statistically by a multiple regression analysis. The effect of the alloying elements on Md were assumed to be additive and to vary linearly with the percentage of the elements by weight [12,30]. Of noteworthy mention is that the characteristic temperature will vary with the method of deformation; in

other words different values will be obtained for deformation by tension or compression [12].

The Md temperature as defined (the highest temperature at which martensite transformation can be mechanically induced) is, however, difficult to determine experimentally (i.e. it is difficult to accurately determine the temperature at the onset of transformation) [12]. Consequently, various authors [12,30,52,57] have used arbitrary combinations of strain levels and volume fraction martensite to express the Md temperature. For example, an Md expression of $M_{d(45/20)}$, refers to the temperature at which 20 % martensite will form after a true plastic strain of 0.45.

Williams et al [30] evaluated a series of Md temperatures (determined under different strain and martensite levels) under compression for 25 different steels covering the AISI 300 series (Table 2.4). Although, the Md values were determined under compression, the behaviour in tension will follow a similar pattern [30]. Therefore, the trend followed by these Md values can be compared with those formulated under tension [30].

Md (°C)	Constant	Cr	Ni	C+N	Mn	Si	Mo
45/50	1171	-30.8	-54.4	-1484	-56.0	14.4	-38.5
45/40	852	-23.2	-38.4	-1133	-32.6	3.3	-26.4
45/30	698	-15.6	-39.0	-611	-30.8	26.4	-17.6
45/20	529	-10.9	-32.4	-301	-20.6	30.7	-12.9
45/10	433	-7.7	-27.6	-170	-16.2	27.7	-11.3
45/5	416	-6.57	-25.8	-189	-17.0	25.4	-11.1
45/2.5	413	-6.03	-24.9	-222	-16.2	20.7	-11.0
50/5	426	-6.59	-25.4	-246	-20.7	22.9	-10.2
30/5	416	-6.88	-26.5	-188	-17.6	23.4	-10.9
10/5	850	-25.2	-38.8	-847	-40.1	3.5	-12.1

Table 2.4: Empirical equations for evaluating the Md of alloys from their chemical compositions. (Md 45/5, for example, refers to Md 45% strain/ 5% martensite. Each factor is multiplied by the weight per cent of the corresponding element). (After Ref 30)

Angel, Pickering and Nohara [12,52,57] chose to express a measure of austenite stability by using a modified version of the Md temperature, termed the $M_{d(30/50)}$ temperature, widely referred to as the M_{d30} temperature. As already explained, the M_{d30} temperature is arbitrarily defined as the temperature at which a total volume fraction of 0.5 martensite is formed after 30% true plastic strain. The following equations were obtained by multiple regression analysis:

$$\textit{Angel [12]: } M_{d30}(°C) = 413 - 462(C+N) - 9.2(Si) - 8.1(Mn) - 13.7(Cr) - 9.5(Ni) - 18.5(Mo) \quad \text{.....(3)}$$

$$\textit{Pickering [52]: } M_{d30}(°C) = 497 - 462(C+N) - 9.2(Si) - 8.1(Mn) - 13.7(Cr) - 20(Ni) - 18.5(Mo) \quad \text{.....(4)}$$

$$\textit{Nohara et al [57]: } M_{d30}(°C) = 551 - 462(C+N) - 9.2(Si) - 8.1(Mn) - 13.7(Cr) - 29(Ni + Cu) - 18.5(Mo) - 68(Nb) - 1.4(GSN - 8.0) \quad \text{.....(5)}$$

where ( ) denotes weight percent of corresponding element and GSN implies ASTM grain size number.

(b) Comparison of the Existing Md Equations

Angel, Nohara and Pickering [12,57,52] discovered that all alloying elements stabilise the austenite. This is indicated by the negative coefficients for each of the elements considered in equations (3), (4) and (5). Contrary to the above trend, Williams et.al [30], found Si to have a destabilizing effect on their Md equations (table 2.4). They [30] seem to agree with other authors [12,52,57] on the behaviour of other elements. Nohara et al [57] included copper, niobium and ASTM grain size number in their equation. Nickel and copper were taken together which assumes their similarity in behaviour in the same way as carbon and nitrogen. Equations (3) to (5) show differences in the constant value and the

coefficient of nickel. But all have the same coefficients for (C+N), Si, Mn, Cr and Mo. The coefficient values from these equations cannot be compared with those of Table 2.4 because the Md equations were determined under compressive mode of deformation and secondly, Williams et al [30] did not consider an M_{d30} relationship for their equations.
Angel [12] conducted a significance test of the individual coefficients statistically using a so-called `Student' t-test. The probability of obtaining coefficient values in equation (3) by chance were found to be:

0.001 for (C+N), 0.01 to 0.001 for Mn,
0.02 to 0.01 for Cr and 0.05 for Mo, Si and Ni

The above probability values mean that results according to commonly accepted standards, are clearly significant for carbon, nitrogen and manganese, just significant for chromium and not significant for molybdenum, silicon and nickel [12]. Angel [12] attributed the results found for the last three elements either to the small amounts of Si and Mo present or to the fact that these elements varied only within a narrow range [12]. He commented that it should be possible to obtain significant results for Ni, Mo and Si by extending the range of the experimental work and by taking into account the interaction between the elements. Williams et al [30] on the other hand, discussed the variation of the coefficients with strain and martensite level for their Md relationships (fig 2.14).

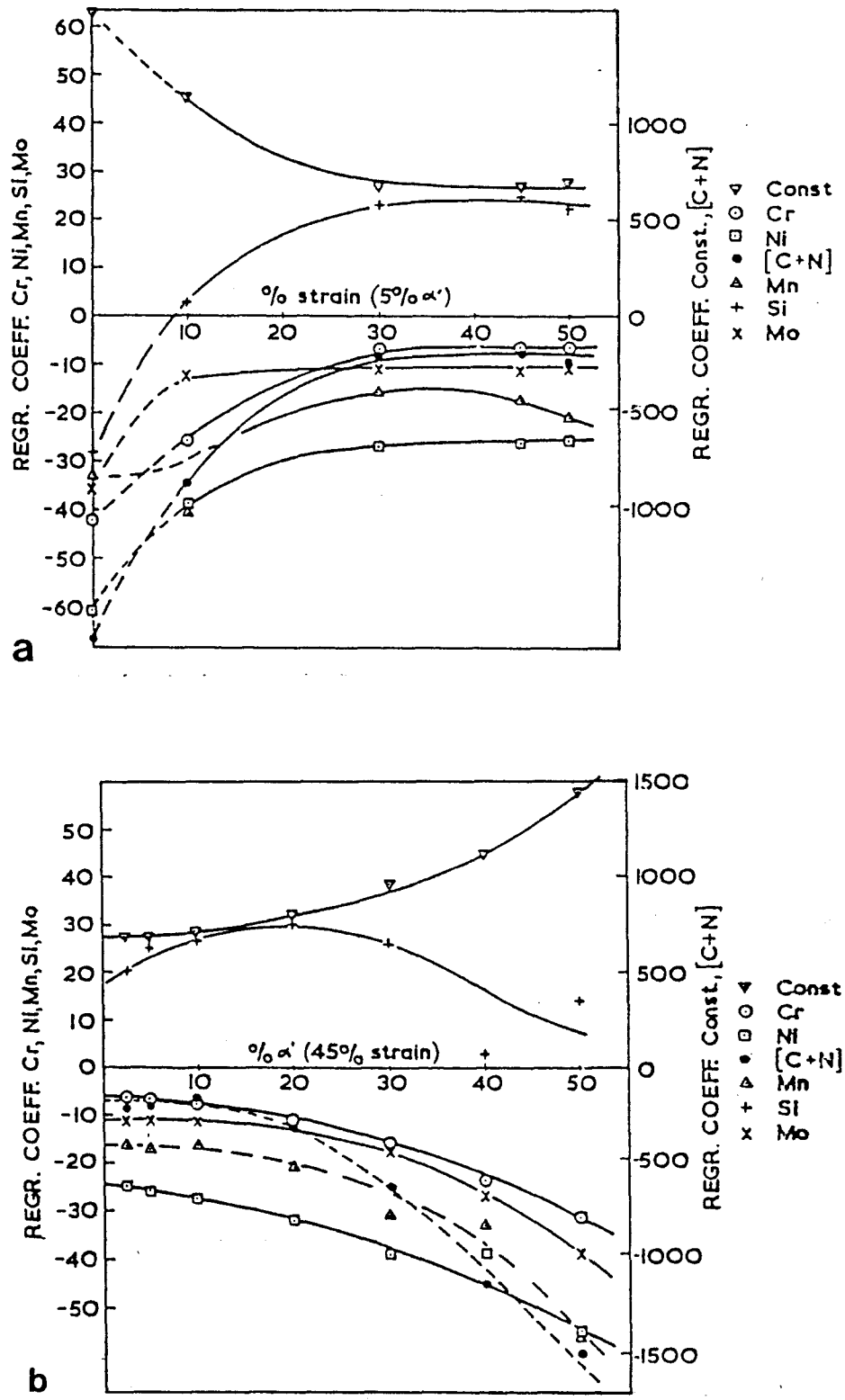

Fig 2.14: Variation of the Md regression coefficients with (a) strain at a constant martensite level and (b) martensite content at a constant strain. (After Ref 30)

They observed that for strains greater than 30% and martensite levels less than 10% the coefficients approach constant values. But at both low strain and high martensite extremes, they found that coefficients of the equations change very rapidly. They concluded that Md values defined in terms of either low strain or a high martensite level must therefore be regarded as somewhat dubious. Furthermore, they regarded Angel's M_{d30} to have a too high martensite level (50%) for most practical purposes. This conclusion by Williams et al [30] might perhaps explain the differences in coefficients for nickel and the constant values in equations 3, 4 and 5. Lenel et al [11] attributes such differences in empirical equations such as the M_{d30} to the fact that each relationship is valid only over the composition range for which it was derived. Generally, values obtained from such equations can differ significantly. Apart from the doubts expressed by Williams et al [30] regarding the use of M_{d30} equations as a measure of alloy stability, these equations (equations (3) to (5)) are widely used as criteria of alloy stability for engineering applications.

2.4 Importance of M_{d30} Temperature in Engineering Applications

The M_{d30} temperature is an important factor which greatly affects press formability of austenitic materials. The effect of drawing on austenitic stainless steels is great, and since this effect is related to the temperature dependence of martensite transformation, it may be predicted that the optimum temperature region will be governed by the austenite stability of the material as indicated in fig 2.15 [57].

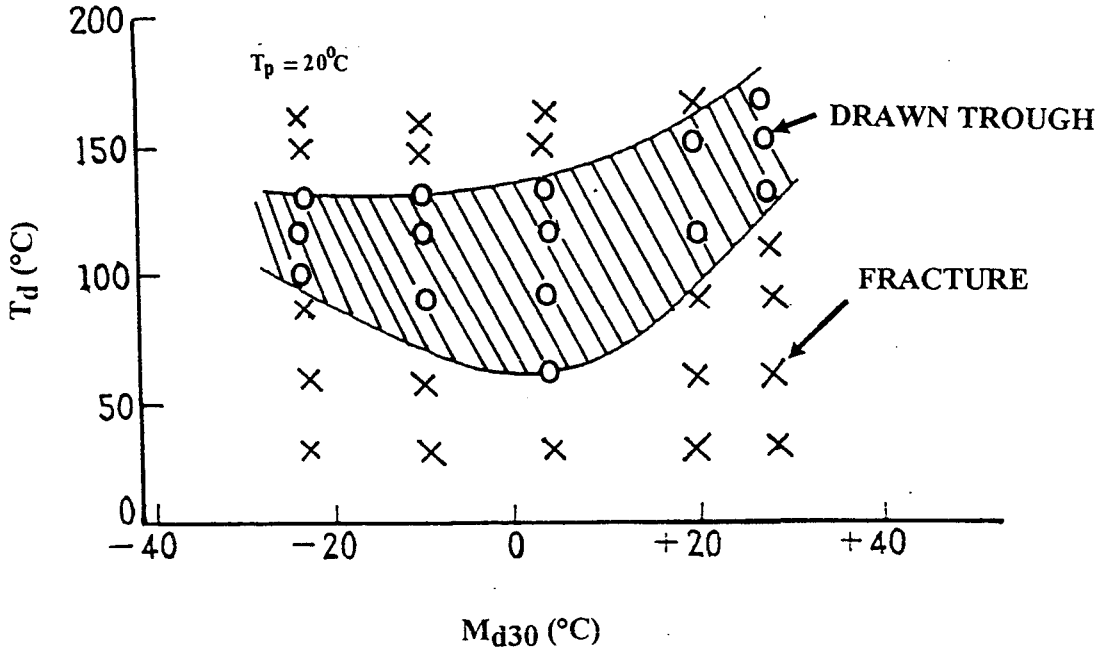

Fig 2.15: Relation between austenite stability (M_{d30}) and drawing temperature (T_d) in austenitic stainless steel. T_p refers to punch temperature. (After Ref 57)

As indicated in fig 2.15, the optimum temperature region changes with M_{d30}. At the optimum M_{d30} temperature of about +5°C, a "drawn trough", which refers to maximum drawing depth, can be achieved over a wide range of drawing temperature (65°C ≤ Td ≤ 135°C (maximum drawing temperature range)). If pressforming is performed at the M_{d30} temperature lower than M_{d30} ≈+5°C, the drawing temperature (Td) range for a "drawn trough" gradually tends towards a minimum. For example, at M_{d30} ≈ -20°C the drawing temperature range is about 35°C as compared to approximately 70°C at the M_{d30} temperature of approximately +5°C. A similar behaviour is evident if pressforming is carried out at M_{d30} temperatures above the M_{d30} temperature of about 5°C. In this case, for example, at the M_{d30} temperature of about 30°C, the drawing temperature range is reduced to about 20°C. As illustrated, failure to accurately predict the M_{d30} temperatures will result in problems in facilities and equipment and deterioration of operational circumstances [57].

2.4.1 Problems Due to Inaccurate Control of the M_{d30} Temperature

Defects which frequently occur when austenitic stainless steel sheets are subjected to deep drawing are delayed fracture and ridging [57]. These problems constitute factors restricting increase in drawing limit as indicated in fig 2.16 [57].

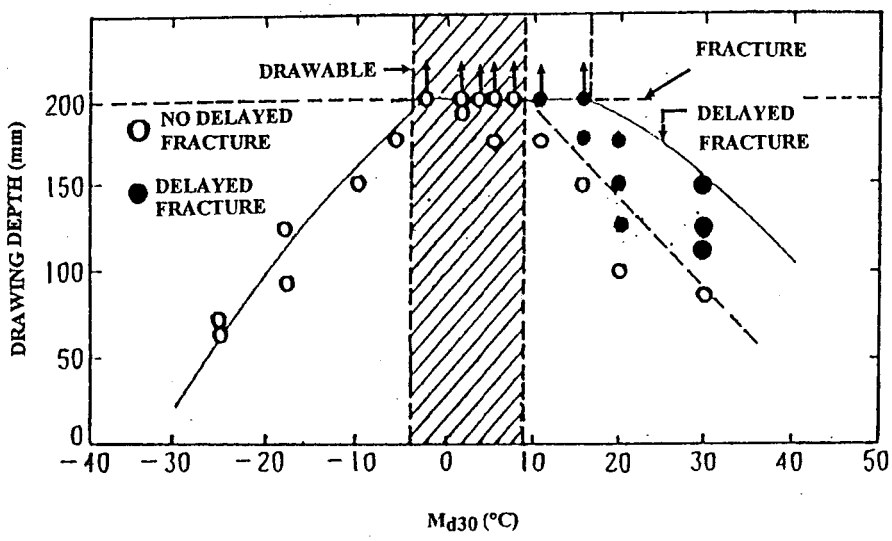

Fig 2.16: Relation between drawing limit and austenite stability (M_{d30}) in drawing room temperature. (After Ref 57)

When M_{d30} is adjusted within the hatched area, a maximum drawing depth is reached without causing drawing fracture or delayed fracture. If M_{d30} is lower than this range, the steel develops drawing fracture before maximum drawability is reached. If M_{d30} is higher than this range, the steel develops delayed fracture (fracture after room temperature drawing) even if maximum drawing depth is reached, or develops drawing fracture before maximum drawing depth. Even if drawing is suspended before drawing fracture occurs in the latter case, drawing down to the depth above the rightward descending dotted line in the figure will cause delayed fractures as shown by black dots [57]. The above-mentioned

problems, highlight the significance for the need of strict control of M_{d30} temperature and chemical composition to secure excellent drawability in austenitic stainless steels.

2.4.2 Limitations of the Existing M_{d30} Empirical Equations

Ms equations (e.g. equation 1 and 2) closely complement the Md-composition relationships [30]. Both Ms and Md relationships are statistically determined first order equations regarding various alloying elements. Lenel et al [11] found that Ms equations do not always give accurate measures of the Ms temperatures for some alloying compositions. The conclusion arrived at, regarding this observation, was that each relationship is valid only over the composition range for which it was derived. Hence, given the close resemblance of these relationships it can be assumed that the same might be the case with the M_{d30} relationships. Another limitation of the M_{d30} empirical equations is the assumption that under isothermal conditions, the amount of martensite due to $\gamma \rightarrow \alpha'$ transformation is unaffected by strain rate changes. As a result, all authors [12,52,57] did not consider the effect strain rate might possibly have on the M_{d30} equations. In some cases strain rates used for tests were not reported (e.g. Williams et al [30]). Only Angel [12] reported a uniaxial tensile strain rate of approximately 10^{-4} s^{-1}. Consequently, there is general use of the slow strain rate M_{d30} equation in predicting high strain rate M_{d30} temperatures. This assumes independence of M_{d30} temperature on strain rate variations.

But it is possible, as discussed in section 2.3.1.(2), that isothermal conditions do not always ensure no changes in the amount of martensite due to $\gamma \rightarrow \alpha'$ transformation if strain rate varies. This means that since M_{d30} temperatures are an indication of austenite stability with respect to $\gamma \rightarrow \alpha'$ transformation, any factor which affects martensite transformation will affect the M_{d30} temperatures. It will then be essential to include strain rate as a parameter of austenite stability against deformation (i.e. M_{d30} equations will be affected by the variations in strain rate).

2.5 Martensite Start Temperature (Ms) as a Criterion of Austenite Stability

Ms temperature was defined in section 2.2 as the temperature at which the $\gamma \rightarrow \alpha'$ transformation starts to occur spontaneously on cooling. This temperature is generally 100 to 200°C below the Md temperature [11]. Although, it is hardly a criterion of austenite stability for engineering applications [30], it can however be used to qualitatively ascertain the Md temperature based on the simple relationship:

$$Ms\ (°C) = Md - \Delta T \quad \text{.....(6)}$$

where $100°C \leq \Delta T \leq 200°C$

As previously mentioned, the Ms temperature can also be expressed as a first order equation concerning individual alloying elements (see equation (1) and (2) in section 2.3.3). Apart from alloy composition, Ms temperature is highly dependent on solution treatment history of an alloy. Such dependence on solution treatment temperature in the austenitizing region (fig 2.17) was illustrated by Irvine et al [58] in fig 2.18.

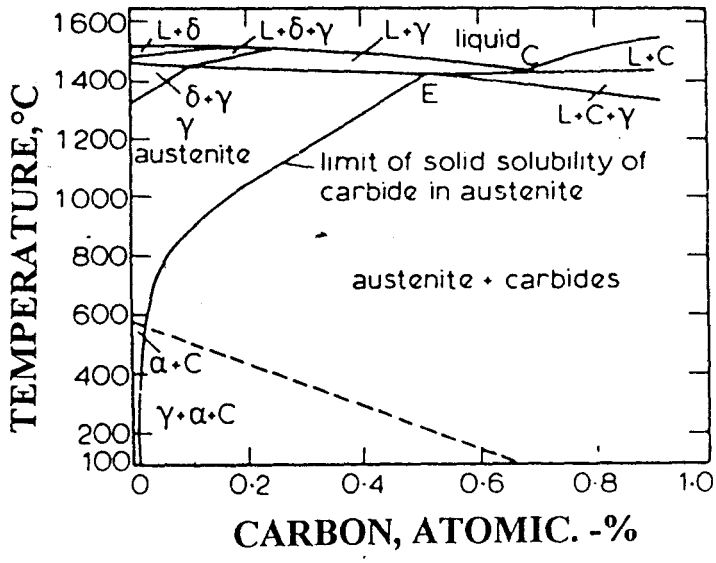

Fig 2.17: Effect of carbon on the solubility of carbides in 18%Cr, 8%Ni steels. (After Ref 22)

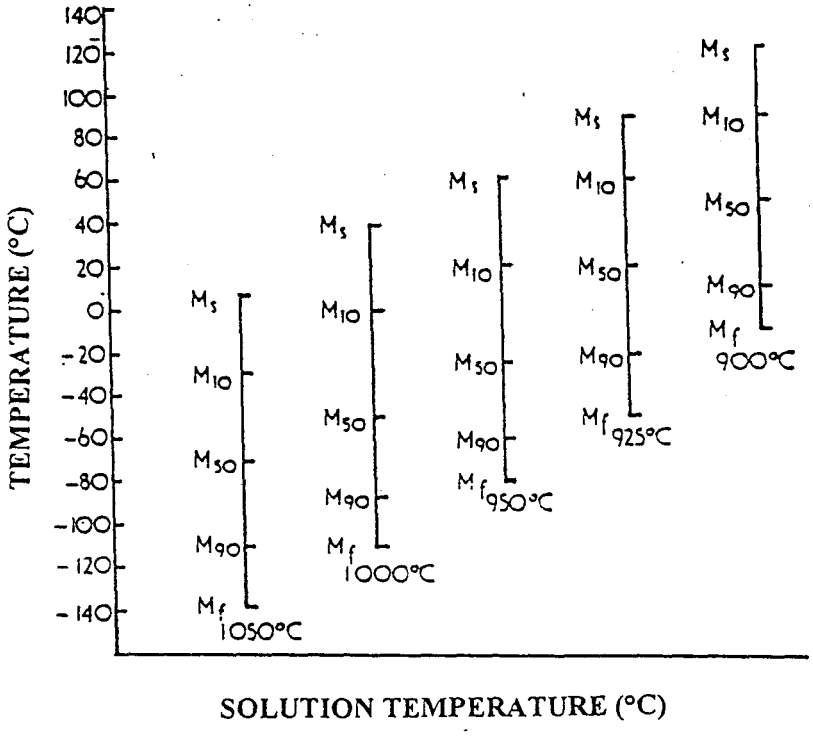

Fig 2.18: Effect of solution treatment on martensite transformation range. (After Ref 22)

The solution treatment temperature can be used to control the amount of carbide which is taken into solution, and hence control the effective composition, both with regard to carbon content and other alloying elements [22]. The effect of C, Mn, Ni, Cr and N_2 in restricting athermal formation of martensite were determined by arbitrarily assigning the value of 1.0 as the potency of Ni. The relative potency of other elements were quoted as follows [32]:

ELEMENT	POTENCY
C	27.3
Mn	0.546
Ni	1.0
Cr	0.682
N_2	27.3

Table 2.5: Relative potencies of different alloying elements in restricting athermal formation of martensite. (After Ref 32)

As illustrated in table 2.5, the interstitial elements, C and N_2 have the greatest effects on austenite stabilisation against transformation. The substitutional elements, Mn, Ni and Cr, generally have much smaller effects on austenite stabilisation [32]. Interstitial solutes increase austenite stability by restricting dislocation movement in the austenitic structures more effectively than substitutional solutes [32]. Since $\gamma \rightarrow \alpha'$ transformation involves volume increase (approximately 4 %), which must be accommodated by the generation and motion of dislocations in the austenite, restriction of dislocation movement will stabilise the austenite [26]. Because of the powerful influence of carbon on austenite stability, depletion of the austenite matrix of carbon and other alloying elements due to precipitation of alloy carbides raises the Ms temperature [26,52]. By lowering the solution treatment temperature, not all carbides are dissolved, and the lower the solution treatment temperature the more carbide is left out of solution [52]. In the example quoted in fig 2.18, if a full solution treatment at 1050°C is used then -70°C will produce only 50% transformation. On the other hand, a solution treatment at 950°C raises the martensite

transformation range sufficiently for about 95% transformation to occur on cooling to -70°C [22]. Thus even if the Ms of the steel is extremely low, heat treatment can be utilised to raise the Ms temperature, and by knowing the amount by which a particular solution treatment temperature raises the Ms temperature, the Ms and the Md can still be compared (see equation 6).

EXPERIMENTAL PROCEDURE

3.1 Materials And Preparation

Experimental alloys used in this study were commercially produced and based on the composition of AISI 304. Materials were received in the annealed condition in sheet form from *COLUMBUS STAINLESS (PTY) LTD.* The average thickness of the materials was approximately 1.4 mm. The chemical compositions and steel classifications are indicated in tables 3.1 and 3.2 respectively.

TYPE	C	N_2	Si	Mn	Cr	Ni	Mo	Cu
30422A	0.03	0.05	0.56	1.56	18.34	8.6	0.06	0.13
30431A	0.04	0.04	0.47	1.52	18.04	8.06	0.08	0.11
30432A	0.06	0.04	0.53	0.98	18.15	8.17	0.07	0.13
30431B	0.05	0.05	0.39	1.61	18.13	8	0.09	0.1
304L	0.03	0.04	0.39	1.77	18.2	8.16	0.06	0.12
30432B	0.06	0.06	0.64	1.05	18.39	8.16	0.12	0.08
30431C	0.05	0.05	0.54	1.55	18.29	8.14	0.05	0.08
30422B	0.04	0.04	0.64	1.79	18.18	8.67	0.02	0.11
30 411	0.05	0.05	0.33	1.89	18.29	8	0.09	0.08

Compositions are expressed in wt%

Table 3.1: Chemical compositions of the experimental alloys of 304 type

ALLOY TYPE	STEEL DESIGNATION
30422	DIN. Specification (German)
30431	Conventional 304
30432	Deep Draw Quality
304L	Extra Low Carbon

Table 3.2: Steel classification of 304 type experimental alloys according to the COLUMBUS STAINLESS production schedule.

3.1.1 Heat Treatment

The experimental materials were solution treated in a vacuum furnace in argon atmosphere. Materials were heated to 1050°C, soaked for 30 minutes and oil-quenched.

3.1.2 Metallography and Grain Size Measurement

To study the representative microstructures after heat-treatment, samples were prepared using conventional metallographic techniques. The final surface finish was obtained by mechanically polishing with a 0.25 μm diamond paste. Electropolishing was necessary to remove any deformation-induced martensite that may have formed during mechanical polishing. The following electropolishing procedure was used:

SOLUTION: 266 ml Glacial Acetic Acid
50g CrO_3 (chrome trioxide)
14 ml Distilled Water
VOLTAGE: 20V
DURATION: 4 Minutes
TEMPERATURE: 0°C

Depending on the information required, samples were analyzed either in the as-polished or etched condition. The various etching techniques used in order to characterize the

microstructures of experimental alloys involved both chemical and electroetching. The solutions and procedures are as follows:

(i) For electroetching, the voltage in the above electropolishing procedure was reduced to 10V.

(ii) Electroetching performed in a 10% oxalic acid solution at a temperature of 23°C. The specimen was anodically polarised at 11V for 90 seconds.

Light microscopy was performed on a REICHERT MeF3A and NIKON optical microscopes. In case of the REICHERT MeF3A, nomarski interference contrast was used to improve grain boundary contrast. As an additional aid to understand representative microstructures, the Schaeffler constitution diagram calculated from nickel equivalent modified for manganese with nitrogen, and X-ray diffraction were used. The theory and procedure for X-ray diffraction are discussed later in this chapter. The nickel and chromium equivalents were calculated from the following equations [64]:

Nickel equivalent:

$$(\%Ni) + 30\,(\%C) + 0.87\,(\%Mn) + 0.33\,(\%Cu) + 30\,(\%N - 0.045) \quad \ldots\ldots\ldots (7)$$

Chromium equivalent:

$$(\%Cr) + \%Mo + 1.5\,(\%Si) + 0.5\,(\%Nb) + 5\,(\%V) + 3\,(\%Al) \quad \ldots\ldots\ldots\ldots (8)$$

Grain size measurements after heat treatment were performed on optical micrographs. For each alloy, three micrographs were used to give an average grain size on randomly selected areas of the specimen. For this exercise, measurement was carried out according to ASTM E112-85 using the Heyn linear intercept method which produces a better

estimate of grain size than other known methods [62]. The ASTM grain size number was calculated from the equation [62]:

$$G = [-6.6457 \log L_3] - 3.298 \quad (L_3, mm) \quad .....(9)$$

where

$$L_3 = L_T / MP \quad .....(10)$$

G is the ASTM grain size number, L_3 is the mean lineal intercept, L_T is the total length of line, M the magnification and P the number of grains intercepted. To achieve good accuracy eight lines (L_T) were used for each micrograph for each alloy.

3.2 Tensile Testing

Uniaxial tensile tests were all carried out at two nominal strain rates. The low strain rate of 10^{-3} s^{-1} and high strain rate of 3 x 10^{-2} s^{-1} were used. All specimens were strained to 0.3 true strain under various testing conditions. Each tensile test was repeated three times to ensure statistical accuracy. The result of a tensile test which differed notably from the other two was excluded in the analysis. But for some of the alloys, due to inadequate amount of specimens, only two tests were used for analysis.

3.2.1 Specimen Geometry

The tensile specimens were machined according to ASTM E-8 standard. The nominal width of the specimens is 10 mm with a gauge length of 50 mm (fig 3.1).

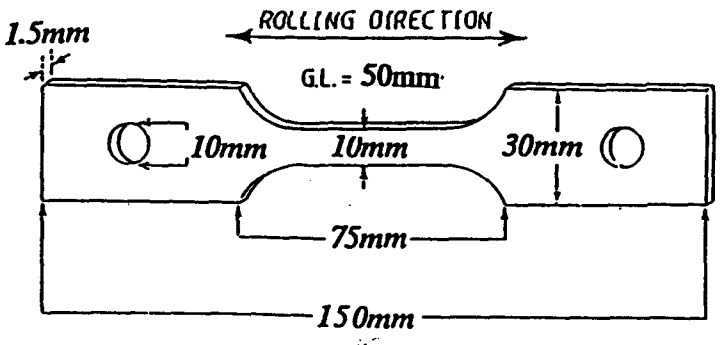

Fig 3.1: Flat tensile specimen for general tensile property evaluation.

3.2.2 Test Apparatus

Tensile tests were performed using a computer-interfaced Zwick 1484 materials tester. The set-up incorporated a temperature bath, regulated by a Eurotherm temperature controller to ± 2°C. The temperature controller was connected to a chromel-alumel thermocouple (Type K) to record specimen temperature. Two types of thermometers (high (mercury) and low (alcohol) temperature thermometers) were used in addition to the thermocouple to determine accurate temperature measurements.

Uniaxial tensile tests were carried to 0.3 true strain at -60, -40, -15, -10, 0, 23, 40 and 55°C at nominal strain rates of 10^{-3} and 3 x 10^{-2} s^{-1}. To ensure constant temperature environments, the tips of the thermocouple and thermometer were positioned in close proximity of the specimen gauge length. To ensure isothermal conditions a mixture of alcohol, liquid nitrogen and dry ice was used for temperatures below 0°C. At 0°C, a mixture of ice and water was used whereas water was used for tests at 23°C. High temperature tests at 40 and 60°C were carried out in an oil bath. The oil was heated by a helical coil which was coupled to the Eurotherm temperature controller positioned over

the gauge length of the specimen. Temperature baths were manually agitated to maintain constant temperature along the gauge length during testing.

Mechanical test data was captured on a computer file and was recorded as force (N), time (s) and gauge length elongation (mm). The data captured by the Zwick software was imported in a spreadsheet package, to obtain final copies of the tensile test records. The elastic machine deflection was subtracted from the total crosshead displacement to obtain engineering strain. The engineering strain was used to calculate the true strain from the equation:

$$\varepsilon = ln\,(1+e) \quad \text{.....(11)}$$

while true stress was calculated from the load data from the equation:

$$\sigma = S\,(1+e) \quad \text{.....(12)}$$

where S and e equal the engineering stress and strain; σ and ε are the true stress and strain, respectively.

The amount of martensite formed as a function of strain was obtained in some of the tension tests by monitoring the progress of the transformation with a magnetic detection device.

3.3 Measurement of Deformation-Induced Martensite

3.3.1 Magnetic Detection Device

(a) Introduction

A rapid, simple and inexpensive method of determining the proportions of austenite and martensite greatly facilitates the study of deformation-induced transformation in

metastable austenitic stainless steels. This is important especially when it is directed towards a technological application, such as determining maximum elongation temperature (M.E.T) and its dependence on stress system and deformation rate [5] or other process variables such as the M_{d30} temperature.

Quantitative metallographic methods are usually the simplest and most inexpensive methods. But these methods are time consuming and in the case of metastable austenitic stainless steels, the morphology of martensite often militates against easy measurement [5]. Maxwell et al [60] found that the martensite plates occurring in sheaves or elongated clusters of laths were too small to be resolved individually. As a result optical microscopy indicated greater amounts of strain-induced martensite than actually existed. The other limitation of quantitative metallography is that if a specimen is required for further deformation, it is impossible to cut from the specimen a sample required for metallography.

The other method which is widely used, is the X-ray diffraction technique. This technique is potentially the most accurate, suitable for definitive measurements and is used in the calibration of other methods [5]. Its main drawbacks, however, are that it is expensive to use in terms of equipment, time consuming due to care which must be taken when analysing data, and samples must be cut from the specimen for analysis.

Various investigators [3,5,12,16,17,30,38] found the use of magnetic techniques to be the least time consuming and easy to use. This technique exploits the fact that during $\gamma \rightarrow \alpha'$ transformation the specimen changes from being non-magnetic (austenitic) to being ferromagnetic (martensitic). When transformation occurs the magnetic permeability of the specimen is increased. Different kinds of instruments incorporating different ways of measuring the amount of martensite have been used [3,5,12,16,17,30,38]. For this study it was decided to use the method according to Maxwell et al [13] and Chapman et al [16].

(b) Development of Magnetic Detection Device

It was reasoned that if a steel specimen were made the core of an electric transformer, then when transformation takes place and the sample becomes magnetic, an emf should be developed in the secondary winding. Thus the magnetic detection device consists of a detection coil of superimposed primary and secondary windings (fig 3.2).

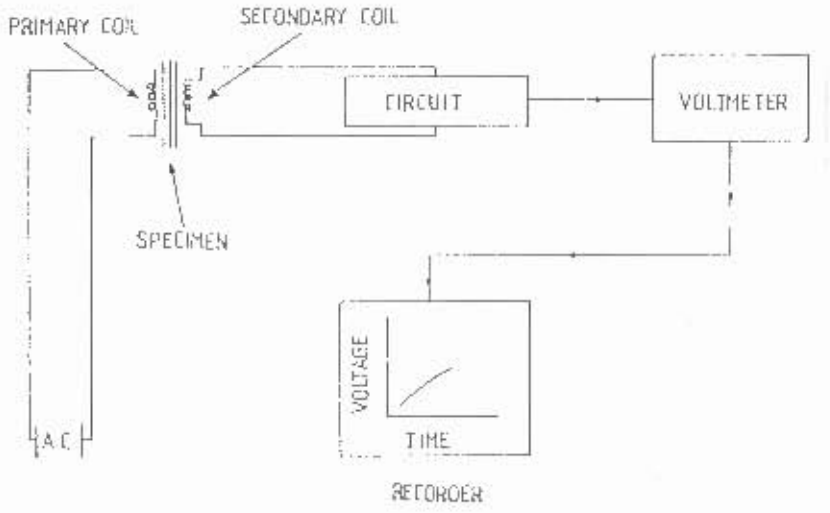

a

A: Control Box of the Magnetic Detection Device

B: Voltage Output Channels to the Recorder

C: Calibration Knob

D: On/Off Button

E: Voltage Display Screen

F: Detection Coil

G: Chart Recorder

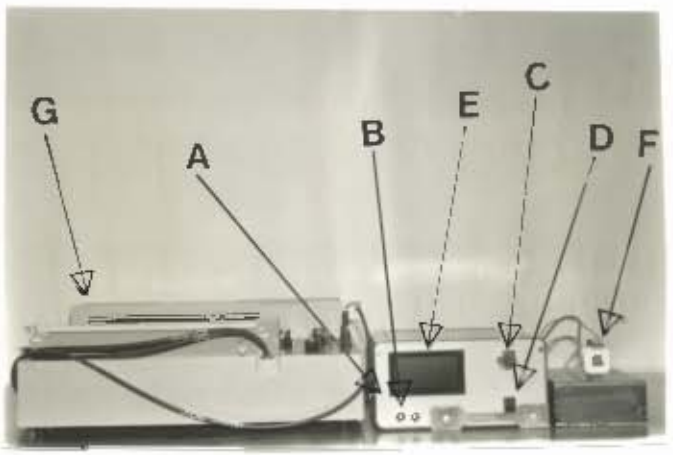

b

Fig 3.2: (a) Schematic diagram of the magnetic detection device. (b) Photograph of the detection device with a chart recorder to register voltage as a function of time.

Since flat specimens (fig 3.1) were used for this study, the secondary and primary coils which formed a transformer were fitted on to the "E" plates which allowed the transformer to be spring loaded on to the flat specimen as indicated in fig 3.3.

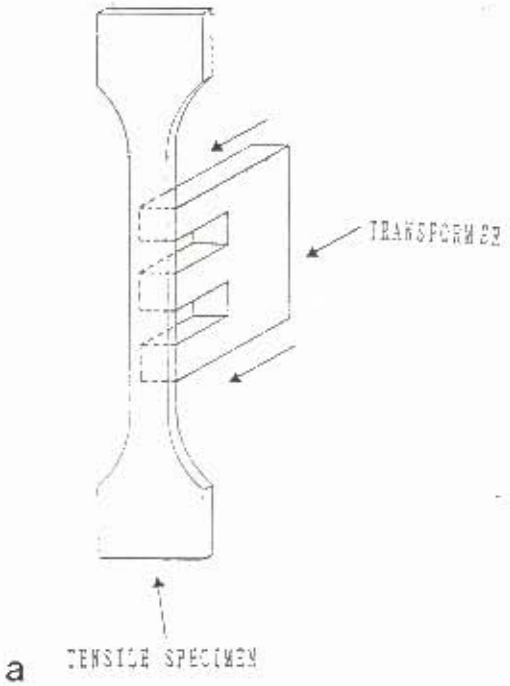

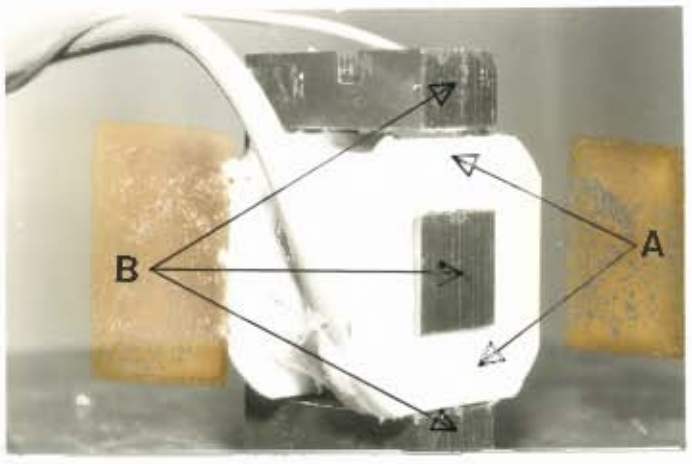

A: Superimposed Primary and secondary windings

B: "E" Plates

Fig 3.3: (a) Schematic diagram of the transformer spring loaded on to the flat tensile specimen. (b) Photograph of the secondary and primary windings fitted on to the "E" plates.

The primary windings are attached to a 220 volt A.C. (alternating current) mains. When an ac (alternating current) input signal was imposed on the primary coil, the output voltage of the secondary coil was proportional to the magnetic permeability of the specimen. It should be pointed out that only non-magnetic materials were used in the construction of the transformer. The voltmeter which is connected to the secondary coil translated magnetic permeability into voltage. The voltmeter was interfaced with a computer which recorded voltage as a function of time using a STAT30 computer program. By maintaining a consistent time base and comparing the time outputs from the magnetic detection device with those from the Zwick tester, it was possible to estimate the amount of martensite that had formed at each level of strain during the tension test.

(c) Operation of the Magnetic Detection Device

The magnetic detection device was spring loaded on to the specimen as indicated in fig 3.3(a) before liquid baths were fitted on to the Zwick tensile tester. After attaching the liquid baths on to the Zwick machine, the control knob of the voltmeter (fig 3.2(b)) was adjusted to read zero volts. This was essential to offset any effect temperature of the testing liquid might have on the voltmeter reading. The computers connected to the magnetic detection device and the Zwick tester were synchronously triggered to start data accumulation up to the end of test. This procedure allowed the voltage output signal of the magnetic detection device to be simultaneously recorded with load, time and extension during tension testing.

(d) Calibration of the Magnetic Detection Device

The magnetic detection device was calibrated by comparing the voltage output with the amount of martensite, as measured by X-ray diffraction. Magnetic output was obtained for each alloy tested at all test temperatures used for magnetic monitoring. This was necessary because the magnetic permeability of both the austenite and martensite varies with composition and temperature [60]. Various authors [7,15,45] have indicated that the

amount of magnetization (which can also be expressed as saturation magnetisation, Magne Gauge readings and force of attraction) is linearly related to the actual volume fraction of martensite. But Livitsanos et al [7] (fig 3.4(a)) indicated that linearity exists only up to approximately 75% martensite after which the curve changes slope. Similar behaviour was also reported by Hecker et al [33] (fig 3.4(b)) where the curve changed slope at about 40% actual volume percentage martensite.

Another important observation is that for both Livitsanos et al [7] and Hecker et al [33] the volume fractions of martensite in fig 3.4, seem to reach a maximum at about 90% martensite. This phenomenon corroborates an observation by Angel [12] who also reported an M_T value (limiting value for martensite content) of about 90%. The observations above imply that a 100% martensite content is never attained. Therefore, it will be erroneous to use an extrapolated magnetic value (such as voltage or saturation magnetisation [12]) for 100% martensite to calibrate specific magnetic values to actual volume fraction of martensite. For this reason, Angel's equation was not used for calibration :

$$M = \sigma_s/\sigma_0 \; X\, 100\% \quad \text{.....(13)}$$

where M is % martensite, σ_s and σ_o are the observed magnetisation value and an extrapolated magnetisation value for 100% martensite.
A similar equation for this study will be:

$$M = V_s/V_0 \; X\, 100\% \quad \text{.....(14)}$$

where V_s and V_0 are observed and extrapolated 100% voltage values respectively.

On the contrary, a linear regression analysis on the volume % martensite against voltage values was performed from the tests carried out at all test temperatures. This method gave linear regression equations based on the values obtained from X-ray diffraction and the magnetic detection device without any extrapolations. The equations were of the form:

$$\%M = mV + c \quad \text{.....(15)}$$

where m is the regression slope, V the voltage and c the y-intercept.

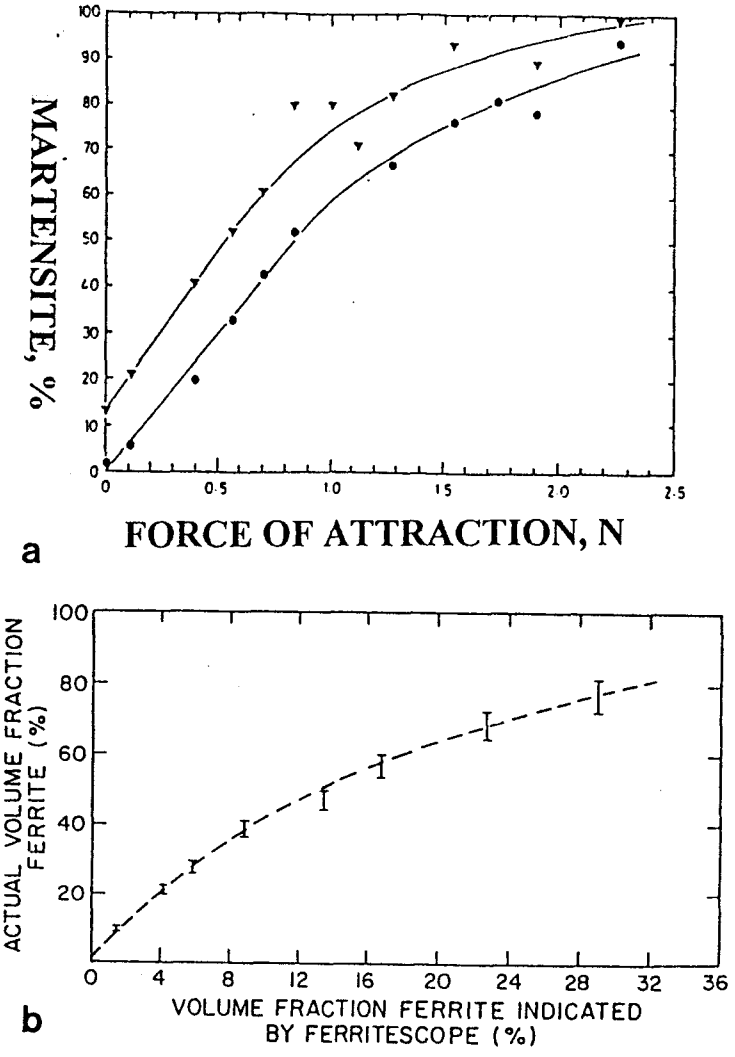

Fig 3.4: Calibration curve of (a) % martensite against force of attraction. Filled triangles represent values obtained from the first austenite and first martensite reflection ((200)$_\gamma$ and (200)α' respectively); whereas filled dots represent values obtained from the first three austenite and the first three martensite reflections ((200), (220) and (311) reflections for austenite and the (200), (211) and (310) reflections for α' martensite). (After Ref 7) and (b) % martensite against saturation magnetisation measurements. (After Ref 33)

As already remarked, since magnetic permeability varies with composition, linear regression equations were determined for all the compositions considered and were henceforth used to estimate the actual volume fraction martensite from subsequent voltage values.

The effect of other variables on calibration other than composition were considered, to ensure the reliability of the device. The effect of testing temperature was determined by immersing the detection coil of the magnetic device into various testing liquids. The variation of voltage against time was determined for the same duration as that taken for an average tensile test procedure. In this way time taken for the magnetic detection device voltage reading to stabilise in a particular testing medium could be determined. This means that for a particular test, the voltage reading can thus be adjusted to 0 mV (millivolts) after it has stabilised allowing accurate voltage values to be recorded. Furthermore, the effect of the gap between the specimen and the transformer and the reduction in contact area between the transformer and the specimen during testing were investigated.

(e) Appraisal of the Reliability of the Magnetic Detection Device

(i) Graphs of Voltage against Time

The curves of voltage against time are indicated in fig 3.5. Fig 3.5(a) shows a curve of a transformed type 301 steel and fig 3.5(b) shows a non-transformed type 304 steel. For a non-transformed steel, voltage remains at 0 V for the duration of the tension test.

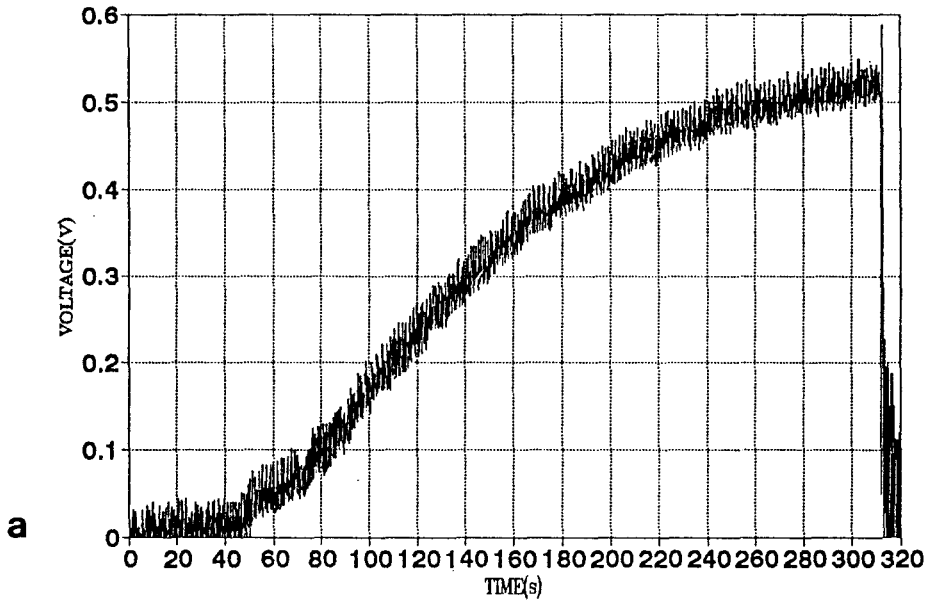

Fig 3.5 (a): Plot of voltage (V) as a function of time for a steel which has undergone transformation.

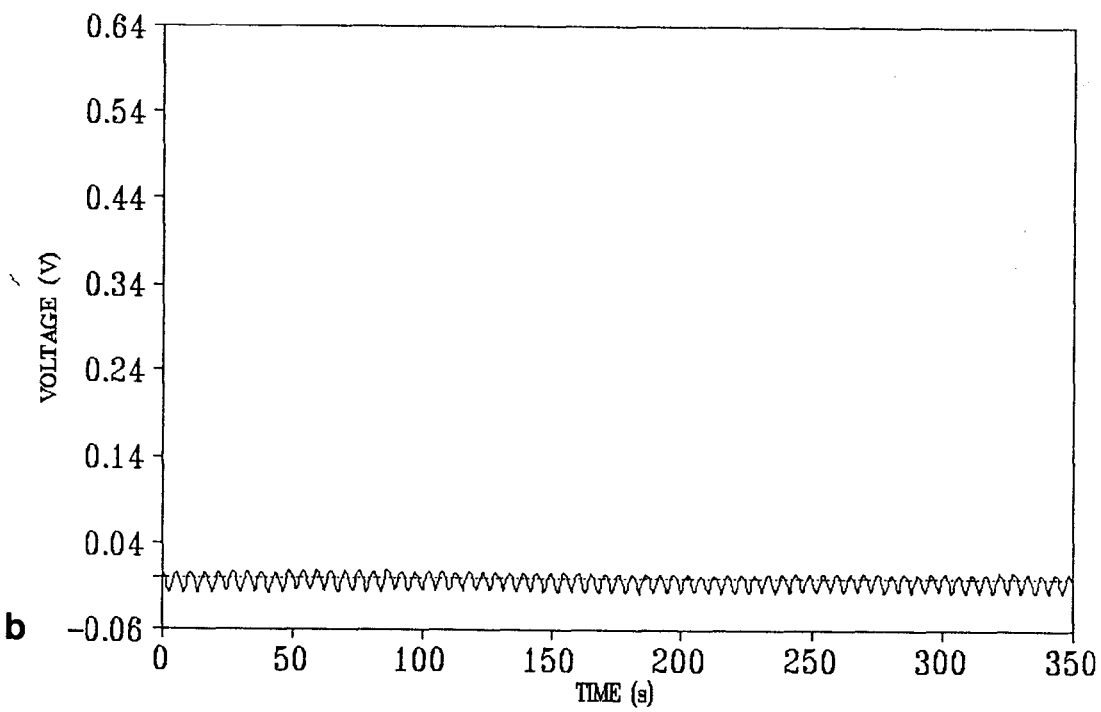

Fig 3.5(b): Plot of voltage (V) as a function of time for a non-transformed steel.

As already mentioned in section 3.3.1 (b), to predict the amount of martensite which formed at each level of strain, time values from the magnetic detection device and the Zwick tensile machine can be related. Fig 3.6 shows curves of voltage (V), true stress and work hardening rate against true strain drawn on the same set of axes. The curves were determined at four different temperatures of -40, 0, 23 and 55°C for alloy 30431A.

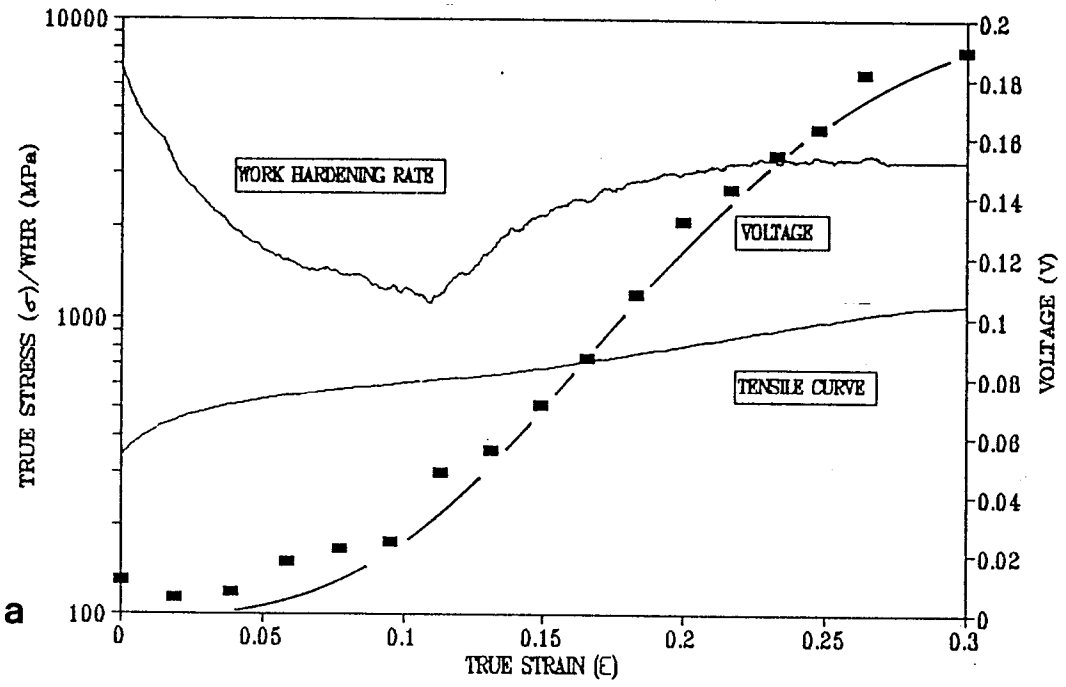

Fig 3.6: (a) Curve of voltage (V), true stress and work hardening rate as a function of true strain at -40°C for alloy 30431A.

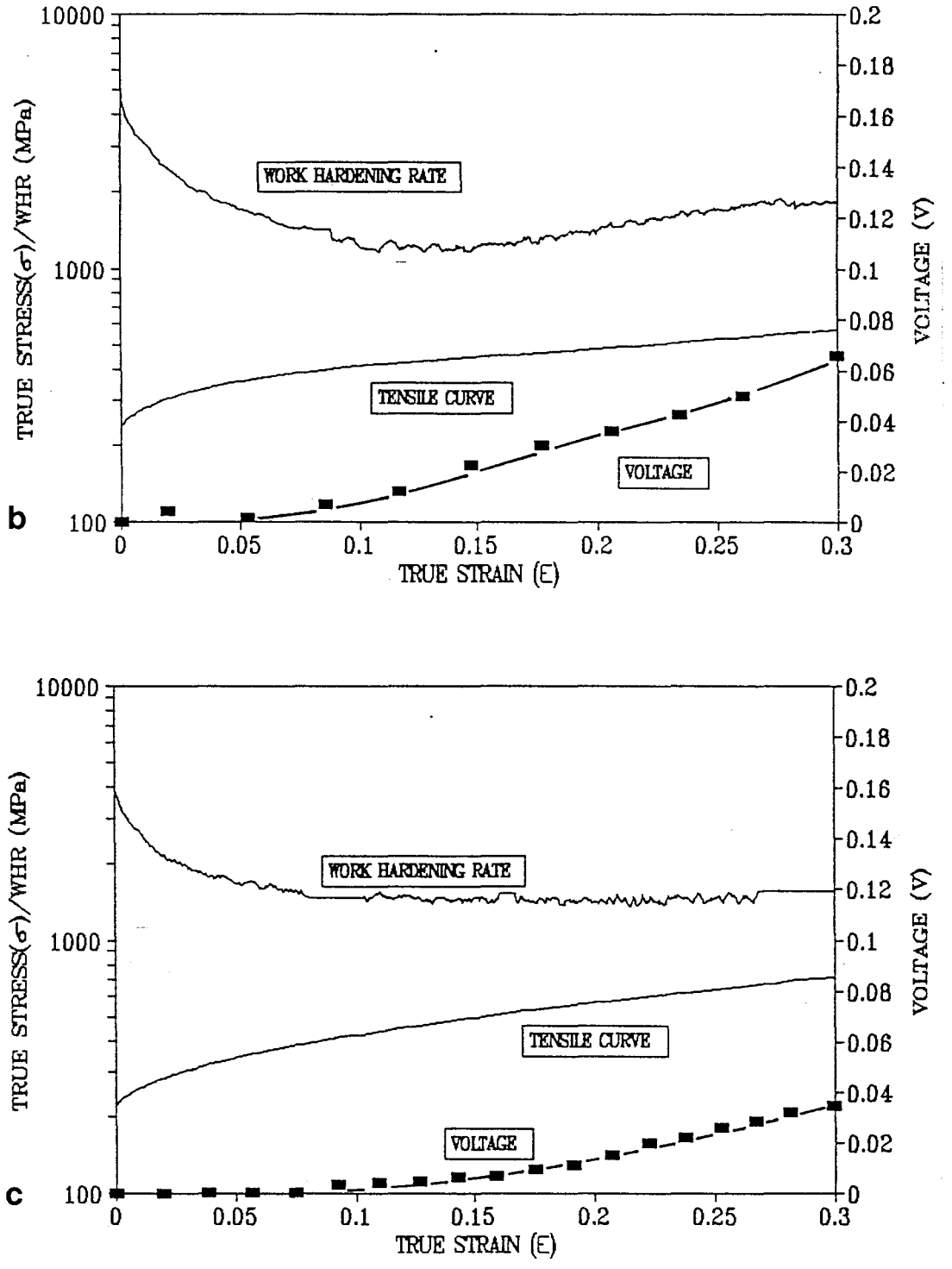

Fig 3.6: Curves of voltage (V), true stress and work hardening rate as a function of true strain at (b) 0°C and (c) 23°C for alloy 30431A.

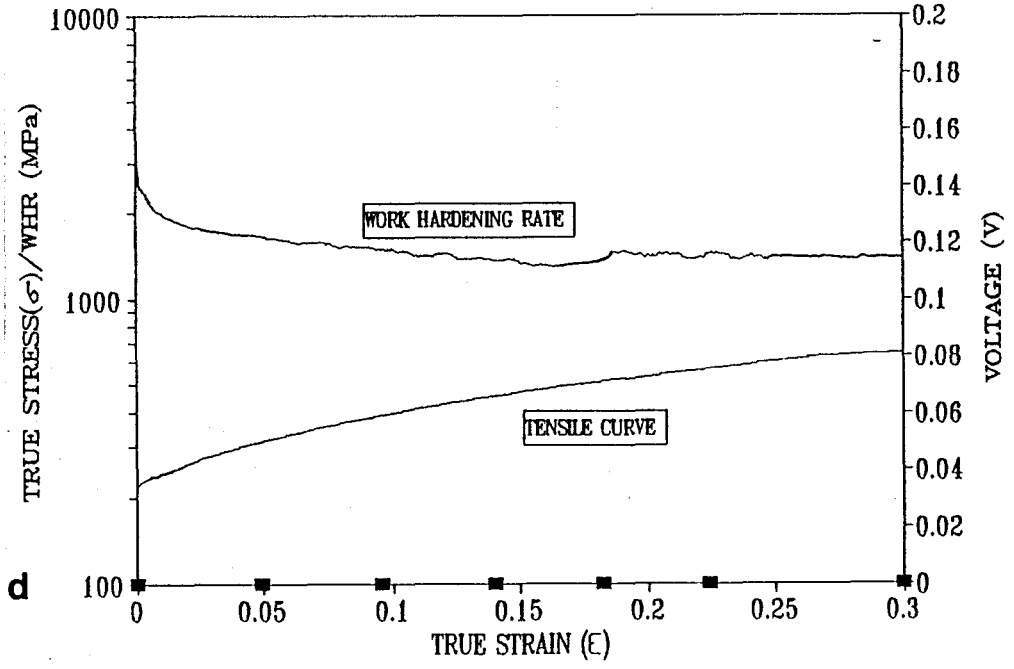

Fig 3.6: Curves of voltage (V), true stress and work hardening rate as a function of true strain at temperatures of (d) 55°C for alloy 30431A.

The work hardening rate of type 300 series austenitic stainless steels has long been known to be dependent on austenite stability and sensitivity to martensite formation during deformation [31]. For a steel undergoing martensitic transformation, the work hardening rate behaviour will be in such a way that initially the curve will decrease gradually as strain increases. But at some strain the martensite embryos become supercritical and begin to grow due to the local stress concentrations at the intersections of the slip bands and/or pile up of dislocations at grain boundaries [43]. Beyond this strain, the transformation rate and correspondingly the martensite volume fraction increases, resulting in an increase in strength due to composite strengthening by continual refinement of the austenite and martensite mixture. This increase in strength, is accompanied by a change in the true stress-true strain curve from a parabolic to sigmoidal shape. Huang et al [31] reported that with a decrease in test temperature and the corresponding increase in the rate of martensite transformation with strain, the stress-strain curves change from a smooth parabolic behaviour at higher temperatures to a sigmoidal shape at low temperatures. This observation is clearly illustrated by comparison of the stress-strain curves at 55 and -40°C

in fig 3.6 (a) and (d). The formation of ferromagnetic martensite can be jointly monitored by magnetic techniques and observation of the changes in the stress-strain and work hardening curves, as borne experimentally and illustrated in fig 3.6.

The specimen tested at -40°C, which showed a pronounced positive work hardening behaviour beyond the true strain of about 0.11 is accompanied by a continuous increase of the voltage curve to higher voltage values and a pronounced sigmoidal shape of the true stress-true strain curve. It is clear, as already remarked by Huang et al [31], that as temperature is increased the sigmoidal behaviour tends to be less pronounced and becomes completely parabolic at temperatures where transformation does not occur (fig 3.6(d)). This disappearance of the sigmoidal behaviour is also accompanied by a gradual decrease of the voltage curves towards lower voltage values and ultimately become zero at 55°C (fig 3.6(d)). It is important to note that the increase of voltage values which corresponds to the formation of martensite (fig 3.6(a) and (b)) does not exactly coincide with the minima of the work hardening rate curves. This is attributed to the fact that deformation induced martensite begins at strains just prior to the minimum work hardening rate [43]. It can be inferred that the unit strength of the first martensite crystals to form impart less strengthening effect to cause an observable change in the stress-strain and work hardening rate curves. The curves in fig 3.6 can be used jointly to provide a qualitative and quantitative transformation behaviour of metastable austenitic stainless steels as a function of temperature and strain. The transformation behaviour against temperature and strain as illustrated in fig 3.6 is commensurate with the observations of other investigators [12,38,30,53].

(ii) Calibration of the Voltage Values to Volume Fraction Martensite

As mentioned in section 3.2 all specimens were strained to 0.3 true strain which was still well within the fracture limit. As a result, specimens could be unloaded from the Zwick machine to determine static voltage values in air. The cross-sectional area of the gauge length of the strained specimen was placed at different positions along the cross-sectional

area of the detection coil of the magnetic device. An average of ten statically determined voltage values was calculated. Subsequently, a mean value between this average voltage value and the dynamically determined voltage value at 0.3 true strain (i.e. voltage value obtained *in situ* as 0.3 true strain is reached in the testing medium) was calculated. The standard deviation value, in this case, gives a measure of error associated with determining voltage dynamically (i.e. in the testing medium at 0.3 true strain) and statically (i.e. in air after straining to 0.3 true strain). Appendix I shows voltage values with the corresponding martensite volume fractions as determined by X-ray diffraction.

(1) Effect of Temperature on Voltage Values

The graphs of voltage against time for the detection coil of the magnetic device immersed in three different testing solutions are indicated in fig 3.7. As evidenced from the graphs, there is virtually no change in the voltage reading at high temperatures (fig 3.7(a) and (b)). This observation, especially at 23°C was accompanied by low differences between dynamically and statically determined values. The highest error noted for tests carried out in water (23°C) was 3 mV. At low temperatures (e.g. fig 3.7(c)) however, the voltage value increases steadily with time up to about 0.05 V (50 mV). This voltage value is reached in 150s after which it remains constant up to the end of the experiment. This observation implies that if a tensile test is carried out before 3 minutes elapses after initially immersing the specimen and the detection coil of the magnetic device in the testing environment, the actual voltage reading can be increased by about 50 mV. This kind of behaviour was observed for some of the alloys tested at temperatures as low as -40°C (see table 3.3).

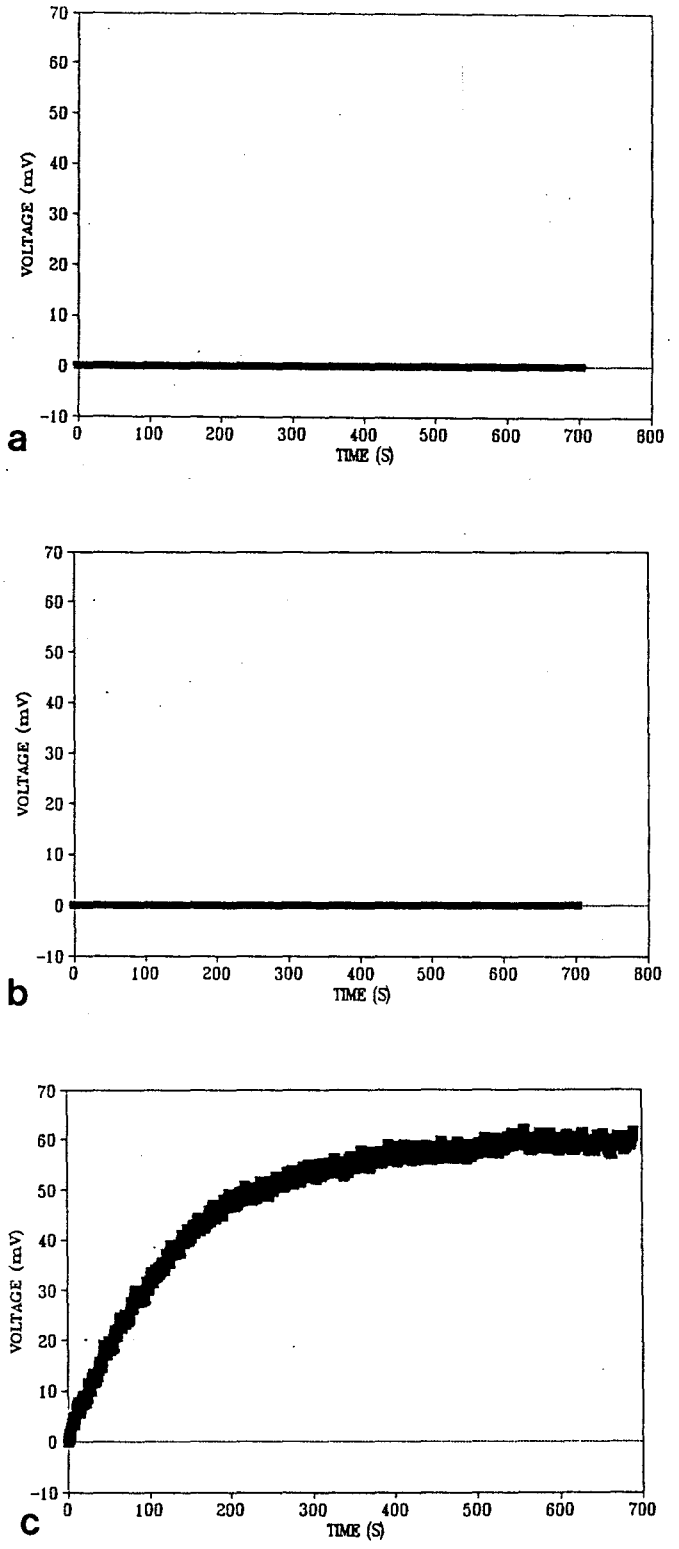

Fig 3.7: Graphs of voltage against time for the detection coil immersed in (a) oil at 55°C (b) water at 23°C and (c) ice at 0°C.

ALLOY TYPE	TEST TEMP (°C)	DYNAMIC VOLTAGE (mV)	STATIC VOLTAGE (mV)	ΔV(mV)
304L	0 -10	112 108	106 90	6 18
30431B	-15 -40	140 210	105 185	35 25
30422A	-40	147	129	13

ΔV (mV) is the difference between the dynamically and statically determined voltage values.

Table 3.3: Influence of testing environment on the voltage value for different experimental alloys.

From table 3.3 it is evident that the effect of testing environment on the voltage reading becomes more pronounced as testing environment temperature decreases. This influence can be minimised by allowing the specimen with the detection coil of the magnetic device to remain in the testing environment, for example at 0°C, for about 5 minutes prior to the commencement of the test. The voltage value is then zeroed after this period to allow a stable starting condition for the test procedure. Generally, the voltage reading on the machine should be allowed to stabilise while the detection coil and the specimen are immersed in the testing liquid, and then adjusted to 0 mV before testing is carried out.

(2) Influence of Areal Reduction on Voltage Readings

The maximum reduction in cross-sectional area for the tests performed to 0.3 true strain was found to be about 10%. The position of the detector with respect to a transformed specimen of alloy 30422A, was varied in order to simulate different reductions in cross-sectional area. When in the normal position (i.e. covering the entire cross-section), a voltage reading of 127 mV was recorded. This reading remained constant after effectively detecting smaller volumes of material, of the same sample to about 13% of the original cross-sectional area (table 3.4).

AREAL REDUCTION (%)	VOLTAGE (mV)
0	127
4	126
8.4	127
13	127

Reported values are mean values calculated from ten readings per areal reduction.

Table 3.4: Influence of areal reduction on voltage reading for a pre-transformed specimen.

The results in table 3.4 indicate that there is virtually no loss in voltage for specimens strained to 0.30 true strain. It can be concluded that areal reduction has no influence on voltage readings for tests performed in this study. Furthermore, for accurate voltage readings the detection coil of the magnetic device must be in full contact with the gauge length area of the specimen.

(3) Regression Equations Relating Voltage to Volume Fraction of Martensite

The voltage and % martensite values reported in appendix I were used to determine linear regression equations for various experimental alloys. Statistical terminology was avoided and only two major statistical tools were used - the *standard error of the estimate* and the square of the *Pearson product moment correlation coefficient*, R^2 [65]. The standard error of estimate indicates the error involved in predicting % martensite from a particular voltage value when the regression equation is used. The R^2 value indicates the amount by which a linear relationship between % martensite and voltage can explain the variability among the % martensite values (predicted values). For example, a high R^2 value (e.g. 0.90) would mean 90% of the variability among the % martensite values could be explained on the basis of the linear relationship between % martensite and voltage. This value indicates a strong linear relationship between the variables involved in the linear

regression equation. The various regression equations for the tested alloys are shown in table 3.5.

ALLOY	REGRESSION EQUATION	ERROR OF ESTIMATE (%)	R^2 VALUE
30422A	%M = 0.22V + 9.0	2.2	0.9943
30431A	%M = 0.28V + 3.7	11.5	0.7555
30432A	%M = 0.24V + 8.4	6.7	0.8793
30431B	%M = 0.22V + 6.0	6.2	0.8976
304L	%M = 0.21V + 5.3	4.1	0.9567
30432B	%M = 0.20V + 6.2	6.8	0.8911

Voltage units expressed in mV (millivolts)

Table 3.5: Linear regression equations to calculate % martensite (%M) from voltage (mV) for tested alloys.

Most alloys show a strong linear relationship between voltage and martensite content. The only exception is alloy 30431A which showed a low R^2 with an large error (11.5 %) of estimate.

3.3.2 X-ray Diffractometry

In the quantitative phase analysis of polycrystalline materials, a method widely used is that of directly comparing the integrated intensities of diffraction lines from each phase in the mixture [61]. This method has a distinct advantage over other methods in that it does not require a set of calibration samples, and is therefore preferred for conditions where it would be difficult to obtain a series of standards.

(a) Sample Preparation for X-ray Diffraction

The samples for X-ray diffraction were prepared according to ASTM E975-84 standard. Two samples of dimension 10 mm x 10 mm were cut from both sides of the midsection of the gauge length of strained specimens. The samples were mounted in resin and ground to a finish using 1000 grit paper. A final surface finish was achieved by using 1 μm diamond paste. Since deformation on the surface can occur during polishing in metastable stainless steels, electrolytic polishing was performed using the procedure outlined in section 3.1.2.

(b) X-ray Equipment and Procedure

A Phillips X-ray diffraction machine was used for quantitative analysis of martensite formed. Molybdenum MoKα radiation with a zirconium (1°) slit was chosen over other types of radiation (e.g. CuKα) because it produces a larger number of diffraction peaks with better resolution [46]. The control settings were as follows:

VOLTAGE: 40 kV
CURRENT: 30 mA
STEP INTERVAL: 0.1
COUNT TIME: 10s
SCANNING ANGLE RANGE: 18° to 48°

(c) Data Analysis

Dickson [61] showed that large errors arose when only a small number of reflections were considered. Generally, it is necessary to use a sufficient number of reflections from martensite and austenite planes to include all major components of the texture (preferred orientation of some planes) [7]. Livitsanos et al [7] recommended the use of (200), (220) and (311) reflections of austenite and the (200), (211) and (310) reflections of α′ martensite. Determination of the integrated area of the (310)α' reflection, is sometimes difficult due to poor resolution of the $(400)_\gamma$ and (310)α' reflections. Although data for higher order reflections such as $(400)_\gamma$ are usually not included, the information obtainable

from these reflections is merely the same as that from lower orders, such as the $(200)_\gamma$ reflection [61]. This information was used by Ball et al [63] to calculate the integrated area of the $(310)\alpha'$ reflection. The procedure is as follows: the integrated intensity of the $(400)_\gamma$ line was calculated from measurement of the $(200)_\gamma$ line and subtracted from the sum of the integrated intensities of the $(400)_\gamma$ and $(310)\alpha'$ lines to give the integrated intensity of the $(310)\alpha'$ line. The relationship between the $(400)_\gamma$ and $(200)_\gamma$ reflections was also observed by Dickson [61] who reported that the $(400)_\gamma$ reflection could be eliminated by the absence of the $(200)_\gamma$ reflection. The peaks were integrated using a program which integrates the background on either side of the peak and subtracts this from the integrated peak area (fig 3.8).

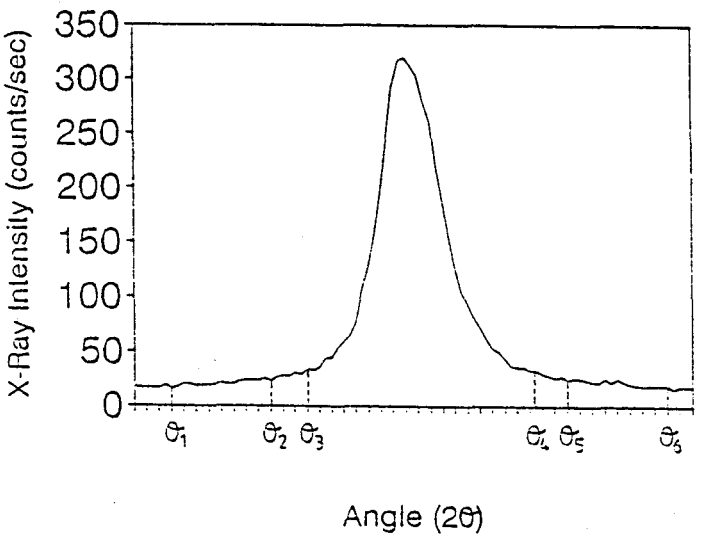

Fig 3.8: Determination of left and right peak angles (θ3 and θ4), as well as angles for determining the left and right backgrounds (θ1, θ2, θ5 and θ6).

The following set of equations were used to calculate the amount of phases in the strained specimens [61]:

Two phases, austenite (γ) and martensite (α') are present in the strained specimens. {N.B. This is true in our case since the solution treatment procedure carried out (section 3.1.1) gives fully austenitic microstructures before tensile testing}. Therefore,

$$C\alpha' + C_\gamma = 1 \quad \text{.....(16)}$$

and $$\frac{C_\gamma}{C\alpha'} = \frac{\frac{1}{n\gamma}\sum\frac{I\gamma}{R\gamma}}{\frac{1}{n\alpha'}\sum\frac{I\alpha'}{R\alpha'}} \quad \text{.....(17)}$$

where $C\alpha'$ and C_γ are volume fractions of martensite and austenite respectively, n_γ and $n\alpha'$ refer to the number of martensite and austenite reflections respectively, $R\alpha'$ and R_γ are the R factors of martensite and austenite respectively. The R factor depends on the Bragg angle θ, the reflecting set of planes and the crystal structure of the phase. $I\alpha'$ and I_γ are the measured integrated intensities of martensite and austenite reflections respectively. The R values used for calculation of the phases using MoKα radiation, were those referenced by Livitsanos et al [7] from Dickson's [61] integrated intensity method.

REFLECTIONS	BRAGG ANGLE (2θ)	FACTOR, R
$(200)_\gamma$	22.8	481
$(220)_\gamma$	32.6	298
$(311)\gamma$	38.4	314
$(200)\alpha'$	28.7	224
$(211)\alpha'$	35.5	413
$(310)\alpha'$	46	132

Table 3.6: Parameters required for calculating volume fraction of martensite using molybdenum (MoKα) radiation by Dickson's integrated intensity method. (After Ref 7)

Finally, the proportion of the two phases was calculated from the equation:

$$C\alpha' = \frac{1}{1+\frac{C_\gamma}{C\alpha'}} \quad \text{.....(18)}$$

The limit of accuracy of this method was given as 2%, which accords with the work of other investigators who found the accuracy of the X-ray method to be 1% [7].

3.4 Clarification of the Discrepancy between Existing M_{d30} Relationships and Measured M_{d30} Values

The M_{d30} values for all the alloys were calculated from equations 3, 4 and 5 described in section 2.3.3. These values will subsequently be compared with those determined from this study.

ALLOY	M_{d30} (°C) (equation 3)	M_{d30} (°C) (equation 4)	M_{d30} (°C) (equation 5)
30422A	24	18	-10
30431A	32	31	10
30432A	19	18	-5
30431B	29	29	8
304L	27	26	3
30432B	13	12	-10
30431C	29	27	5
30422B	29	22	-5
30411	29	29	9

Table 3.7: Calculated M_{d30} temperatures from equations 3, 4 and 5 described in section 2.3.3. (After Ref 12,52,57)

3.4.1 Test Statistics for Analysis of Regression Results

Two types of regression analyses are used in this study: the multiple and linear regression analyses. Both procedures use the method of least squares to give a prediction equation. The multiple regression analysis is used to predict an M_{d30} temperature value from the knowledge of the compositions of the alloying elements. The accuracy of the predicted M_{d30} values in relation with experimentally determined M_{d30} values, is established by performing a linear comparison (linear regression) between these two sets of values.

(a) Multiple Regression Analysis

A multiple regression analysis deals with the estimation of a dependent variable, Y, from several independent X variables. The basic equation relating these variables may be written in the form:

$$Y = \beta_0 + \beta_1 X_1 + \beta_2 X_2 + \ldots + \beta_P X_P \quad \ldots\ldots\ldots\ldots\ldots\ldots (A)$$

For this study, the Y value is the predicted M_{d30} value, X values are the compositions of various alloying elements considered in the equation, and are expressed in weight percent (wt%). The β values are the correlation coefficients, where β_0 is the constant coefficient and β_1, ...,β_p are the coefficients associated with the alloying elements. For ease of interpretation, the M_{d30} value and the compositions of the alloying elements shall henceforth be referred to as Y and X respectively.

A regression M_{d30} equation such as equation A above, is determined by taking into account the experimentally determined M_{d30} values for various experimental alloys. These Y values together with corresponding compositions (in wt%) for various alloying elements for each alloy, are input into a *STATGRAPHICS* computer package, to give an equation of the form of equation A, above.

The test statistics: *standard error of estimate* and *multiple correlation coefficient, R,* are used to test for a good relationship between the Y value and a linear combination of the alloying elements compositions (i.e. X values). The standard error of estimate provides a measure of error made in estimating an M_{d30} temperature value from the compositions of elements considered in the equation (of the form of equation A). However, since the standard error of estimate also depend on the variances of X and Y, a better measure is provided by the R value which is independent of variances in X and Y. The R value has the following properties:

1. R ranges in value between 0 and +1. If R = 0, there is no linear relationship between the Y value and the linear combination of the X variables. A value of R = +1 implies a perfect relationship between Y and the linear combination of the X values.

2. Interpretation of the relationship between Y and the X variables is carried out by using the square of the R value, R^2. For example, $R^2 = 0.61$ will imply that the linear combination of the X variables accounts for approximately 61% of the variance in the Y value [65].

Therefore, it can be concluded that a large R^2 value and a small error of estimate will imply a relatively strong relationship between the Y value and a linear combination of the X values.

However, in multiple regression analysis, each correlation coefficient ($\beta_0,...,\beta_p$) has to be tested statistically as to whether or not the effect observed was due to an assignable cause or chance. This is achieved by using the test statistic, *level of significance or the p-value,* which is explained as the percent of time a particular coefficient could be wrong. For this study, the p-value (level of significance) at the *5% level* is used as a test of significance. At this level of significance, a particular coefficient is not significant unless it achieves a p-value of 0.05 or less [66]. Furthermore, a *95% confidence interval* formed by the *lower and upper limits,* was determined for each coefficient. The interval formed, should enclose the value of a particular coefficient [66].

(b) Linear Regression Analysis

The linear relationship between the experimental and calculated M_{d30} values was evaluated by using linear regression equations of the form:

$$Y = a + bX \quad \text{.....(B)}$$

Y is regarded as the dependent variable because its value depends on that of X. The Y values in this study, are the calculated M_{d30} values, whereas the X values are the experimentally determined M_{d30} values. The constants a and b determine the position of the line of the graph. a is called the Y intercept when X = 0, whereas b is the slope of the line and is equal to the increase in Y divided by the corresponding increase in X.

As with the multiple regression case, a measure of error made in predicting Y from X is provided by the *standard error of estimate* and the *linear correlation coefficient, R.* But the R value in the linear regression case has a slightly different property, in that the R value in this case ranges from -1.00 to +1.00. Therefore, R = -1.00 or +1.00 when a perfect linear relationship between X and Y exists; and there is no linear relationship between X and Y if R = 0. The interpretation of the relationship between the Y and X values is also carried out by using the R^2 value. For example, if R = 0.7 then R^2 = 0.49, which implies that 49% of the variance in the Y value could be "explained" on the basis of the linear relationship with the variable X

As with the multiple regression case, the strength of the relationship between X and Y variables is evaluated by considering the sizes of the linear correlation coefficient and the standard error of estimate.

3.5 Martensite Start Temperature (Ms) Qualitative Tests

Specimens for qualitative determination of Ms temperatures were cut from steel plates provided by *COLUMBUS STAINLESS (Pty) LTD.* The specimens were solution treated at 900, 950 and 1050°C under a protective argon atmosphere in a vacuum furnace for 30 minutes. The specimens were then quenched in water at 23°C and quickly transferred into liquid nitrogen (-196°C) within 20 seconds after water quenching. Irvine et al [22] highlighted that reaction rates become sluggish at very low temperatures, so that transformation rates become extremely slow. Hence, to ensure adequate time for transformation to occur, specimens were immersed in liquid nitrogen for 12 hours.

The specimens were then mechanically polished and electropolished to remove surface martensite that might have formed during quenching or mechanical polishing. The electropolishing procedure stated in section 3.1.2 was used. The specimens were tested for magnetism using a hand magnet and only specimens which indicated some magnetism were considered for X-ray diffraction.

For ease of comparison between the qualitative tests and the calculated Ms temperatures, equations 1 and 2 presented in section 2.3.3, were used to calculate Ms temperatures for all experimental alloys.

ALLOY	Ms (°C) (equation 1)	Ms (°C) (equation 2)
30422A	-186	-92
30431A	-145	-72
30432A	-190	-99
30431B	-153	-76
304L	-166	-89
30432B	-207	-106
30431C	-159	-78
30422B	-174	-79
30411	-152	-78

Table 3.8: Calculated Ms temperatures from equations 1 and 2. (After Ref 9,52)

4 EXPERIMENTAL RESULTS

4.1 Microstructural Analysis

4.1.1 Phase Compositions

The calculated nickel and chromium equivalents from equations 7 and 8 (presented in section 3.1.2) are indicated in table 4.1.

ALLOY TYPE	Ni Equivalent	Cr Equivalent
30422A	11.05	19.78
30431A	10.62	19.38
30432A	11.7	19.53
30431B	10.75	19.33
304L	10.97	19.36
30432B	11.23	20.04
30431C	10.63	19.72
30422B	10.95	19.67
30411	10.72	19.44

Table 4.1: Calculated Ni and Cr equivalents for the experimental alloys.

A plot of the values in table 4.1 on the Schaeffler diagram is shown in fig 4.1. From the Schaeffler diagram, the alloys are expected to contain between 0 and 10% δ-ferrite (delta ferrite). However, microstructural examination of the alloys after heat treatment at 1050 °C by light microscopy indicated an absence of δ-ferrite in all instances. A typical microstructure is shown in fig 4.2.

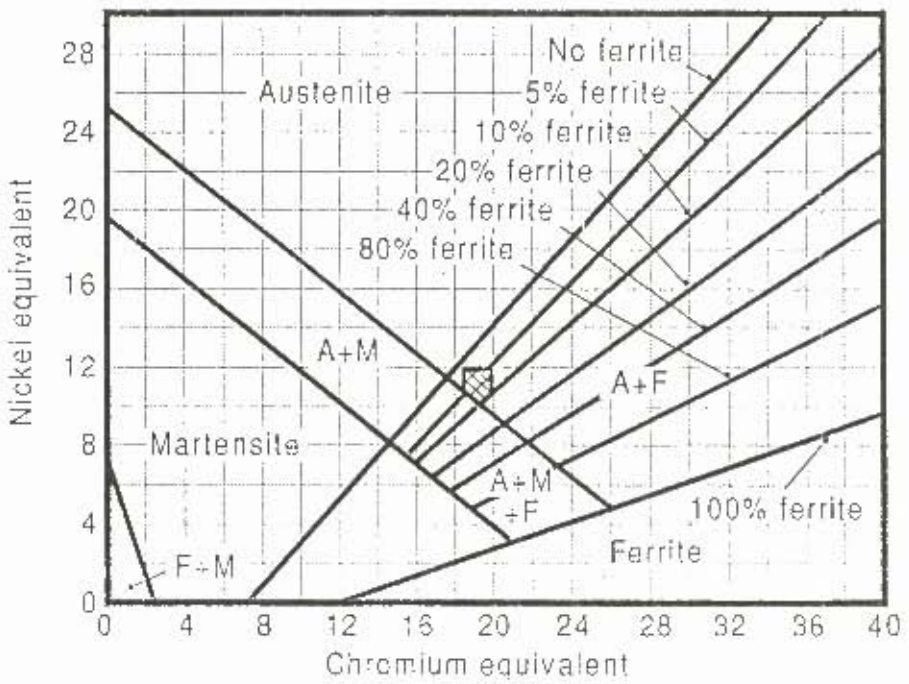

Fig 4.1: Schaeffler diagram to predict microstructural constituents of the experimental alloys. The expected phases in the alloys are indicated by the hatched area in the diagram.

Fig 4.2: An optical micrograph of alloy 30422A after solution heat treatment at 1050°C for 30 minutes, indicating a fully austenitic microstructure.

The absence of δ-ferrite was further supported by X-ray diffraction results obtained for all experimental alloys as shown in table 4.2.

ALLOY	RETAINED AUSTENITE (%)
30422A	98 ± 2
30431A	99 ± 1
30432A	98 ± 1
30431B	100
304L	100
30432B	99 ± 1
30431C	99 ± 1
30422B	100
30411	98 ± 2

Table 4.2: Phase compositions of the experimental alloys after solution treatment at 1050°C, as determined by XRD.

From the results above, it can be inferred that a single phase austenitic structure existed at the solution temperature (1050°C) and after rapid quenching to room temperature.

4.1.2 Grain Size Measurement

The ASTM grain size numbers for the tensile tested alloys are indicated in table 4.3.

ALLOY	GRAIN SIZE NUMBER, G
30422A	8.6
30431A	8.5
30432A	7.8
30431B	7.9
304L	7.9
30432B	8.0

Table 4.3: Calculated ASTM grain size numbers using Heyn linear intercept method.

The average grain size after heat treatment is approximately ASTM No. 8 which translates to approximately 20 μm in diameter [62].

4.2 Alloy Stability with Respect to Temperature and Strain Rate

Alloy stability with respect to temperature was determined at both low and high strain rates (10^{-3} and $3x10^{-2}s^{-1}$ respectively). The temperature range used was -60 to 55°C. However, only alloys which indicated a martensite volume fraction of less than 50% at -40°C, were tested at -60°C. In some cases, due to inadequate amount of specimens, tests at -40°C were only performed at the low strain rate.

4.2.1 Qualitative Assessment of Influence of Temperature and Strain Rate towards Martensite Formation

(a) Influence of Temperature on Martensite Formation

Influence of temperature on $\gamma \rightarrow \alpha'$ transformation was qualitatively followed by comparing voltage outputs (at 0.30 true strain) on the voltage versus temperature graphs, and microstructural changes obtained when testing temperature was varied. The results for alloys used for tensile tests are shown in fig 4.3.

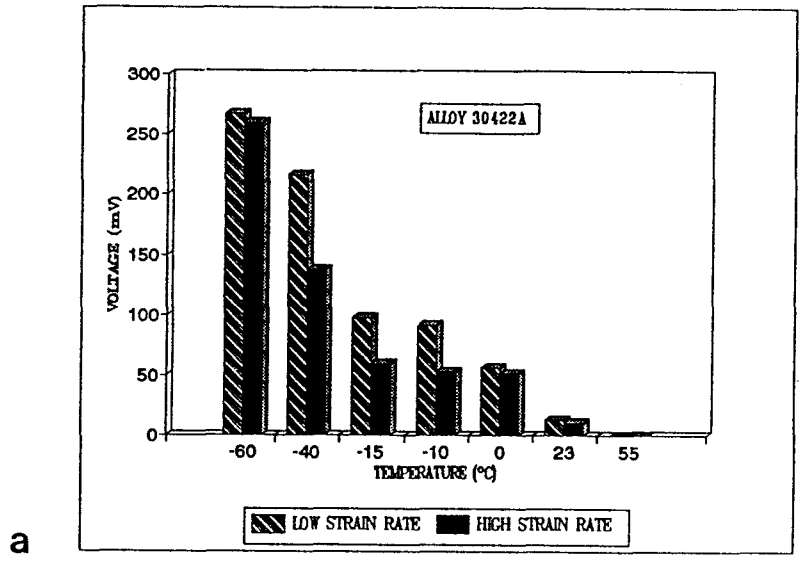

a

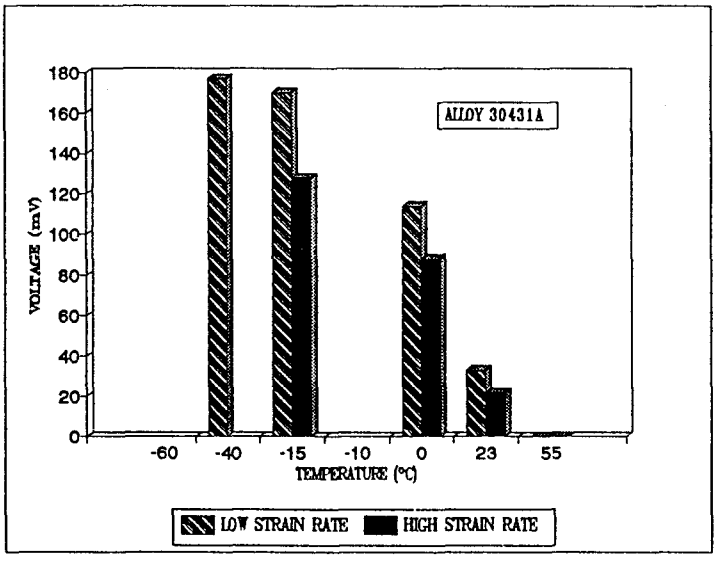

b

Fig 4.3: Graphs of voltage (mV) against temperature for alloy (a) 30422A, (b) 30431A

c

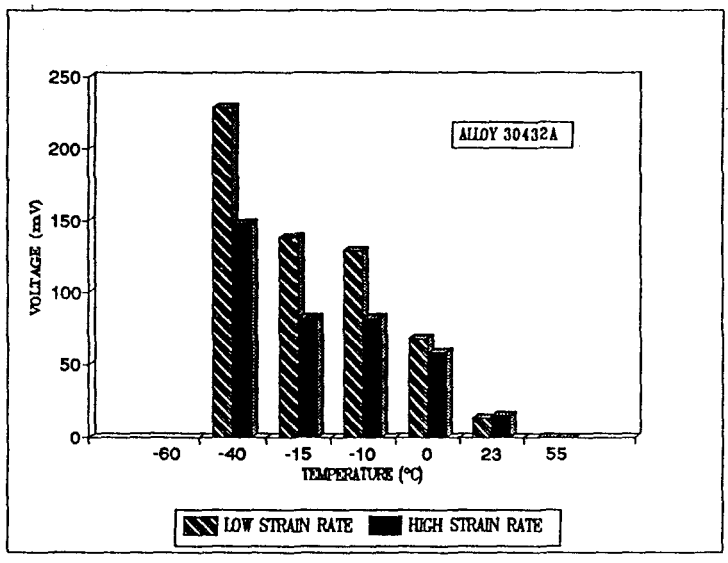

d

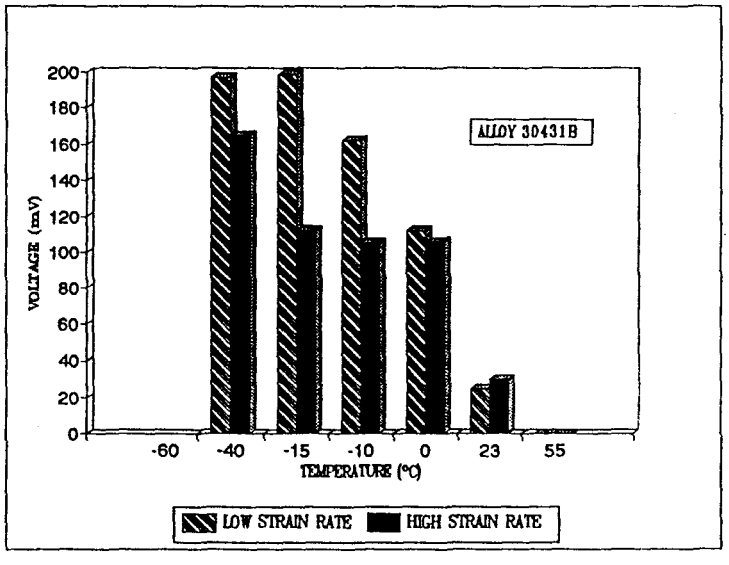

Fig 4.3: Graphs of voltage (mV) against temperature for alloy (c) 30432A, (d) 30431B

e

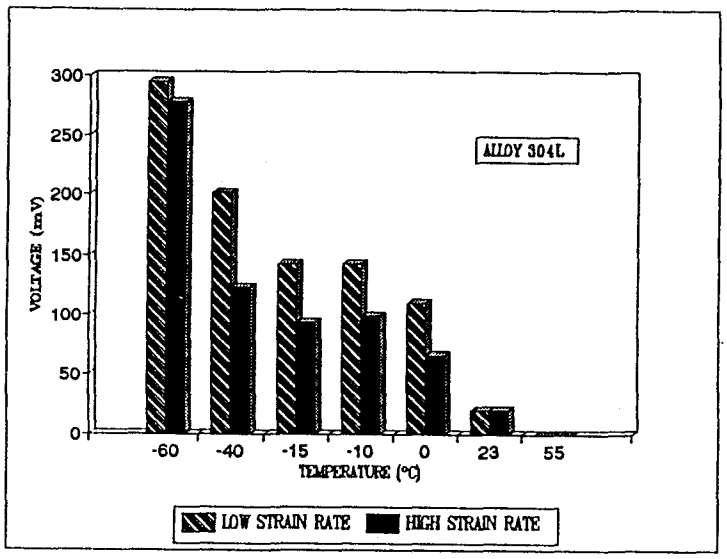

f

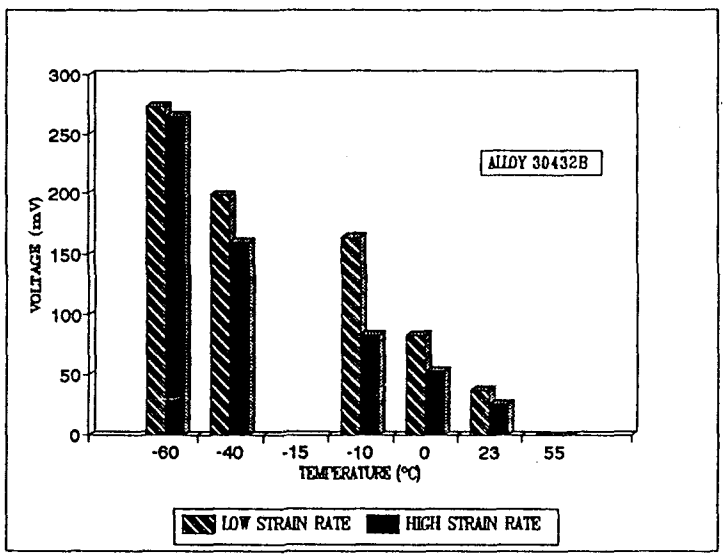

Fig 4.3: Graphs of voltage (mV) against temperature for alloy (e) 304L, and (f) 30432B

The voltage values for all alloys indicate that alloy stability decreases as temperature is decreased. This is indicated by increases in voltage outputs as temperature decreases; which implies an increase in the martensite content. At higher temperatures (e.g 55°C) at 0.3 true strain, no voltage responses were evidenced for all alloys, which indicates that no transformation occurs at this temperature. Metallography was performed on alloy 30422A tested at temperatures of 23°C, 0°C and -15°C at the low strain rate. The microstructures are indicated in fig 4.4.

Fig 4.4(a) indicates surface relief along active slip planes of the austenite, in some grains. This indicates preferential nucleation of martensite along active slip planes. X-ray diffraction indicated a martensite volume fraction of 10%. In fig 4.4(b), the micrograph shows a high density of surface relief associated with the active slip planes, within the austenite grains. A martensite volume fraction of 24% was measured. The micrograph also illustrates preferential growth of martensite at twin boundaries and along the grain boundaries. The micrograph for the specimen deformed at -15°C, indicates a preponderance of surface relief associated with the formation of α' martensite crystals. Furthermore, the preferential growth of α' martensite parallel to active slip planes, twin boundaries and along grain boundaries is evident. X-ray diffraction indicated a martensite volume fraction of 30%.

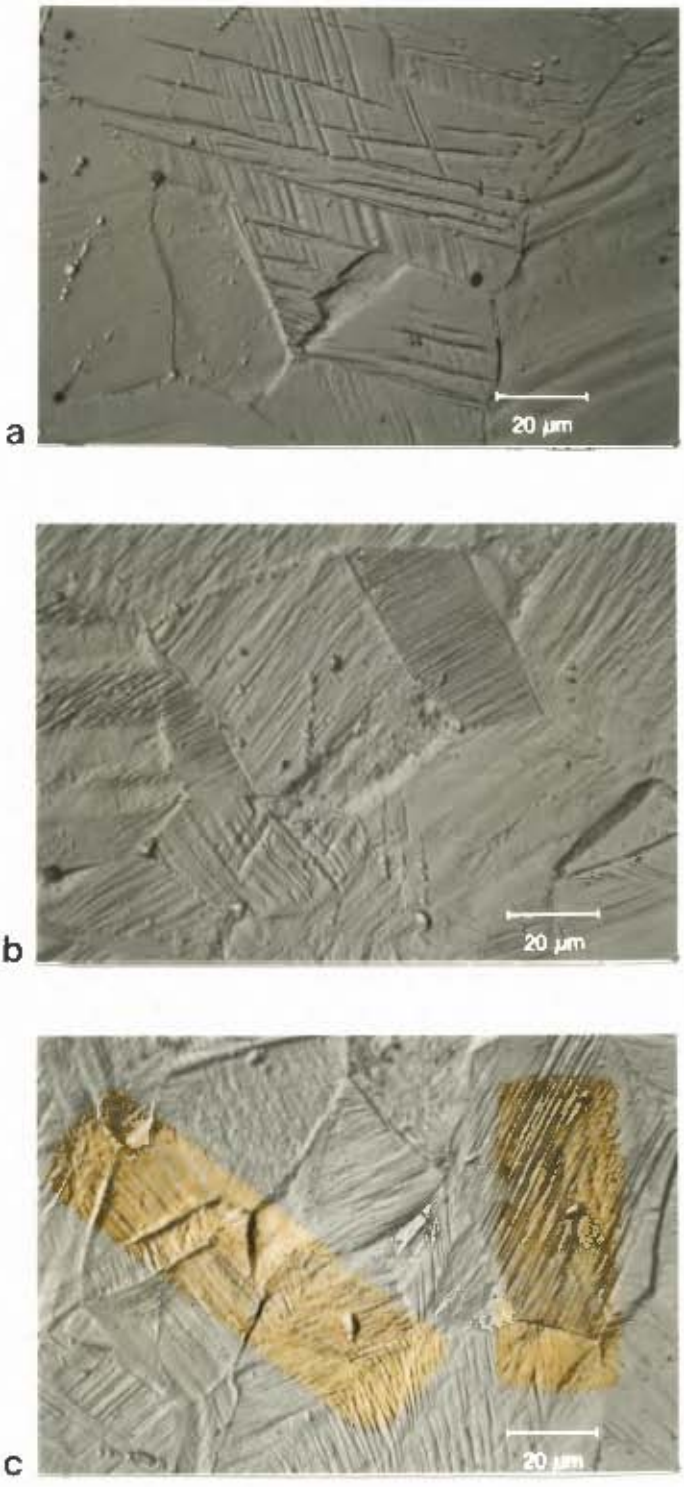

Fig 4.4: Optical micrographs of alloy 30422A deformed at low strain rate in tension to 30% true strain at (a) 23°C (b) 0°C and (c) -15°C.

(b) Influence of Strain Rate on Martensite Formation

Comparison of voltage values for low and high strain rates at a particular temperature indicated that at low temperatures ($T \leq 0°C$), low strain rate tests gave higher voltage values than high strain rate tests. This implies that at low strain rates an increased amount of martensite is expected. At higher temperatures ($T \geq 23°C$) however, martensite content with respect to strain rate varied from alloy to alloy. Alloys 30431A, 30432B and 30422A indicated slightly higher volume fractions at low strain rates, whereas alloys 30431B and 30432A showed slightly higher martensite contents at the high strain rate. Equal amounts of martensite were realised for alloy 304L. No transformation occurred at 55°C for all alloys tested.

Another important observation from the graphs is that the differences in voltage values between the low and high strain rates (10^{-3} and $3 \times 10^{-2} s^{-1}$ respectively) are more pronounced at temperatures between -40 and 0°C. This trend is clearly evident for alloys 30422A, 30431A, 30432B and 304L (fig 4.3(a), (b), (c) and (e)). On the contrary, at both low and high temperature extremes (at $T \approx -60°C$ and $T \approx 23°C$) voltage differences between the two strain rates tend to decrease as seen in fig 4.3 (a), (e) and (f).

4.2.2 Quantitative Assessment of Influence of Temperature and Strain Rate on Transformation to Martensite

(a) Martensite Transformation during Deformation

In some tests, the relative amounts of martensite were determined by magnetic measurements made *in situ* during testing. This was achieved by mounting the magnetic detection coil on the specimen. Hence precise measure of magnetism as a function of plastic strain was obtained. The linear regression equations listed in table 3.5 (in section 3.3) relating %martensite to voltage, were used to convert voltage values to specific amounts of martensite.

The progress of martensite was studied at 0°C and -40°C at the low strain rate of $10^{-3}s^{-1}$, and the results are shown in fig 4.5 (a) and (b). It was further attempted to relate the formation of martensite during straining with the true stress-true strain curves. The superimposed curves for alloy 30431A at both 0 and -40°C (at the low strain rate) are indicated in fig 4.6 (a) and (b). Similar curves were obtained for other alloys but are not shown here. It was difficult to obtain good results at the high strain rate ($3 \times 10^{-2}s^{-1}$) because of the difficulty of maintaining an accurate time base between the magnetic device and the Zwick tensile machine data.

In fig 4.5(a), all alloys are stable up to about 0.075 true strain after which transformation starts to occur. At the true strain of 0.2 the difference in the rate of martensite transformation between alloys is clearly evident. At this strain level, alloy 30431A is the most transformable whereas alloy 30422A is the least transformable. At 0.3 true strain, alloy 30431A has formed the greatest amount of martensite ($\approx$ 27%) whereas alloy 30422A has formed least amount of martensite ($\approx$ 10%). Alloy 304L and 30431B formed nearly the same amounts of martensite ($\approx$ 20%). Interestingly, alloys of the same type formed different amounts of martensite. Alloy 30431A formed more martensite than 30431B (approximately 27 and 20% respectively). For the 30432 type alloys, 30432A showed higher martensite content than alloy 30432B (about 16 and 13% respectively).

In fig 4.5 (b), all alloys are stable up to about 0.025 true strain. At the true strain of 0.2, alloy 30431A has formed the highest amount of martensite (about 28%) as compared to other alloys. However, at 0.3 true strain, alloy 30432A has formed the highest amount of martensite. Interestingly, alloy 30422A has formed more martensite than alloys 304L, 30431B and 30432B. As noted in fig 4.5(a) (at 0°C), alloy 30431A still formed more martensite than alloy 30431B. Similarly, alloy 30432A has also formed more martensite than 30432B.

The main observation on comparing fig 4.5 (a) and (b) is that transformation does not start until a certain value of strain has been achieved. This value of strain is lower for tests performed at -40°C (0.025) as compared to the strain value of 0.075 for the tests performed at 0°C. The quantity of martensite increases as strain is increased and as the

temperature of straining is lowered. In addition, the variation in tendency to form martensite as a function of alloy type is greater at 0°C than at -40°C.

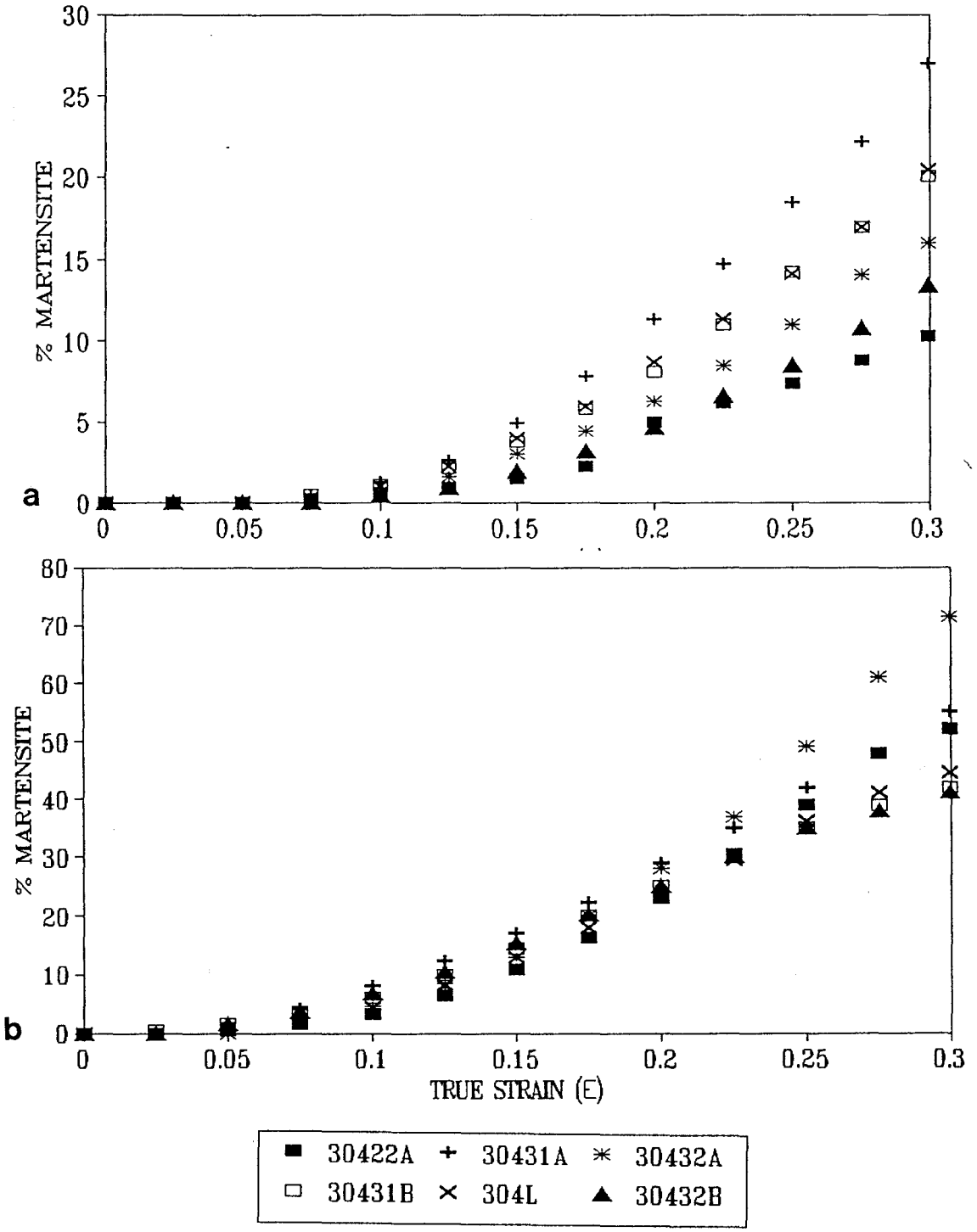

Fig 4.5: Graphs of % martensite as a function of true plastic strain during deformation at: (a) 0°C and (b) -40°C for alloys tested.

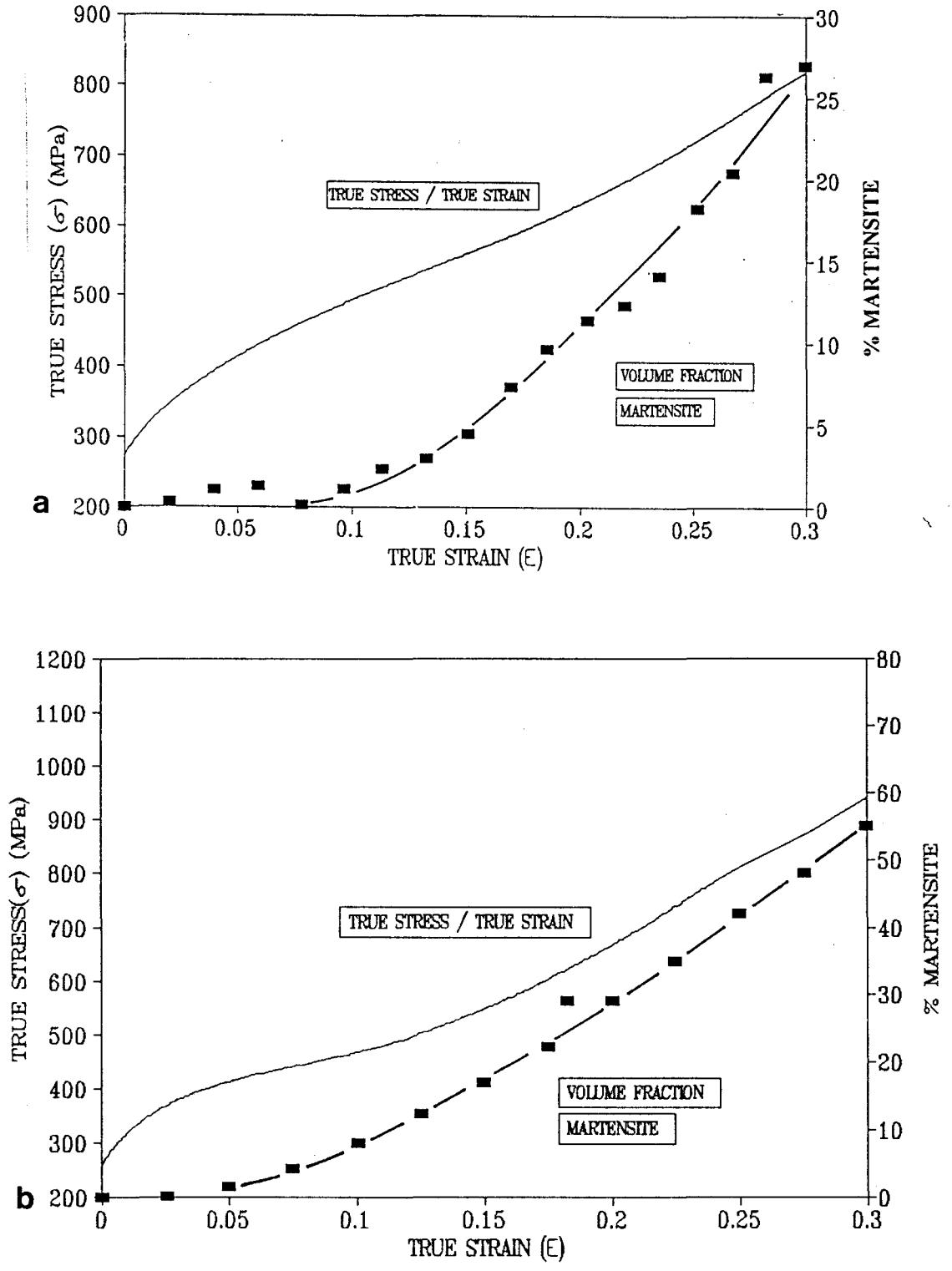

Fig 4.6: Graph of true stress and % martensite against true strain for alloy 30431A at: (a) 0°C and (b) -40°C

Comparison between fig 4.6 (a) and (b) indicates that the true stress-true strain curve at -40°C (fig 4.6 (b)) has a more pronounced sigmoidal shape than the curve at 0°C. In both cases, the region where the true stress-true strain curves are sigmoidal in shape, coincide with areas where martensite content increases rapidly with increasing strain, as indicated by the % martensite-true strain curves. But it is important to note that the increase in martensite does not exactly coincide with the point where the true stress-true strain curves changes from parabolic to sigmoidal shape. However, an important observation is that the rate of martensite formation is more rapid at -40°C than at 0°C.

(b) Martensite Transformation as a Function of Temperature

Actual volume fractions of martensite (at 0.3 true strain) at all temperatures, were obtained from X-ray diffraction results. Although, volume fractions can be calculated reliably from regression equations in table 3.5 (in section 3.3.1), the use of actual X-ray diffraction results will eliminate possible error introduced by the regression equations. Curves of % martensite versus temperature were obtained for both strain rates and are indicated in appendix II. For ease of reference, low and high strain rate curves were plotted on the same set of axes and are shown in fig 4.7.

As already observed in section 4.2.1, high strain rate tensile tests gave decreased amounts of martensite as compared to low strain rate tests between 0 and -40°C. This caused a shift of the high strain rate curves towards lower temperatures along the temperature axis (fig 4.7(b)). Furthermore, at both strain rates, alloys 30431A, 30432B and 30431B gave higher volume fractions of martensite at temperatures less than 23°C compared to alloys 30422A, 304L and 30432B. This observation indicates the differences in temperature sensitivity of martensite formation for these alloys. Graphs of (-dM/dT) versus temperature were therefore determined to assess the temperature sensitivities of martensite formation for these alloys (M and T imply % martensite and temperature (°C) respectively).

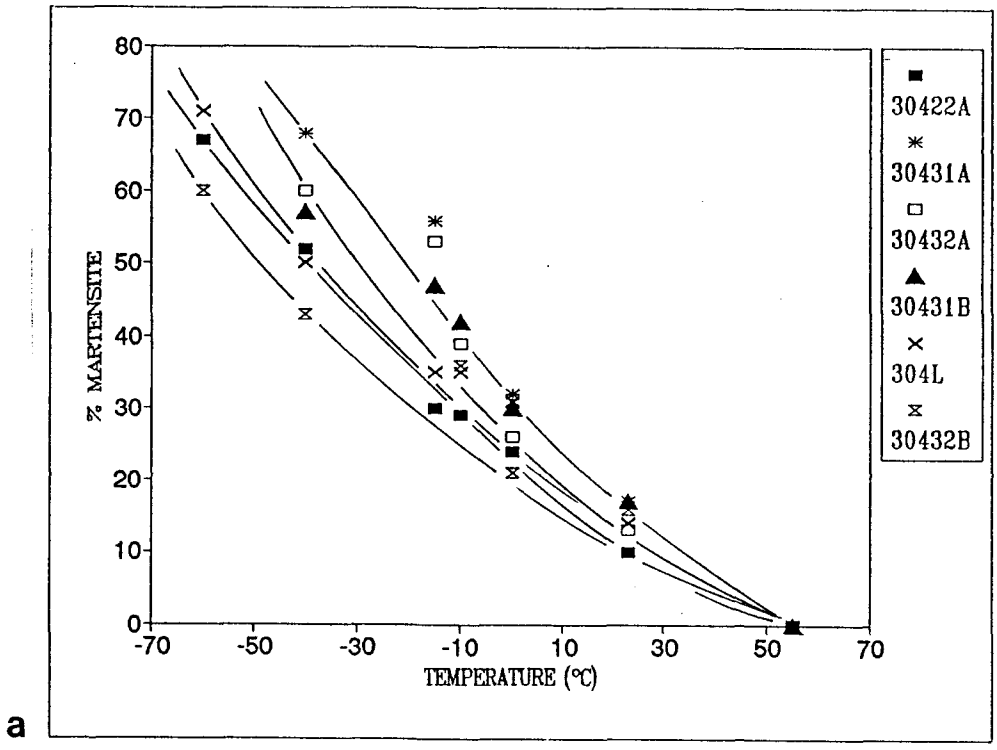

a

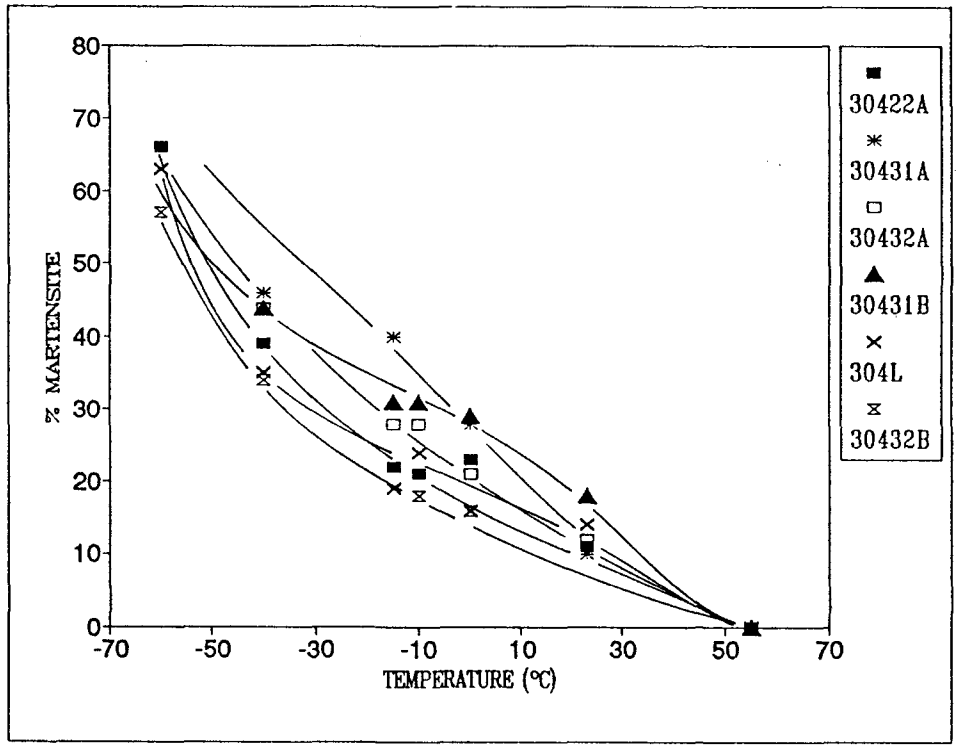

b

Fig 4.7: Curves of % martensite versus temperature for experimental alloys tested at the (a) low strain rate ($10^{-3}s^{-1}$) and (b) high strain rate ($3 \times 10^{-2}s^{-1}$).

(c) Temperature Sensitivity of Martensite Formation against Temperature

Curves of (-dM/dT) versus temperature for all alloys were obtained by measuring the slopes of all the appropriate curves in appendix II, and are presented in fig 4.8.

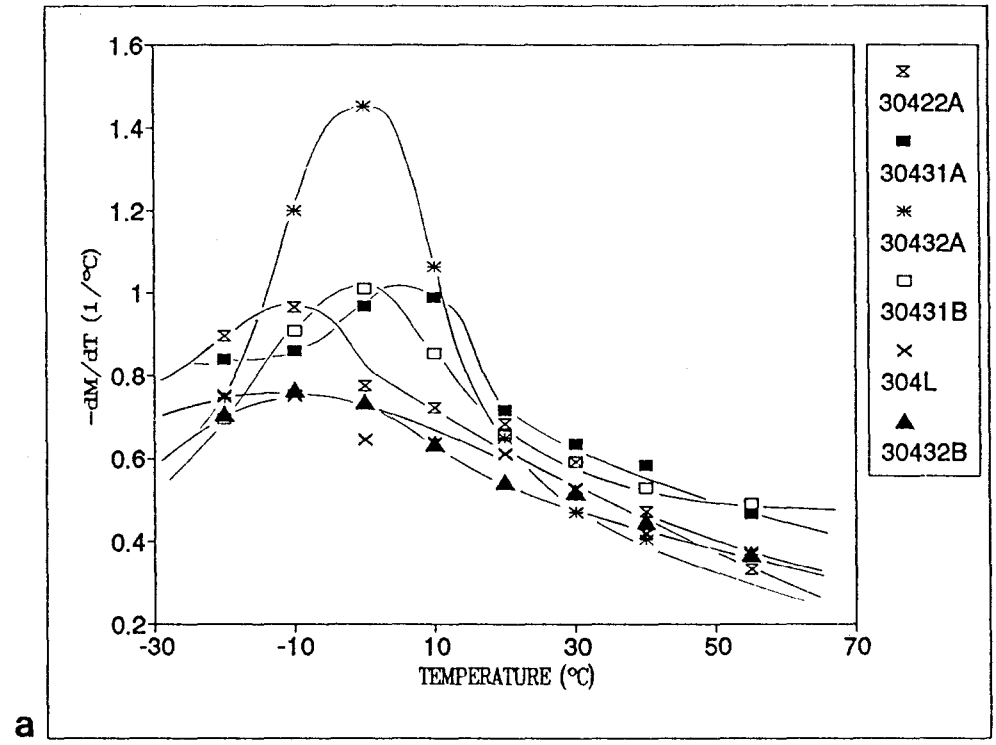

a

Fig 4.8: Graphs of (-dM/dT) versus temperature for tests performed at (a) low strain rate

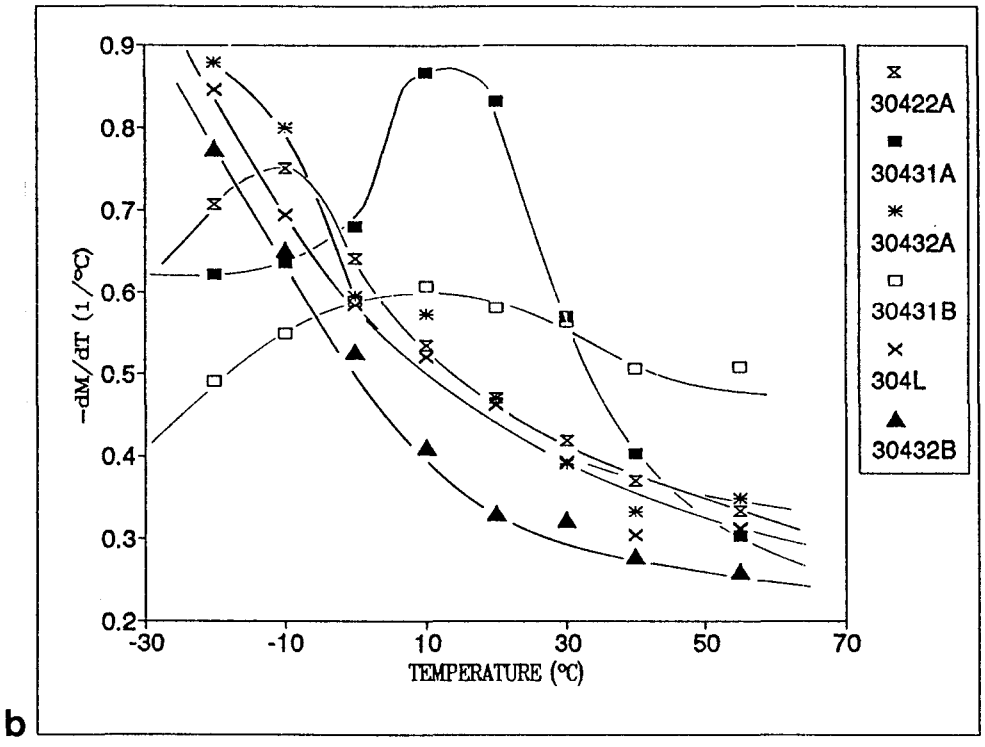

Fig 4.8: Graphs of (-dM/dT) versus temperature for tests performed at (b) high strain rate for all experimental alloys.

At both strain rates, the temperature sensitivity of martensite formation is low at high temperatures (e.g. at ≈ 50°C). At the low strain rate, the sensitivity gradually increases with decreasing temperature and goes through a maximum between -10 and 10°C after which it decreases with decreasing temperature. The peaks correspond to regions of maximum slopes on the % martensite versus temperature curves where martensite transformation occurs rapidly over a small temperature change. The peaks for alloys 30432A, 30431A and 30431B at the low strain rate occurred at higher temperatures (≈ 0 to 10°C) whereas alloys 30422A, 304L and 30432B showed peaks at about -10°C. At the high strain rate, alloys 30431A and 30431B are more transformable than alloys 30422A, 30432B, 30432A and 304L as evidenced by higher (-dM/dT) values in the temperature range of 0 to 40°C. The (-dM/dT) maxima for alloys 30431A, 30431B and 30422A still

occur at approximately 10 and -10°C respectively. Peaks of alloys 30432A, 304L and 30432B are not observed, but the indications are that they occur at < -30°C.

Comparison of (-dM/dT) versus temperature curves for high and low strain rate cases, indicates that generally the temperature sensitivities of martensite formation are higher at the low strain rate as shown in fig 4.9. In addition, temperature sensitivity tends to peak at lower temperatures at the high strain rate.

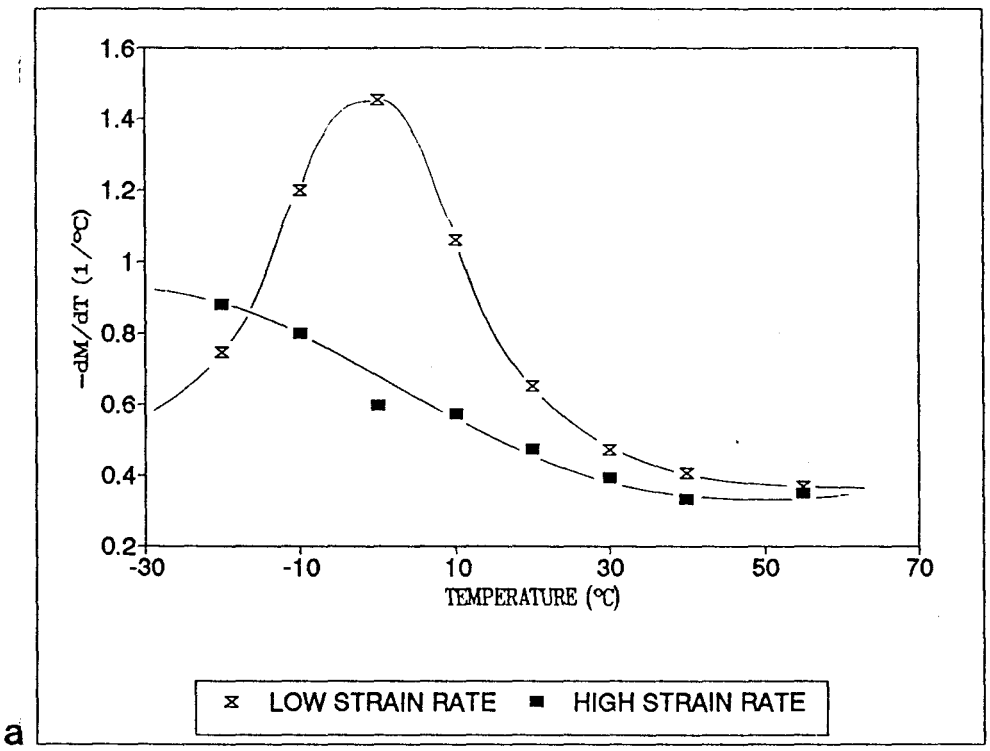

Fig 4.9: Graphs of (-dM/dT) versus temperature at both strain rates for alloy (a) 30432A (the graphs for other alloys are shown in appendix IV).

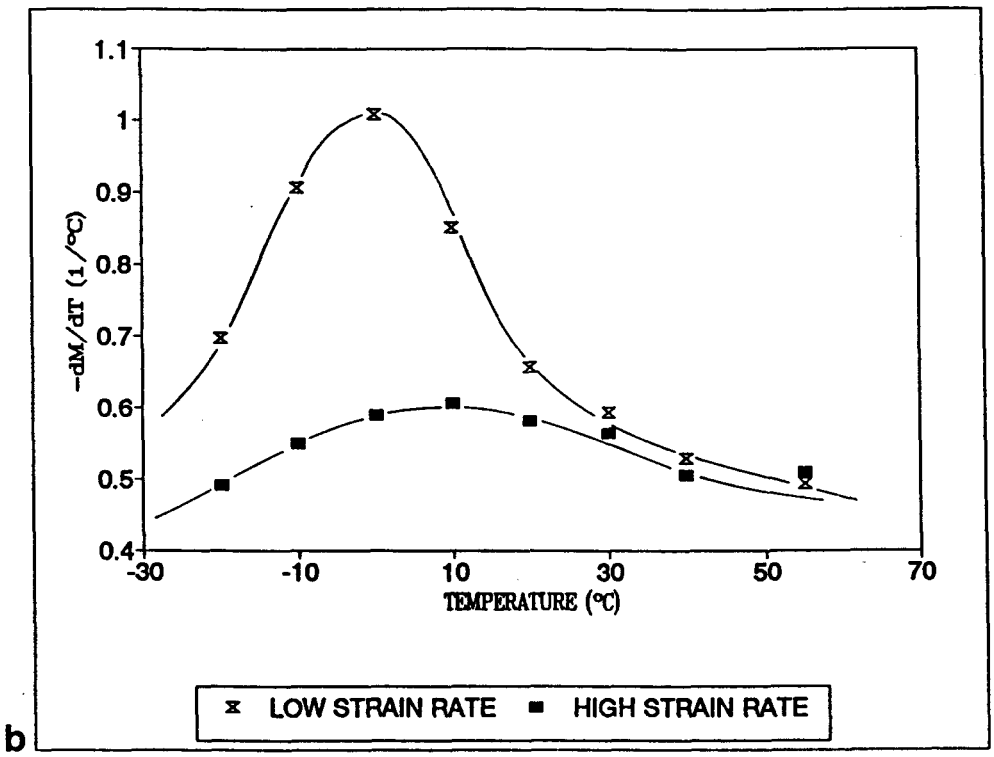

Fig 4.9: Graphs of (-dM/dT) versus temperature at both strain rates for alloy (b) 30431B (the graphs of other alloys are shown in appendix IV)

For most alloys, the maximum difference between (-dM/dT) values between the two strain rates is at a maximum in the temperature range of -10 to 10°C. This difference tends towards a minimum at higher and lower temperatures (≥ 23°C and ≤-15°C) as seen in fig 4.9 (a) and (b). This phenomenon accords well with observations in figure 4.3 (a) to (f) where the difference in voltage values between the two strain rates were found to be minimal at both low and high temperature extremes (T ≈ -60°C and T ≈ 23°C).

(d) Determination of M_{d30} Temperatures

From the results in sections 4.2.1 and 4.2.2 (c) it is clear that alloys 30431A, 30431B and 30432A are less stable towards $\gamma \rightarrow \alpha'$ transformation on plastic deformation than alloys 304L, 30432B and 30422A. It is expected that the least stable alloys will have higher M_{d30}

values in comparison with the more stable alloys. In addition, since high strain rate tests gave decreased amounts of martensite it is expected that M_{d30} values will be lower than those determined at the low strain rate. The M_{d30} values were determined from the curves in appendix II and are shown in table 4.4.

ALLOY	M_{d30} (°C) (Low Strain Rate)	M_{d30} (°C) (High Strain Rate)
30422A	-33	-44
30431A	-16	-31
30432A	-16	-39
30431B	-19	-36
304L	-33	-41
30432B	-33	-48
30431C	-22	-40
30422B	-28	-37
30411	-33	-42

Table 4.4: Experimentally determined M_{d30} values at low and high strain rates.

(i) Formulation of the M_{d30} Equations

A multiple regression analysis was made using experimental alloys given in table 3.1 (9 in all). It was attempted to consider and express elements in the same order as fitted in Pickering, Angel and Nohara et al's equations (equations 3, 4 and 5 in section 2.3.3). The equations were determined on the assumption of additivity, linearity and no element interaction. Limited statistics is used to explain the accuracy of each equation.

1. M_{d30} equations according to Elements considered in Angel and Pickering's Equations (eqns 3 and 4)

M_{d30} (°C)	Constant	C + N	Si	Mn	Cr	Ni	Mo
Low Strain Rate (19)	883	-728	-14	-47	-33	-20	-63
High Strain Rate (20)	717.5	-308	+4.1	-10.1	-36.5	-6.3	+9.3

( ) implies equation 19 and 20.

Table 4.5: Formulated equations according to the elements considered by Angel [12] and Pickering [52].

The following test statistics were obtained for the two equations indicated in table 4.5 and are shown in table 4.6.

M_{d30} (°C)	CORRELATION COEFFICIENT, R	R^2 (%)	STANDARD ERROR (°C)
Low Strain Rate (19)	0.98	95.62	3.2
High Strain Rate (20)	0.99	99.84	0.4

R and R^2 are multiple correlation coefficient and the square of the multiple correlation coefficient respectively. The other test statistics are shown in appendix III.

Table 4.6: Test statistics to evaluate the accuracy of equations 19 and 20.

The large R^2 values in the low strain rate case implies that about 96% of the variation in the calculated M_{d30} values from the low strain rate equation (19) can be explained by the alloying elements considered. For the high strain rate case 99.8% of the variation of M_{d30} temperatures as calculated from equation 20 can be explained by the alloying elements. The errors for using the equations listed in table 4.6 for the low and high strain rate are 3.2 and 0.4°C respectively.

To test the accuracy of the formulated M_{d30} equations in table 4.5, a linear regression analysis between the calculated and observed M_{d30} values was performed. The results are shown in table 4.7 (see appendix III).

M_{d30} (°C)	LINEAR CORRELATION COEFFICIENT, R	R^2 (%)	STANDARD ERROR OF ESTIMATE (°C)
Low Strain Rate (19)	0.98	95.67	1.7
High Strain Rate (20)	0.99	99.83	0.2

Table 4.7: Linear regression analysis between calculated and observed M_{d30} values for equations in table 4.5 (equations 19 and 20).

The test statistics in table 4.7 indicate large R^2 values which in the low strain rate (19) case means that about 96% of the variation in the calculated M_{d30} values can be explained by the observed M_{d30} values. For the high strain rate (20) case 99.8% variation in the calculated M_{d30} values can be explained by the observed M_{d30} values.

2. M_{d30} Equations according to Elements considered in Nohara et al's Equation (equation 5)

For equations according to elements considered in Nohara et al's equation, Nb was excluded since some alloys did not contain Nb in their alloy compositions.

M_{d30} (°C)	Constant	C + N	Si	Mn	Cr	Ni + Cu	Mo	GSN - 8.0
Low Strain Rate (21)	889	-1382	-15.3	-70	-32	-13	+79.1	-15
High Strain Rate (22)	721	-384.4	+3	-12	-37	-5.3	+18	-1

( ) refers to equation number. GSN means grain size number (ASTM)

Table 4.8: Formulated equations according to the elements considered by Nohara et al [57].

The following test statistics were obtained for equations 21 and 22 in table 4.8.

M_{d30} (°C)	CORRELATION COEFFICIENT, R	R^2 (%)	STANDARD ERROR (°C)
Low Strain Rate (21)	0.99	99.92	0.6
High Strain Rate (22)	0.99	99.92	0.4

Table 4.9: Test statistics to evaluate the accuracy of equations 21 and 22 in table 4.8. The other test statistics are indicated in appendix II.

The large R^2 values in both cases implies that almost 100% of the variation in the M_{d30} values predicted by equations 21 and 22 can be explained by the elements considered in these equations. The standard errors associated with using equations 21 and 22 were found to be 0.6 and 0.4°C for low and high strain rates respectively.

Accuracy of these equations was further tested by performing a linear regression analysis between calculated and observed M_{d30} values and results are shown in table 4.10

M_{d30} (°C)	LINEAR CORRELATION COEFFICIENT, R	R^2 (%)	STANDARD ERROR OF ESTIMATE (°C)
Low Strain Rate (21)	0.99	99.96	0.2
High Strain Rate (22)	0.99	99.92	0.1

Table 4.10: Linear regression analysis between calculated and observed M_{d30} values for equations 21 and 22 in table 4.8.

The test statistics in table 4.10 show R^2 values of approximately 100%, which implies that almost 100% of variation in the calculated M_{d30} values can be explained by the experimentally determined M_{d30} values. The standard errors observed for equations 21 and 22 are 0.2 and 0.1°C respectively.

(c) Relationship between Observed M_{d30} values and Alloying Elements

To assess the effect of alloying elements on the M_{d30} temperature, graphs of M_{d30} versus alloying elements considered were obtained for both strain rates. Typical results are shown in Fig 4.10 and 4.11.

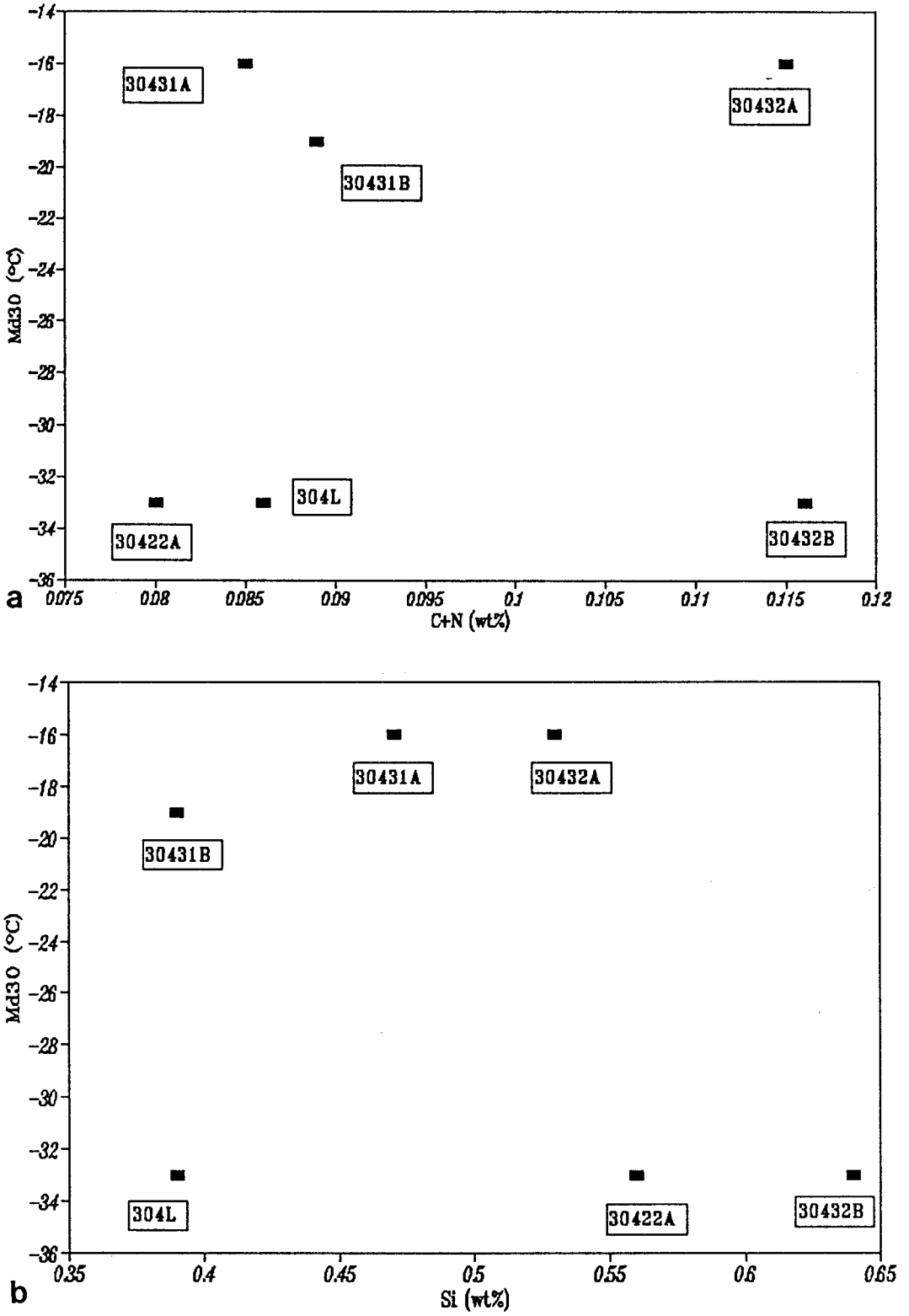

Fig 4.10: Effect of alloying elements on M_{d30} temperature at the low strain rate: (a) C+N, (b) Si

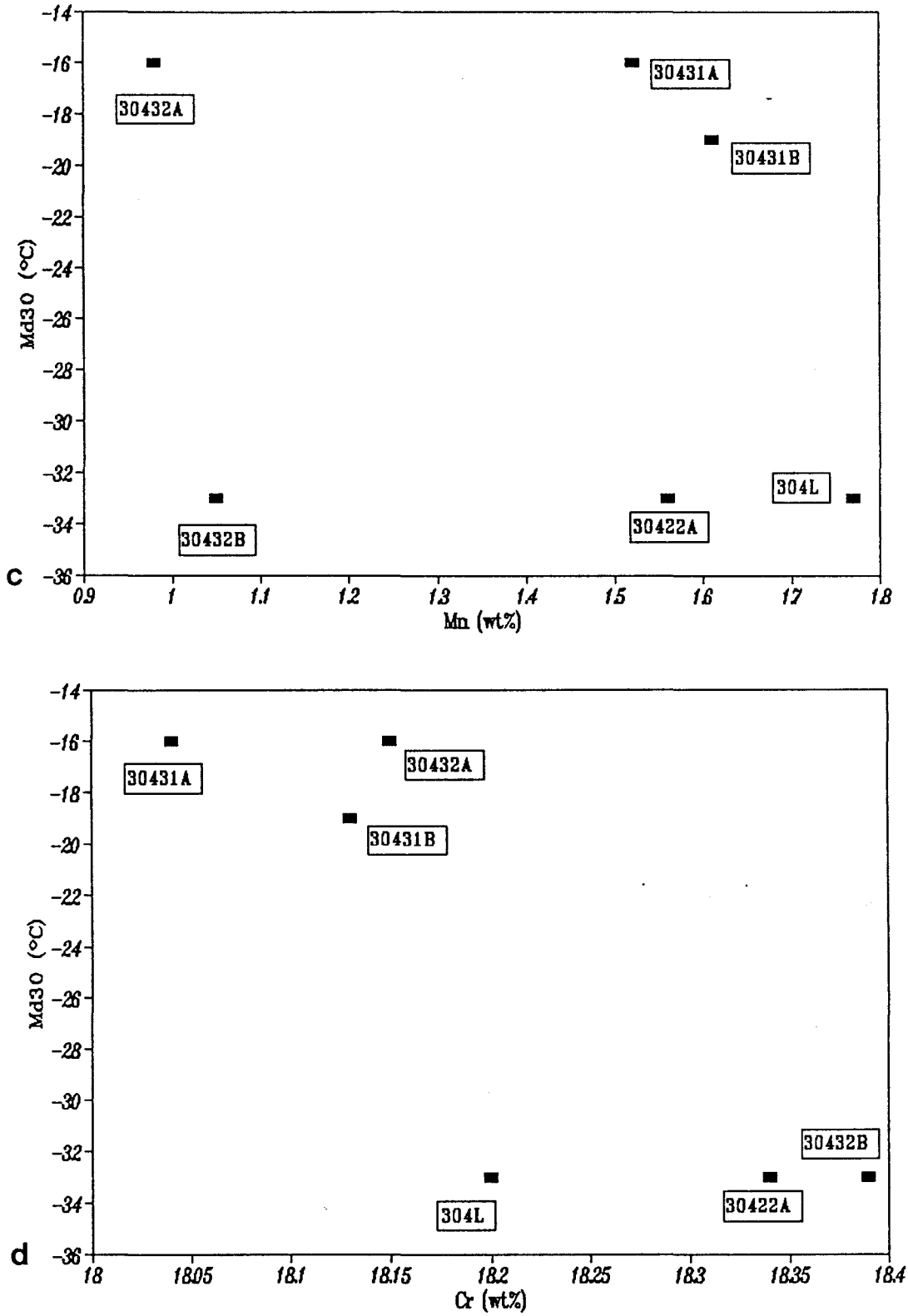

Fig 4.10: Effect of alloying elements on M_{d30} temperature at the low strain rate, (c) Mn, (d) Cr

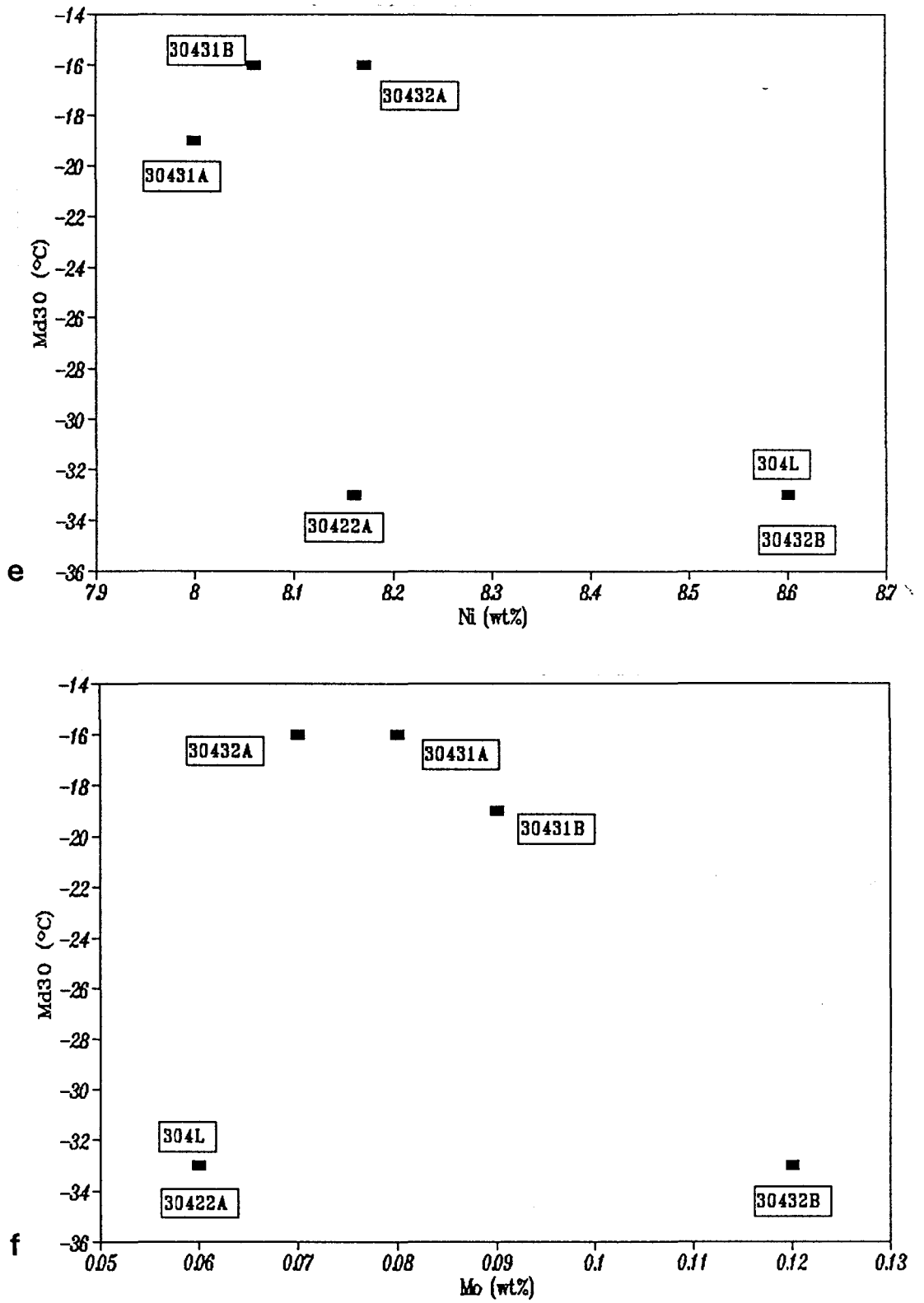

Fig 4.10: Effect of alloying elements on M_{d30} temperature at the low strain rate: (e) Ni and (f) Mo

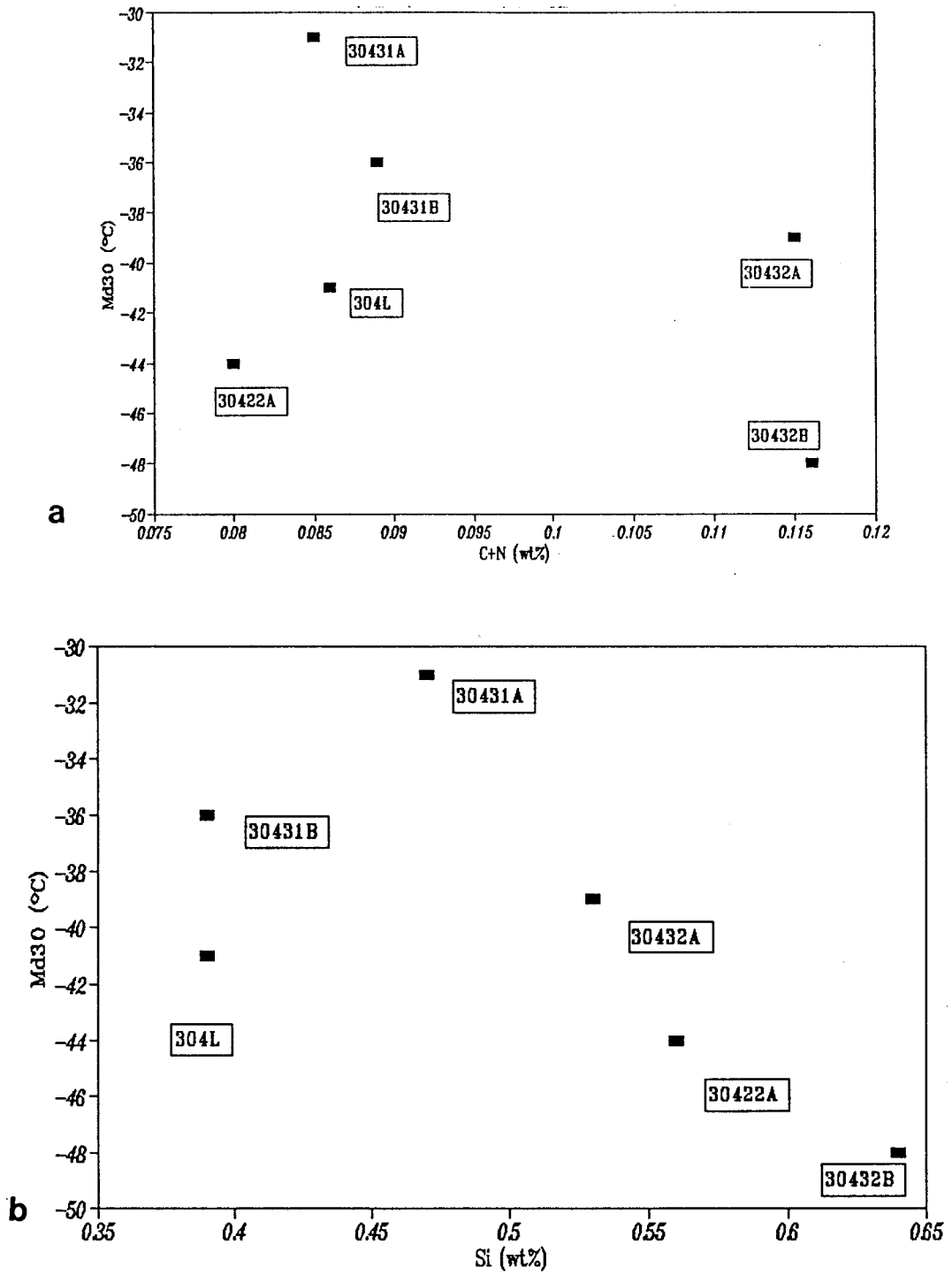

Fig 4.11: Effect of alloying elements on M_{d30} temperature at the high strain rate : (a) C+N, (b) Si

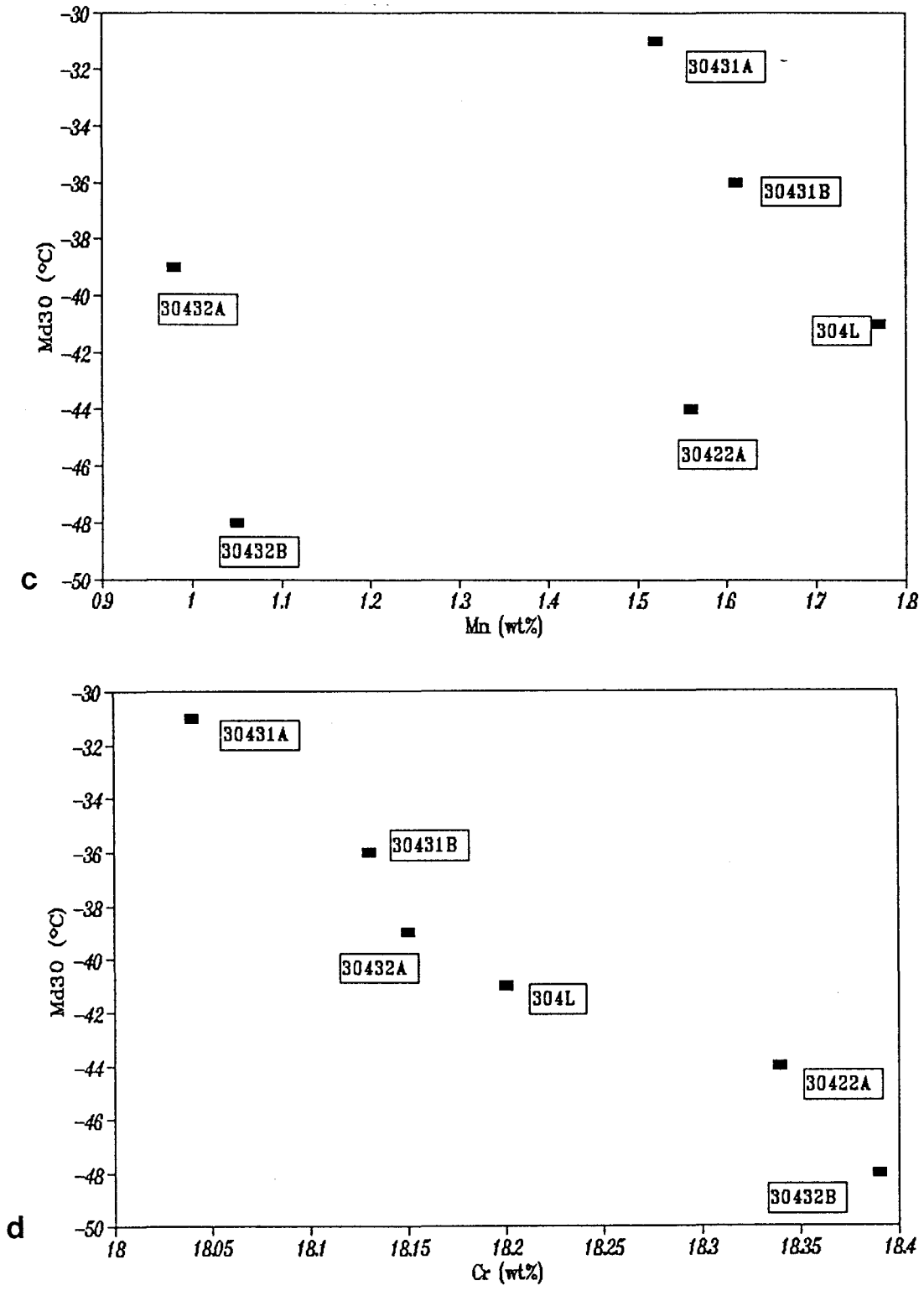

Fig 4.11: Effect of alloying elements on M_{d30} temperature at the high strain rate: (c) Mn, (d) Cr

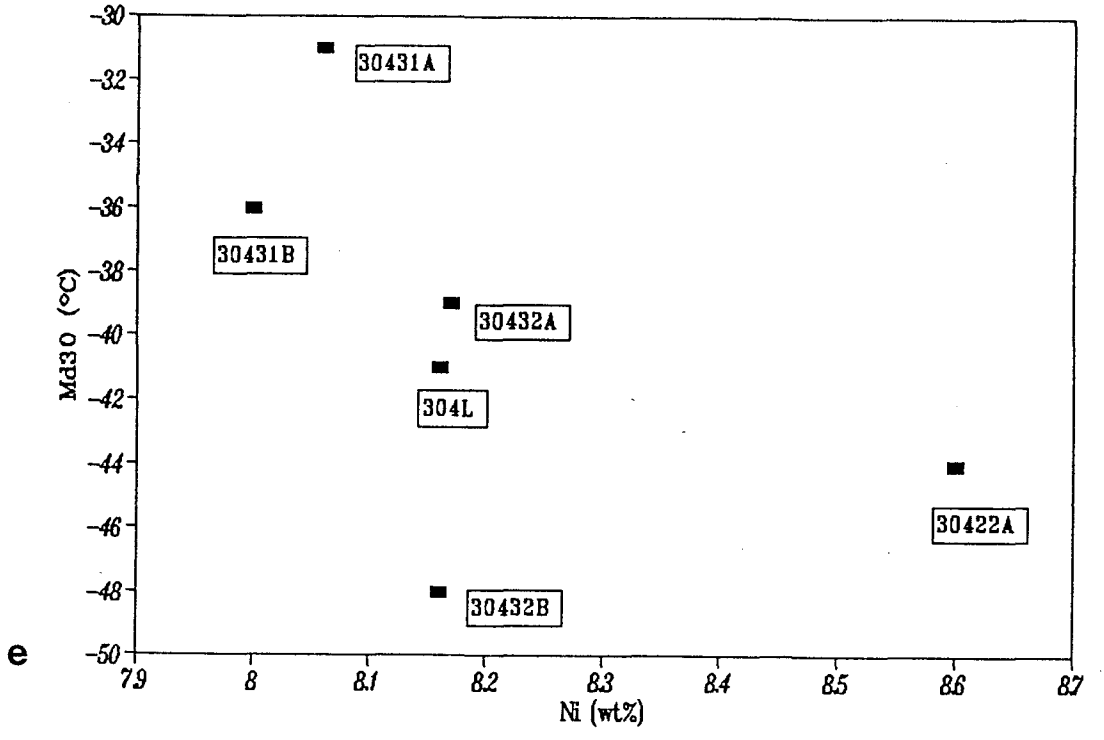

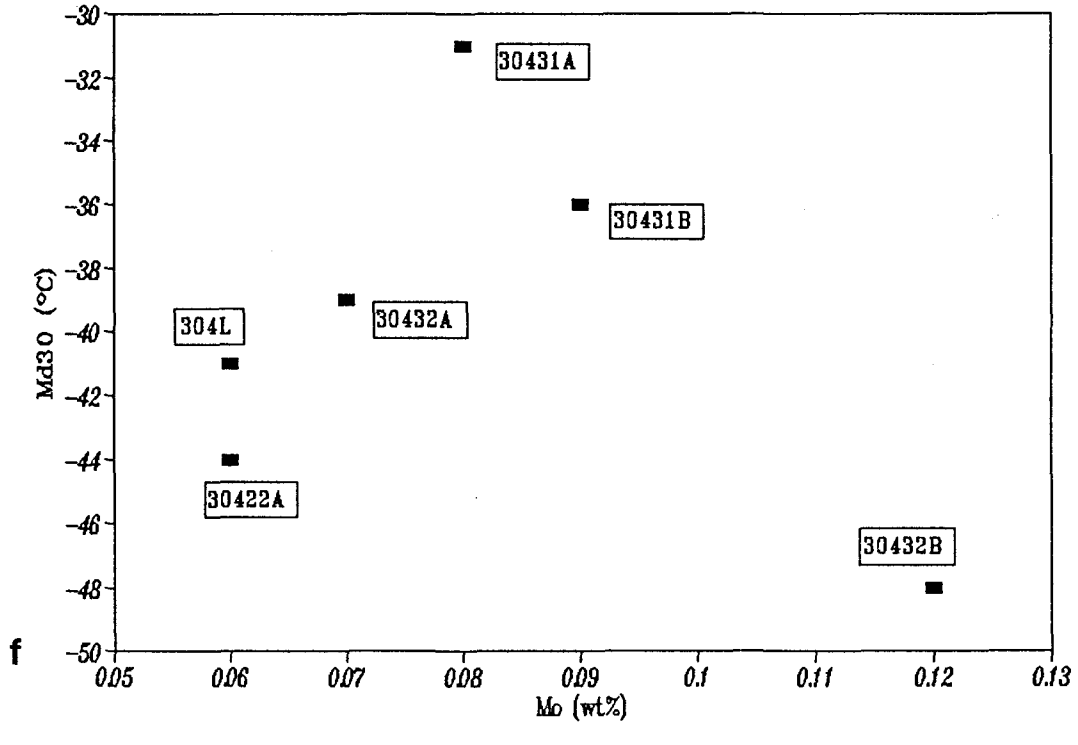

Fig 4.11: Effect of alloying elements on M_{d30} temperature at the high strain rate: (e) Ni and (f) Mo

For the low strain rate results, only the relationships of M_{d30} versus Cr demonstrate a discernible trend. For this element, the general trend is that lower compositions are associated with higher M_{d30} temperatures (alloys 30431A, 30431B and 30432A). The relationship of M_{d30} versus Si, although doubtful indicates that higher M_{d30} temperatures (alloys 30431A, 30431B and 30432B) are also associated with lower Si compositions. The only exception is 304L, which showed a low M_{d30} temperature at a low Si composition. Alloys 30431A and 30431B showed similar behaviour for all the elements. This behaviour compares well with their comparable M_{d30} temperatures (-16 and -19°C respectively). Alloys 30432A and 30432B behaved differently. Alloy 30432A which showed a lower M_{d30} temperature (-16°C compared to -33°C for alloy 30432B) is associated with lower compositions for all elements except for C+N and Ni where compositions are comparable.

For high strain rate tests, only the relationship of M_{d30} versus Cr showed a clear behavioural trend. The M_{d30} temperatures decreased with increasing Cr content. The relationship of M_{d30} versus Si was not clearly explained as a result of alloy 304L, which showed low M_{d30} value at low Si composition. But there is a better trend observed for Si at the high strain rate than at the low strain rate. Except for alloy 304L, generally M_{d30} gradually decreases with increasing Si content. As with the low strain rate case, alloys 30431A and 30431B showed comparable behaviour with respect to all elements. This similar trend again compares well with their M_{d30} temperatures (-31 and -36°C respectively). For alloys 30432A and 30432B, a higher M_{d30} temperature was observed for alloy 30432A compared to alloy 30432B (-39 and -48°C respectively).

4.3 Alloy Stability on Refrigeration

All alloys were found to be magnetic after quenching from 900, 950 and 1050°C, into liquid nitrogen at -196°C. The specimens were then mechanically polished and subsequently electropolished to remove any martensite which might have formed as a result of quenching strains or mechanical polishing. The specimens were again tested for

magnetism using a hand magnet. Most of the alloys indicated no magnetism except alloys 30431A and 30431B quenched from 900°C which showed some slight magnetism. These specimens were electropolished and prepared for X-ray diffraction; and the traces obtained are shown in fig 4.12. It is clear from the XRD traces that no $\gamma \rightarrow \alpha'$ transformation occurred. It was concluded that the slight magnetism observed was probably due to inadequate initial electropolishing after quenching to -196°C. However, it is not clear whether the magnetism is due to quenching to 23°C or after quenching to -196°C. To explain this, specimens were quickly tested for magnetism after quenching to 23°C and were all found to be magnetic. This implies that the magnetism observed after quenching to -196°C is not due to spontaneous $\gamma \rightarrow \alpha'$ transformation. The transformation is probably due to some deformation on the surface of the specimens as a result of quenching strains when specimens were quenched from the solution treatment temperatures to 23°C. Hence, it can be concluded that the Ms temperatures of these alloys are well below -196°C.

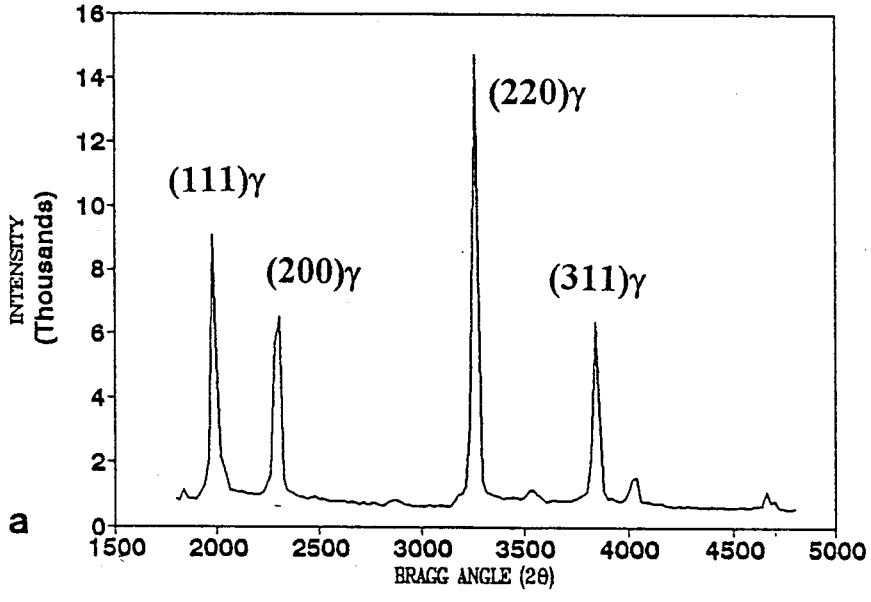

Fig 4.12: X-ray trace for alloy (a) 30431A at the solution temperature of 900°C.

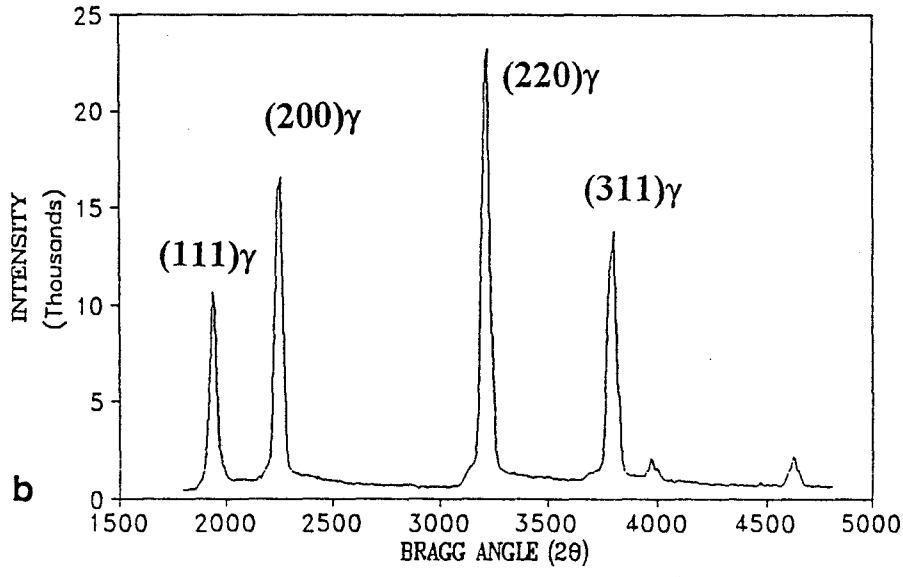

Fig 4.12: X-ray trace for alloy (b) 30431B at the solution temperature of 900°C.

5 DISCUSSION

5.1 Temperature and Strain Rate Influence Towards Martensite Formation

5.1.1 Martensite Transformation during Deformation

The present investigation has shown that where transformation is possible, $\gamma \rightarrow \alpha'$ transformation increases with increasing strain. On comparison of tests carried out at 0°C and -40°C, it was found that transformation at -40°C started at lower strains ($\approx$ 0.075 true strain) compared to transformation at 0°C which started at higher strains ($\approx$ 0.2 true strain). Furthermore at a particular strain, tests at -40°C formed large amounts of martensite as compared to tests conducted at 0°C. These observations are consistent with the findings of various investigators [12,17,70] who found that during plastic deformation the quantity of martensite increases as the strain is increased, and as the temperature of straining is lowered. The start of martensite transformation was also found to be a function of temperature and level of strain. Fiedler et al [70] reported that generally, at a particular temperature, transformation does not start until a certain value of strain has been obtained. In addition, this value of strain is generally higher, the higher the temperature.

The addition of alloying elements in table 3.1 (in section 3.1) showed that alloy 30431A, 30432A and 30431B have compositional sums (total alloy elements) of approximately 28 wt% (28.3, 28.1 and 28.3 wt% respectively). Alloys 30422A, 304L and 30432B showed compositional sums of approximately 29 wt% (29.2, 28.6 and 28.5 wt% respectively). Barclay and Williams et al [17,30] remarked that martensite transformation is also a criterion of austenite stability. They indicated that a less stable alloy (less highly alloyed) undergoes transformation sooner, and has more martensite at a given strain than a more stable alloy (highly alloyed). It is thus expected that less highly alloyed steels (28 wt%)

will generally show higher amounts of martensite than the more highly alloyed steels (29 wt%).

This appears to be the case at 0°C, except for alloy 304L which gave a similar amount of martensite to alloy 30431A at 0.3 true strain (fig 4.5(a)). X-ray diffraction results also indicated comparable volume fractions of martensite of 32% for alloy 30431A and 31% for alloy 304L. This suggests that at this temperature, the rates of martensite formation are similar for these alloys. At -40°C, alloy 30422A indicated a higher amount of martensite than alloy 30431B at 0.3 true strain (fig 4.5(b)). This increase in martensite content for alloy 30422A is dubious since X-ray diffraction results actually gave a lower amount of martensite (52% for alloy 30422A and 68% for alloy 30431B) at 0.3 true strain. This low martensite value for 30431B is probably due to an error associated with voltage recording during straining at -40°C.

The difference in the amount of martensite at 0.3 for this set of alloys can be explained by considering relative potencies of C, Mn, Ni, Cr and N_2 in restricting strain-induced transformation. Addition of these elements tend to stabilise the austenite against transformation. Ludwigson et al [32] reported the relative potencies of these five elements as follows:

ELEMENT	POTENCY
C	21.6
Mn	0.683
Ni	1.0
Cr	0.515
N_2	17.1

Table 5.1: Relative potencies of different alloying elements in restricting strain-induced formation of martensite. (After Ref 32)

On comparing alloy 30432A and alloy 30432B, both alloys have similar amounts of C and Ni, (0.0623 and 0.056% C and 8.17 and 8.16% Ni respectively). However, alloy 30432B consists of higher amounts of N_2 ,Cr and Mn (0.06, 18.39 and 1.05 respectively) as compared to (0.042, 18.15 and 0.98 respectively) for alloy 30432A. Hence, since alloy 30432B contains higher amounts of N_2, Cr and Mn, strain-induced martensite transformation will be more suppressed for this alloy compared to alloy 30432A.

Alloys 30431A and 30431B, both contained similar amounts of Ni (8.06 and 8%Ni respectively). However, alloy 30431B contained higher amounts of C, Mn, Cr and N_2 (0.047, 1.61, 18.13 and 0.0527 wt% respectively), whereas alloy 30431A contained lower composition (0.044, 1.52, 18.04 and 0.041 wt% respectively). Hence, alloy 30431B is expected to be less transformable than alloy 30431A on plastic deformation.

5.1.2 Martensite Transformation as a Function of Temperature

The variation in the rate of martensite formation as a function of temperature during deformation has been well documented by various authors [12,13,28]. In this study, the results (figs 4.3 and 4.7) indicated that generally at a particular temperature, high strain rate tests give decreased amounts of martensite compared to low strain rate tests. These observations accord well with the findings of Bressanelli et al [53] (fig 2.11) and Livitsanos et al [5] (fig 2.10) where decreased amounts of martensite were observed at high strain rates despite the fact that tests were performed under isothermal testing conditions. The conclusion arrived at [53] was that at the lowest temperature, the large amount of heat generated by the martensite reaction was not as thoroughly removed from the specimens strained at the high strain rate as from those at the slow strain rate.

Various investigators [5,12,13] have reported that there is a critical temperature range on the % martensite versus temperature curves, in which there is rapid increase in the amount of martensite. By measuring the slopes of the %martensite versus temperature curves, Rosen et al [13] showed that this narrow critical temperature range coincide with the

peaks on the (-dM/dT) versus temperature curves which represent the regions where martensite formation is highly temperature sensitive. Schematically, the above discussion can be represented as follows:

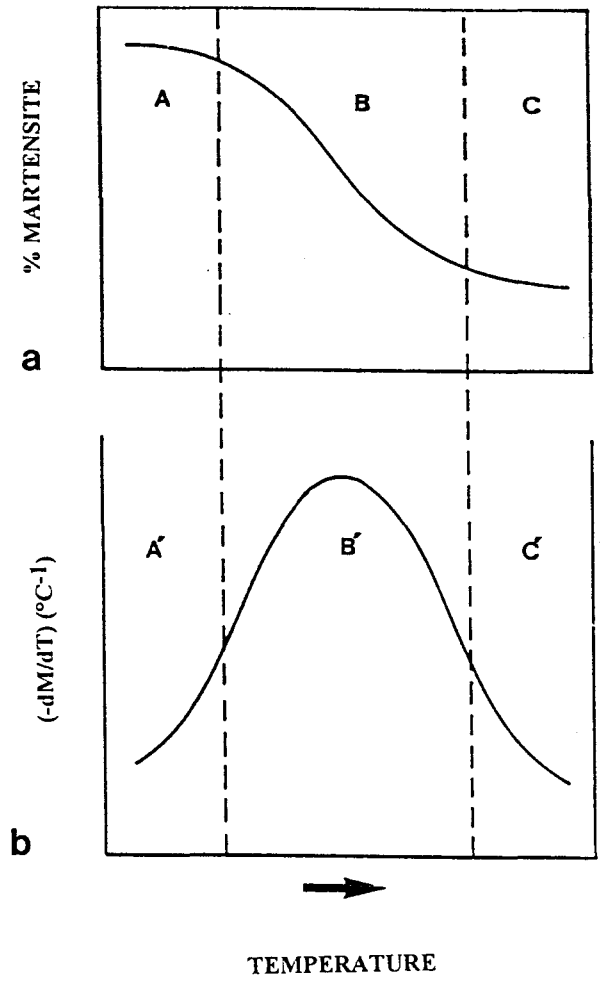

Fig 5.1: Schematic representation of various areas of temperature sensitivity of martensite transformation at a particular value of true strain: (a) and (b) show curves of % martensite and (-dM/dT) with respect to test temperature.

Livitsanos et al [5] further indicated that this critical temperature range is dependent on strain rate. The strain rate dependence of this critical temperature range was clearly explained by Rosen et al's [13] results which indicated that a change in strain rate causes a

shift of %martensite versus temperature curves along the temperature axis. This implies a subsequent shift of the peaks of the (-dM/dT) curves along the temperature axis. This shift of the peaks can be schematically represented as follows:

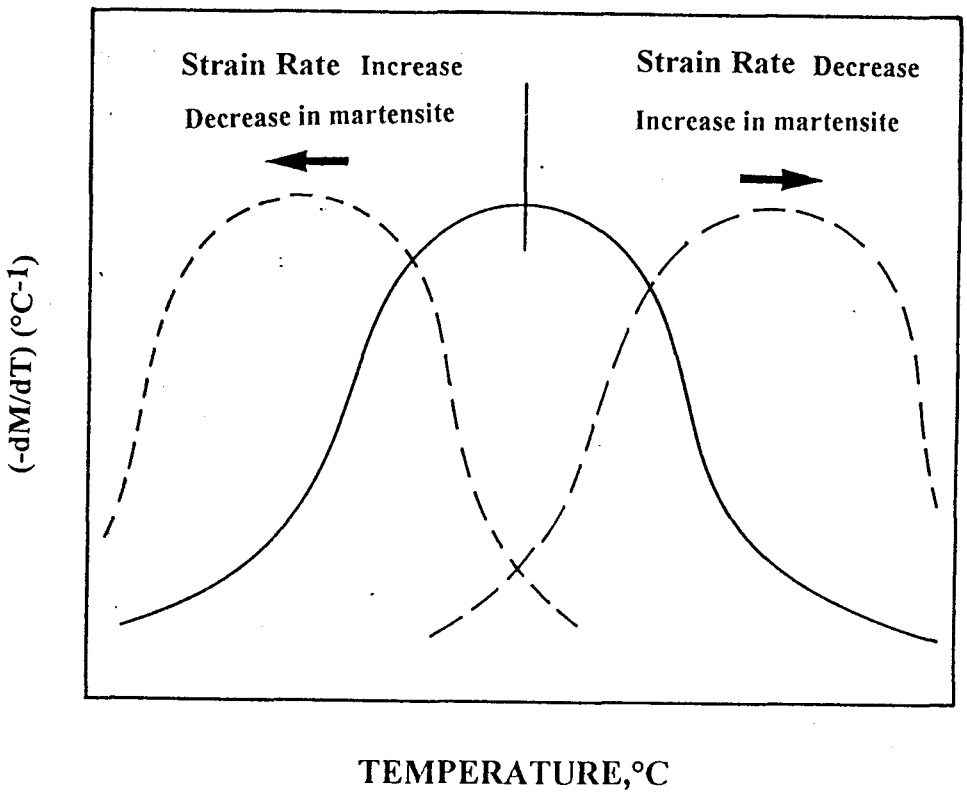

Fig 5.2: The shifting of (-dM/dT) versus temperature curves due to variations in martensite content on the %martensite versus temperature curves. For this study at the high strain rate curves shifted to the left whereas at the low strain rate curves shifted to the right.

Furthermore, Fukase et al [39] reasoned that in such a temperature range (i.e. critical temperature range) that $\gamma \rightarrow \alpha'$ transformation is clearly temperature dependent, the influence of test speed is considered to be most pronounced. In this study, the propensity of alloys to form martensite was more pronounced at the temperature range of approximately -40 to 0°C, as shown by high (-dM/dT) values at the low strain rate ($10^{-3}s^{-1}$) (fig 4.8(a)). This temperature range will coincide with regions B and B' in fig 5.1. The

present investigation indicated that in this region, the effect of strain rate was significant. Closer examination of fig 4.9(a) and (b) (also see appendix IV) showed that the difference in martensite content between the two strain rates was greatest at the temperatures coinciding with the peaks at the low strain rate. For most alloys, the high strain rate curves shifted towards lower temperatures, which as already remarked above, is a further indication that less amount of martensite was formed at the high strain rate (see schematic representation in fig 5.2). The only exceptions were alloy 30422A and 30431A in which high strain rate curves did not indicate clear shifts towards lower temperatures. But of interest is that these alloys at a particular temperature, indicated lower (-dM/dT) values at the high strain rate, which implies less formation of martensite.

The high temperature sensitivity of transformation at the temperature range of -40 to 0°C (which corresponds to high (-dM/dT) values at the low strain rate (fig 4.6(b)), compares well with the pronounced voltage differences between the two strain rates (fig 4.3 (a) to (f)) It can thus be inferred that at this temperature range, adiabatic heating as a result of high strain rate will greatly affect $\gamma \rightarrow \alpha'$ transformation resulting in reduced amounts of martensite.

For tests performed at 23°C, the effect of strain rate was not adequately explained as martensite contents between the two strain rates was not consistent; and even where martensite contents varied, the difference was no more than 2%. On close examination of the (-dM/dT) curves at the low strain rate, low (-dM/dT) values are evident at 23°C which means that transformation is less sensitive to temperature. This temperature (23°C) lies in the regions C and C' in fig 5.1. It can therefore be concluded that an increase in temperature due to adiabatic heating at high strain rate, did not significantly affect the extent of transformation due to low temperature sensitivity of transformation at this temperature. Similarly, at low temperatures ($\approx$-60°C) which coincide with regions A and A' in fig 5.1, voltage differences (martensite content) between the two strain rates were minimal (fig 4.3(a), (e) and (f)). This provides further evidence that due to low temperature sensitivity of martensite formation at low temperatures, adiabatic heating due to high strain rate will not result in large martensite content variations.

It can thus be concluded that strain rate will have a large effect on transformation at those temperatures where transformation is highly sensitive to temperature (regions B and B' in fig 5.1). Martensite transformation will be virtually strain rate independent at regions of low temperature sensitivity (above 23°C and below -60°C), which coincide with regions A, A', C and C' in fig 5.1. The strain rate dependence of transformation at various temperatures was also noted by Livitsanos et al [5] on tests performed on a Type 301 stainless steel (fig 2.10). They reported that at very low test temperatures (i.e. 40°C), transformation is relatively independent of strain rate. For a Type 304 stainless steel however, the temperature at which transformation will be independent of strain rate, would certainly be much lower than 40°C given that Type 304 stainless steels (highly alloyed) are more stable than Type 301 stainless steels (less highly alloyed) [5].

5.2 The Effect of Strain Rate on The M_{d30} Temperature

Angel [12] reported that within a narrow temperature range on the %martensite versus temperature curves (corresponding to regions B and B' in fig 5.1), a radical change in austenite stability is observed. In this range a characteristic temperature, M_{d30} , was chosen as a measure of austenite stability. Hence according to the present results, the M_{d30} temperature will be greatly affected by changes in strain rate. This is clearly illustrated by the experimental M_{d30} results observed in this study as shown in table 5.2.

ALLOY	M_{d30} (°C) (Low Strain Rate)	M_{d30} (°C) (High Strain Rate)	$\|\Delta T\|$(°C)
30422A	-33	-44	11
30431A	-16	-31	15
30432A	-16	-39	23
30431B	-19	-36	17
304L	-33	-41	11
30432B	-33	-48	15

$|\Delta T|$ is the M_{d30} temperature difference between the low strain rate and high strain rate.

Table 5.2: The M_{d30} temperatures for experimental alloys at the low and high strain rates with associated differences for each alloy.

The M_{d30} temperatures for alloys 30431A, 30432B and 30431B (-16,-16 and -19°C respectively) corresponded to regions where (-dM/dT) values at the low strain rate were still quite high (fig 4.8 (a) (the extrapolated values for (-dM/dT) are approximately 1, 0.8 and 0.84 ($°C^{-1}$) for alloy 30432A, 30431B and 30431A respectively)). These high temperature sensitivities suggest that adiabatic heating due to high strain rate will produce large decreases in the amount of martensite which will subsequently result in large decreases in the M_{d30} temperature at the high strain rate. This seemed to be the case, especially for alloy 30432A which showed quite a high sensitivity. The reduction in the M_{d30} temperature for this alloy was found to be 23°C. Alloys 30431A and 30431B which had lower sensitivities compared to alloy 30432A, showed much lower M_{d30} temperature reductions of 15 and 17°C respectively when comparing the two strain rates.

Alloys 30422A, 304L and 30432B indicated extrapolated (-dM/dT) values of approximately 0.75, 0.7 and 0.58 respectively at -33°C at the low strain rate. This was accompanied by much lower $|\Delta T|$ values between the low and high strain rates for alloys 30422A and 304L (11°C). The only exception is alloy 30432B which showed a higher $|\Delta T|$ value of 15°C. But it is interesting to note that alloys 30422A and 304L which showed comparable (-dM/dT) values indicated similar $|\Delta T|$ values. It can be concluded that since temperature sensitivity of martensite formation is low at this temperature

(-33°C) adiabatic heating due to high strain rate will not result in large reductions in martensite content and hence M_{d30} temperatures.

5.3 The Effect of Alloy Chemistry on the M_{d30} Temperature

5.3.1 Qualitative Effect of Alloy Chemistry on the M_{d30} Temperature

Alloy composition affects the M_{d30} temperature by influencing martensite reaction. Increasing the alloy content of the steel (highly alloyed) will result in the formation of less martensite than alloys with lower alloy content [53]. This observation has been previously noted by Angel [12] and Williams et al [30] who both investigated the transformation behaviour of various austenitic stainless steels (fig 2.13). Less highly alloyed steels form martensite at a high rate and are expected to have higher M_{d30} temperatures as indicated in fig 5.3.

In this investigation at the low strain rate, alloys 30431A, 30432A and 30431B which are less highly alloyed (compositional sum of approximately 28) showed higher M_{d30} values (-16 to -19°C) as compared to more highly alloyed steels (30422A, 304L and 30432B with compositional sum of approximately 29) which showed very low M_{d30} temperatures (-33°C). This relationship was also observed for the high strain rate M_{d30} values although with not as much clarity as in the low strain rate case. The above analysis only provides a qualitative effect of chemical composition on austenite stability and hence the M_{d30} temperature. To obtain quantitative data on the specific influence of the alloying elements on the M_{d30} temperature, statistical analysis is used.

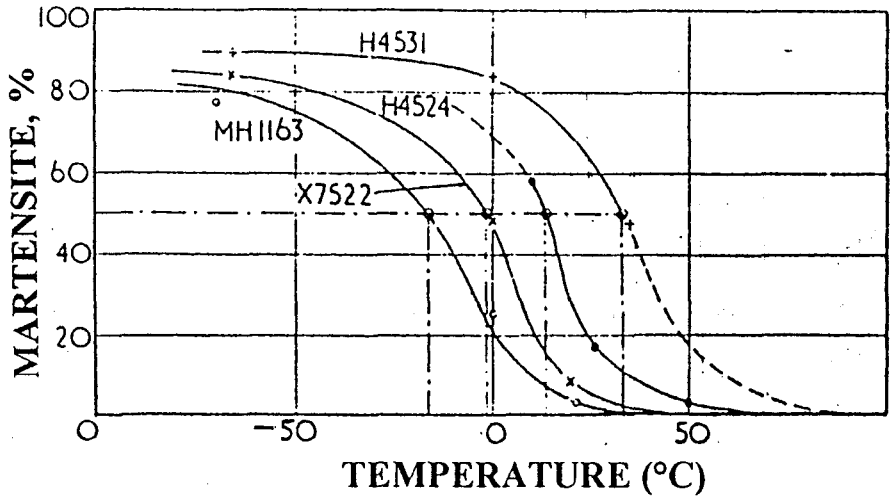

HEAT	C	N_2	Si	Mn	Cr	Ni	Mo	M_{d30} (°C) exp	M_{d30} (°C) calc
H 4531	0.06	0.02	0.39	0.33	18.4	8.6	0.06	34	33
MH 1163	0.12	0.01	0.81	0.95	19.2	8.4	0.07	-15	-8

Fig 5.3: Transformation/temperature curves at a true strain of 0.30 plastic strain, showing the less highly alloyed steel with the lowest M_{d30} temperature. The M_{d30} temperatures shown are calculated (calc) and experimental (exp). (After Ref 12)

5.3.2 Quantitative Effect of Alloy Chemistry on the M_{d30} temperature

The effect of elements in a statistical equation is deduced by comparing the coefficients associated with them. A statistical analysis made on the data for equation 19 (low strain rate case) shows that Mn was the only significant element affecting this M_{d30} equation (p-value = 0.03). For equation 20 (high strain rate case) all elements were significant except Mo. The results for equation 19 compares to some degree with Angel's [12] findings who also found his equation to be significant for Mn and insignificant for Mo, Si and Ni. It is also important to note that the coefficient of Cr in equation 19 although insignificant, has less probability of occurring by chance (p-value = 0.08) compared to the

other insignificant elements (C+N, Si, Ni and Mo showed p-values of 0.14, 0.62, 0.18 and 0.49 respectively). The only similarity between Angel's equation (equation 3) and equation 20 (high strain rate) is that both are insignificant for Mo. Of noteworthy mention is that Angel's equation was formulated at the low strain rate ($10^{-4}s^{-1}$) which possibly explains the close similarity of the significance of various elements considered for equation 19. For equation 21, in which elements were fitted in the same order as Nohara's equation (equation 5), statistical analysis showed that C + N, Mn and Cr are the only significant elements affecting the M_{d30} temperature (p-values are 0.05, 0.04 and 0.05 respectively). For equation 22, Cr (p-value is equal to 0.03) is the only significant elements affecting the equation. The significance of Cr, Mn and C + N for equation 21 and Cr for equation 22, compares well with those found by Angel [12].

The significance of Cr in equations 20, 21 and 22 corroborates the results obtained in fig 4.10(d) and 4.11(d). It was found that for both low and high strain rate cases, the relationship between M_{d30} versus Cr showed a clear trend where M_{d30} temperatures decreased with corresponding increase in Cr. The significance of other alloying elements, as already remarked by Angel [12], can be obtained by extending the range of experimental work. The statistical equations (19, 20, 21 and 22) for this study, were formulated from only 9 alloys of similar composition, as compared to Angel [12] and Williams et al [30] who based their investigations on 11 and 25 alloys respectively. The very small range of compositions considered implies that the formulated equations will give accurate calculated M_{d30} temperatures only for alloys with compositions comparable to the 9 alloys considered in this investigation. This was noted by Lenel et al [11] who concluded that empirical equations, such as the M_{d30} are generally valid for the composition range for which they were derived. To test the validity of the preceding statement, two alloys used by Angel (alloys H4531 and MH1163 in fig 5.3) were considered. Alloy H4531 closely resembled the chemical compositions of experimental alloys used for this study whereas alloy MH1163 had a very different compositional content. The M_{d30} temperatures as calculated from equation 19 (low strain rate) was compared with the M_{d30} temperature reported by Angel [12] and are shown in table 5.3.

ALLOY	M_{d30} (°C)		
	EXPERIMENTAL	CALCULATED	EQUATION 19
H4531	34	33	23
MH1163	-15	-8	-71

Table 5.3: Comparison of M_{d30} temperatures from Angel [12] and formulated equation (equation 19).

It is clear that equation 19 gives a reasonable approximation of the M_{d30} temperature value reported by Angel [12] for alloy H4531 and a very inaccurate M_{d30} temperature value for alloy MH1163. Of noteworthy mention is that equation 19 gives a better M_{d30} temperature approximation for alloy H4531 compared to Angel's equation (equation 3) which gives very inaccurate M_{d30} values for the range of alloys used in this study (see table 3.6). This high discrepancy could be accounted for by the fact that only one alloy (H4531) in the alloy range considered by Angel [12] had comparable composition to the alloy range used in this study. It can thus be concluded that the formulated equations (equations 19 to 22) including equations by other authors [12,52,57] will give accurate M_{d30} temperature approximations for alloys covered by the alloy range for which they were derived. Therefore the formulated M_{d30} relationships (equations 19 to 22) are valid for the following composition limits indicated in table 5.4:

ELEMENT	COMPOSITIONAL LIMIT (%)
Cr	18.04 to 18.39
Ni	8.00 to 8.67
Si	0.33 to 0.64
C	0.025 to 0.063
N_2	0.041 to 0.06
Mn	0.98 to 1.89
Mo	0.05 to 0.09
Cu	0.08 to 0.13

Table 5.4: Compositional limits for accurate M_{d30} temperature calculations from formulated equations (equations 19 to 22).

5.3.3 Austenite Stabilising Effect of Elements in the M_{d30} Equations

For ease of comparison of the formulated equations with the existing equations, all the equations are presented in a tabular form in tables 5.5 and 5.6 below.

M_{d30} Equation Number	Constant	C + N	Si	Mn	Cr	Ni	Mo
3 (Angel)	497	-462	-9.2	-8.1	-13.7	-20	-18.5
4 (Pick)	413	-462	-9.2	-8.1	-13.7	-9.5	-18.5
19 (Low Strain Rate)	883	-728	-14	-47	-33	-20	-63
22 (High Strain Rate)	717.5	-308	+4.1	-10.1	-36.5	-6.3	+9.3

Table 5.5: Comparison of M_{d30} empirical equations by Angel [12] and Pickering [52] with formulated M_{d30} equations (19 and 20).

M_{d30} Equation Number	Constant	C + N	Si	Mn	Cr	Ni + Cu	Mo	GSN - 8
5 (Nohara)	551	-462	-9.2	-8.1	-13.7	-29	-18.5	-1.4
21 (Low Strain Rate)	889	-1382	-15.3	-70	-32	-13	+79.1	-15
22 (High Strain Rate)	721	-384.4	+3	-12	-37	-5.3	+18	-1

Table 5.6: Comparison of Nohara et al's M_{d30} empirical equation with the formulated M_{d30} equations (21 and 22).

Most alloying elements in tables 5.5 and 5.6 stabilise the austenite with regard to martensite transformation. The only exceptions are Mo in equations 20, 21 and 22, and Si in equation 22 which indicated a destabilising effect. The destabilising effect of Mo has not been reported in literature unlike Si which was found to have a destabilising effect by Williams et al [30] as indicated in table 2.4 in section 2.3.3. However, no significance can be attached to the destabilising effects of these alloying elements in this study. The reason is that, except for Si in equation 20 (p-value = 0.02), all the coefficients for these two elements were insignificant in the formulated equations (see appendix III). This means that the observed effects are not due to assignable causes but to chance [69]. For all the formulated equations, (C+N) has the greatest stabilising effect of all the elements considered, as indicated by the most negative coefficient associated with it. This effect is also evidenced in the pre-existing M_{d30} relationships (equations 3, 4 and 5 in section 2.3.3).

The coefficients of the formulated equations are significantly different from those appearing in equations 3, 4 and 5. Williams et al [30] explained the rapid change in coefficients by plotting the variation of the Md regression coefficients (table 2.3) with strain at a constant martensite level, and martensite content at a constant strain (fig 2.14). From these plots they reached the conclusion that coefficients of the equations change very rapidly at both low and high martensite extremes, moving in both cases roughly towards the coefficients of the Ms equation (equation 1 in section 2.3.3). They regarded the M_{d30} temperature to have too high a martensite level (50%) and therefore it can be inferred that coefficients of the M_{d30} equations are expected to vary rapidly with small changes in parameters such as composition and strain rate. This probably explains the vast variation of coefficients as strain rate is varied. For example, the coefficients in equation 19 are significantly different from those obtained in equation 20. A similar observation is also noted for equations 21 and 22. Interestingly, the coefficients of equations 19 and 21 (low strain rate equations) showed comparable values for the constant, Si and Cr. For equations 20 and 22 (high strain rate equations) similar coefficient values for the constant value, Si, Mn and Cr were observed.

5.4 Assessment of the Accuracy of the Formulated M_{d30} Equations

A multiple regression analysis deals with the estimation of a random variable, the M_{d30} temperature in this case, from several variables, which are the alloying elements for this study. The accuracy of a multiple regression equation is evaluated by considering the size of the square of the multiple correlation coefficient R^2, and the standard error of estimate. All the formulated equations showed large R^2 values, which indicates that there is a significant relationship between the M_{d30} temperature and the linear combination of the alloying elements. However, equation 19 showed a "moderately strong" relationship between the M_{d30} temperature and the alloying elements. This is indicated by the standard error of estimate of 3°C.

A further test of accuracy is performed by carrying out a linear regression analysis between the observed values and the calculated values. The calculated and the observed M_{d30} values for all formulated equations are shown in appendix III. As with the multiple regression case, a good relationship between the two sets of values is evaluated by using the linear correlation coefficient R^2, and the standard error of estimate. All the equations indicated a very strong linear relationship between the calculated and the predicted values. The R^2 values for equations 20, 21 and 22, indicated that almost 100% of the variance in the calculated M_{d30} values can be accounted for by the linear combination of the compositions of the alloying elements; and in addition, the standard error of estimate was not more than 0.2°C for all equations. However, for equation 19, a "less strong" relationship between the calculated and observed values occurred which is indicated by an R^2 value of about 96% (i.e. about 96% of the variance in the calculated M_{d30} values can be accounted for by the linear combination of the alloying elements compositions) with a standard error of estimate of about 2°C.

The practical implication of the accuracy analysis above is that, these equations will give accurate M_{d30} temperature predictions, for alloy compositions within the range of the

alloys considered for this study. This high sensitivity to alloy composition was clearly illustrated by the M_{d30} calculations carried out on two steels considered by Angel for his equation (see table 5.3). Of noteworthy mention is that a better linear relationship between the observed and calculated M_{d30} values was achieved for the equations determined in this study (errors between calculated and observed M_{d30} values for equations 19, 20, 21 and 22 were found to be 1.7, 0.2, 0.2 and 0.1°C respectively), as compared to Angel's equation which showed a standard deviation of ± 8°C between calculated and observed values [12].

5.5 Austenite Stability on Spontaneous Transformation to Martensite

The solution treatment temperature can be used to control the amount of carbide which is taken into solution, and hence control the effective matrix composition, both with regard to the content of carbon and other alloying elements [52]. As already indicated in fig 2.18, lower solution treatment temperatures raises the Ms temperatures. The fact that all the experimental alloys resisted transformation even at the lowest solution treatment temperature of 900°C, means that these alloys are highly stable. This high austenite stability with respect to spontaneous martensite transformation, is supported by results of previous investigators [68], who reported an Ms temperature of approximately -250°C for a Type 304 stainless steel (10.6% Ni, 18.1% Cr and 0.055% C).

However, Lenel et al's [11] assertion that Ms and Md usually differ by about 100 to 200°C is questionable. If this was true, some transformation would have been noticed even for alloys solution treated at 1050°C, based on Ms predictions as calculated from equations 1 and 2 (table 3.7). The Md of these alloys was noted to be around 40°C which according to Lenel et al [11], approximates the Ms temperature to about -160°C which is well above the liquid nitrogen temperature. Consequently, for alloys solution treated at 900°C a high content of spontaneously transformed martensite is expected as was indicated in section 2.6. The experimental alloys were quenched from the solution

treatment temperatures (900, 950 and 1050°C) into water at 23°C before quenching to -196°C. All the specimens were magnetic upon rapid quenching to 23°C which indicates some degree of deformation-induced martensite formation. It was however found that after mechanical polishing and electropolishing procedures this magnetism disappeared. This indicates that martensite was formed at the specimen surface while the remainder of the specimen is still austenite. Fahr [26] highlighted that austenite of a given composition is further stabilised by thermal treatments. Large amounts of deformation of the austenite increase its dislocation density and thus make the co-operative movement of atoms during formation of martensite more difficult. Moreover, the volume of the martensite is larger than that of the austenite from which it forms. This volume increase must be accommodated by the generation and motion of dislocations in the austenite. A high dislocation density in the austenite makes it more difficult. However, in this case, deformation due to quenching strains is not large enough to have a significant effect on the dislocation density of the untransformed austenite. Although some degree of austenite stabilisation might occur, it will not be high enough to have a significant effect on the Ms temperatures. Therefore, Ms and Md temperatures may differ by more than 200°C depending on alloy composition.

Furthermore, experiments carried out in this work suggests that Ms temperatures for the present set of alloys are lower than indicated by Ms temperature-composition relationships stated in section 2.3.3 (equations 1 and 2). These results confirm Lenel et al's [11] conclusion that Ms temperature-composition relationships in general, are valid only for the composition range for which they were derived. Therefore, the reliability of equations 1 and 2 in predicting Ms temperature values for these alloys is questionable.

As already discussed above, there is a relationship between the Ms and Md temperatures. For example, Williams et al [30] reported a calculated Ms temperature (from equation 1) of -292°C and an observed Md temperature of 15°C for a Type 304 stainless steel (19.05% Cr, 9.5% Ni and 0.06% C). Furthermore, at a true tensile strain of approximately 0.3, only 69% martensite was achieved at -269°C (4.2 K in a tensile testing cryostat). Based on this observation, 50% martensite at 0.3 true strain (i.e. M_{d30}

temperature) can be expected at very low temperatures (possibly about -100°C). Given the very high sensitivity of the Ms temperature on composition [30], the Ms temperatures of the present set of alloys are expected to be higher than -292°C. This will be the case taking into account that the present set of alloys are less highly alloyed (18.04 to 18.39% Cr, 8.06 to 8.67%Ni and 0.025 to 0.0623% C) and hence less stable, than the type 304 stainless steel considered by Williams et al. The present investigation indicated that the Ms temperatures are much lower than -196°C, with observed Md temperatures of approximately 40°C at the low strain rate ($10^{-3}s^{-1}$). This austenite stability (Ms < -196°C) affirms the low M_{d30} temperatures observed for these alloys at both low and high strain rates (10^{-3} and $3x10^{-2}s^{-1}$ respectively). Generally, it can be concluded that the more stable the alloy, the lower will be its Ms and Md temperatures and hence the M_{d30} temperature.

6 CONCLUSIONS

6.1 Introduction

This chapter serves to present a summary of significant findings during the course of this thesis. Although these are not all embracing, they however represent a meaningful contribution to the understanding of the transformation behaviour of type 304 austenitic stainless steels.

6.2 List of Conclusions

1. The magnetic detection device was found to provide a rapid , simple, reproducible and widely applicable method of determining the amount of martensite in metastable austenitic stainless steels. The dependence of magnetic response on alloy chemistry as reported by other investigators was confirmed.

2. The amount of martensite was also found to be directly related to a decrease in temperature as already reported by other investigators.

3. It was found that the progress of martensite formation during straining can be qualitatively (by observing voltage change) and quantitatively (by converting voltage values to absolute amounts of martensite) followed by observing the true-stress/true strain and voltage (martensite content) against true strain curves. At low temperatures (e.g. -40°C) the pronounced sigmoidal shape of the true strain/true-strain as strain was increased, was accompanied by very rapid formation of martensite, as indicated by sudden increase in voltage during straining. Furthermore, voltage (martensite content) was found to be directly proportional to the amount of strain. At high temperature (e.g. 55°C) where

the true-stress/true strain curves showed a parabolic shape, no voltage was recorded, which implies an absence of martensite formation.

4. The amount of martensite transformed was found to be inversely related to strain rate at the sensitive temperature range. This occurred despite the fact that uniaxial tensile tests were performed under isothermal testing conditions.

5. It was found that the parameter (-dM/dT) could be used to explain transformation behaviour of metastable austenitic stainless steels under various temperature conditions. The region around a peak in a (-dM/dT) versus temperature curve, corresponds to a temperature range where there is rapid increase in the amount of martensite formed as test temperature is decreased. The M_{d30} temperature exists around this peak region.

6. The effect of strain rate on martensite transformation was found to be significant at the temperatures which indicated high (-dM/dT) values. The effect of strain rate on martensite transformation was found to be less effective at very low ($\approx$ -60°C) and high temperatures ($\approx$ 23°C) where transformation is least sensitive to temperature change as indicated by low (-dM/dT) values.

7. The formulated M_{d30} empirical equations were found to vary significantly with strain rate and showed regression coefficients similar to those of the Ms equations.

8. Most alloying elements stabilise the M_{d30} temperature with the exception of Mo and Si in some of the M_{d30} relationships. The destabilising effect of Mo has not been reported in literature. Although the destabilising effect of Si has been reported in literature, no significance can be attached to the destabilising effects observed in this study; since for most equations the coefficients of these elements (Mo and Si) were found to be insignificant. It was observed that alloys with similar alloying degree gave similar M_{d30} temperatures. Highly alloyed steels gave low M_{d30} temperatures compared to high M_{d30} temperatures for less highly alloyed steels.

9. The M_{d30} equations are very sensitive to alloy chemistry. A particular empirical M_{d30} equation will give accurate M_{d30} temperature estimations only for compositions with alloy chemistries similar to alloys for which a particular equation was derived. The relationship between the observed M_{d30} temperature and various alloying elements could only be explained by Cr. The plots of observed M_{d30} against Cr at both high and low strain rates showed that M_{d30} temperature decreased with increasing chromium content

10. All alloys are very stable under spontaneous martensite transformation on cooling. This indicates that they all have Ms temperatures below -196°C. This provides evidence for their observed low M_{d30} temperatures at both strain rates.

6.3 Recommendations

6.3.1 Magnetic Detection Device

The magnetic detection device provides a more expeditious way of estimating martensite content as compared to X-ray diffraction. It was found that during the course of this research, the magnetic device gave consistent magnetic values for materials tested under similar conditions but at different times. On the contrary, X-ray diffraction gave significantly different results for tests carried out under similar conditions but at different times which required a continuous use of a standard (a 50% austenite alloy) to determine accurate results. It is based on this that the use of the magnetic device requires further investigations for more accurate and all embracing use. The following need to be considered:

(i) It was difficult to record accurate voltage results during the course of the tensile tests for high strain rate tests. This was complicated by the fact that since data collection for voltage and strain was carried out separately and with high strain rate tests taking less testing time, synchronous data collection was sometimes not feasible. Hence, it is

recommended that the magnetic detection device should be interfaced with the Zwick tensile testing machine to eliminate such impediments.

(ii) The detection coil of the magnetic device should be modified for different specimen shapes. The present set-up only allows for plate-like specimens to be tested.

(iii) The device needs to be calibrated for occurrence of preferred orientation by comparison of results obtained for tensile specimens oriented at various directions to the rolling direction. Furthermore, the effect of calibration by the stress system under which the steel was deformed needs closer examination.

6.3.2 Limitations of the Formulated M_{d30} Empirical Equations

It must be emphasised that these equations are not general since they were determined from alloys covering a small range of alloy compositions. As already stated, usage of these equations for significantly different alloy compositions will result in very large errors associated with the M_{d30} temperatures. However, equations determined provide a rough guide of the possible M_{d30} temperatures to be expected under different strain rates.

It is therefore recommended that for an all inclusive M_{d30} equation, a wide range of compositions covering the austenitic "family" should be used. This will allow formulation of an equation which will be less sensitive to alloy composition, as compared to the existing M_{d30} relationships.

REFERENCES

1. J. REISSNER et al, *Proceedings of International Conference on Stainless Steel*, 1991, CHIBA, ISIJ, 779

2. J. SINGH, *J. Mat. Sci*, 20 (1985) 3157

3. P.C. MAXWELL et al, *Met.Trans.*, 5 (1974) 1305

4. I. TAMURA et al, *J.Japan Inst. Metals*, 33 (1969) 1376

5. C.P. LIVITSANOS et al, *Mater.Sci.Eng*, 30 (1977) 93

6. M.T.JAHN et al, *J.Mat.Sci*, 21 (1986) 2866

7. C.P.LIVITSANOS et al, *J.Mat.Sci*, 12 (1977) 2209

8. I. TAMURA, *Metal Science*, 16 (1982) 245

9. D.R. HARRIES, *Int. Conf. Mech. Behaviour and Nuclear Applications of Stainless Steels at Elevated Temperatures*, Varese, May 1981, London, Metals Society

10. F. LECROISEY, *Met.Trans*, 3 (1972) 387

11. U.R. LENEL et al, *Met.Trans*, 18a (1987) 767

12. T. ANGEL, *J.Iron Steel Inst*, 177 (1954) 165

13. A. ROSEN et al, *J.Mat.Sci*, 7 (1972) 870

14. B. CINA, *J.Iron Steel Inst*, 177 (1954) 406

15. L.E. MURR et al, *Met.Trans*, 13a (1982) 627

16. R.D. CHAPMAN et al, *Trans.Amer.Soc.Metals*, 47 (1955) 869

17. W.F. BARCLAY, *ASTM, STP*, 369 (1965) 26

18. R. CASTRO et al, *Metal Treatment and Drop Forging*, 1 (1964) 245

19. S.C. TJONG et al, *J.Mat.Sci*, 24 (1989) 1257

20. B.N. FERRY et al, *Journal of Materials, JMLSA*, vol 5 No.1 (1970) 99

21. P.D. HODGSON et al, *Metals Forum*, vol 4 Part 4 (1981) 192

22. K.J.IRVINE et al, *J.Iron Steel Inst*, 207 (1969) 1017

23. G.B. OLSON et al, *Met.Trans*, 13A (1982) 1907

24. V. SEETHARAM, *Bull.Mater.Sci*, vol 6 No.4 (1984) 703

25. E.R. PARKER et al, *Trans.Amer.Soc.Metals*, 30 (1942) 68

26. D. FAHR, *Met.Trans*, 2 (1971) 1883

27. V. SEETHARAM et al, *J.Mat.Sci*, 16 (1981) 523

28. R. JACKSON, *Sheet Metal Forming and Energy Conservation - 9th Biennial Congress of IDDRG*, ASM, (1976)264

29. X.F. FANG et al, *Mater.Sci.Eng A*, 141 (1991) 189

30. I. WILLIAMS et al, *Proc.6th Int. Cryogenic Conf.*, GRENOBLE, May 1976, 337

31. G.L. HUANG et al, *Met.Trans*, 20A (1989) 1239

32. D.C. LUDWIGSON et al, *J.Iron Steel Inst*, 207 (1969) 63

33. S.S. HECKER et al, *Met.Trans*, 13A (1982) 619

34. R.A. AYERS, *Met.Trans*, 16A (1985) 37

35. A. KUMAR et al, *Met.Trans*, 19A (1988) 1021

36. M.T. JAHN et al, *J.Mat.Sci*, 20 (1985) 2757

37. V.F. ZACKAY et al, *A.S.M TRANS*, 60 (1967) 252

38. G.W. FORM et al, *Trans.Amer.Soc.Metals*, 48 (1956) 475

39. Y. FUKASE et al, *Trans.Japanese Inst. of Metals*, SEDAI, JAPAN, 32 (1968) 38

40. P. MARSHALL, *AUSTENITIC STAINLESS STEELS: MICROSTRUCTURE AND MECHANICAL PROPERTIES*, ELSEVIER APPLIED SCIENCE PUBLISHERS, LONDON, 1984

41. J.N. HARRIES, *MECHANICAL WORKING OF METALS: THEORY AND PRACTICE, Int. Series on Material Science and Technology*, PERGAMON PRESS, NEW YORK

42. M. TAKAHASHI et al, *J.Mater.Sci.Lett,* 8 (1989) 477

43. O. SCHMIDT, *M.Sc Thesis, University of Cape Town*, Cape Town, R.S.A., 1992

44. M.G. SCOTT, *Analytical Proceedings Royal Society of Chemistry,* 18(10) (1981) 437

45. W.T. DELONG et al, *AWS National Spring,* BUFFALO, May 1956, NEW YORK

46. C.F. YATCZAK et al, *RETAINED AUSTENITE AND ITS MEASUREMENTS BY X-RAY DIFFRACTION, Society of Automotive Engineers, Inc.*, WARRENDALE, PA., 1980

47. R. JENKINS et al, *AN INTRODUCTION TO X-RAY POWDER DIFFRACTOMETRY, N.V. PHILLIPS,* GLOEILAMPENFABRIEKEN, EINDIHOVEN, HOLLAND

48. M.FUJIKARA et al, *Trans.Iron Steel Inst. JPN,* 15 (1975) 464

49. G. JONES et al, *Proceedings, American Society for Testing Materials,* 40 (1940) 610

50. L.H. FRY, *Proceedings, American Society for Testing Materials,* 40 (1940) 508

51. C.W. MACGREGOR, *Proceedings, American Society for Testing Materials,* 40 (1940) 508

52. F.B. PICKERING, *PHYSICAL METALLURGY AND THE DESIGN OF STEELS,* APPLIED SCIENCE PUBLISHERS LTD, ENGLAND, 1978

53. J.P. BRESSANELLI et al, *Trans. A.S.M.*, 59 (1966) 223

54. D. PECKNER et al, *HANDBOOK OF STAINLESS STEELS,* McGRAW-HILL COMPANY, NEW YORK, 1977

55. J.D. VERHOVEN, *FUNDAMENTALS OF PHYSICAL METALLURGY,* JOHN WILEY AND SONS, NEW YORK, 1975

56. A. GOLDBERG et al, *Mater.Sci.Eng,* 13 (1974) 211

57. K. NOHARA et al, *Kawasaki Steel Technical Report,* (14 March 1986)131

58. M.B. BEAVER, *ENCYCLOPEDIA OF MATERIALS SCIENCE AND ENGINEERING,* vol 4, PERGAMON PRESS LTD, OXFORD, 1986

59. G.B. OLSON et al, *J.Less Common Metals,* 28 (1972) 107

60. P.C. MAXWELL et al, *Metall.Trans,* 1 (1970) 2759

61. M.J. DICKSON, *J.Appl.Cryst,* 2 (1969) 176

62. G.F. VAN DER VOORT, *METALLOGRAPHY PRINCIPLES AND PRACTICE,* McGRAW-HILL COMPANY, NEW YORK, 1984

63. C.J. BALL et al, *Metal Science,* 16 (1982) 332

64. J.S. STANKO et al, *MANGANESE IN CORROSION RESISTANT STEELS,* SAMANCOR LIMITED (South Africa), June 1991

65. R.H. LINDENMAN et al, *INTRODUCTION TO BIVARIATE AND MULTIVARIATE ANALYSIS,* SCOTT, FORESMAN AND COMPANY, U.S.A, 1980

66. L. OTT et al, *UNDERSTANDING STATISTICS*, DUXBURY PRESS, DALLAS, 1985

67. ASTM 975-84, *ASTM Committee E-4 on Metallography (Subcommittee E04.06 on X-ray methods)*, (1984)1050

68. G.W. Powell et al, *Trans. ASM*, 50 (1958) 478

69. C.K. DIVERS, *Metal Progress*, August (1964) 115

70. H.C. FIEDLER et al, *Trans. American Society for Metals*, 47 (1955) 267

APPENDIX I

Table AI:1: Voltage (mV) and volume fraction martensite values used for calibration. Error associated with the voltage readings and % martensite readings show calculated standard deviations obtained from static and dynamic values; and three tests per alloy respectively.

ALLOY	VOLT (mV)	ERROR (mV)	% MART	ERROR (% MART)
30422A	13	± 1	10	± 2
	57	± 10	24	± 1
	98	± 9	30	± 2
	267	± 2	67	± 5
30431A	22	± 3	7	± 2
	34	± 2	17	± 7
	88	± 3	38	± 1
	114	± 9	32	± 2
	134	± 3	46	± 2
	170	± 14	56	± 7
	177	± 9	68	± 2
30432A	13	± 1	13	± 2
	58	± 4	17	± 4
	68	± 11	26	± 1
	82	± 8	28	± 5
	120	± 1	30	± 1
	138	± 6	53	± 2
	228	± 38	60	± 9

ALLOY	VOLT (mV)	ERROR (mV)	% MART	ERROR (% MART)
30431B	25	± 1	12	± 2
	30	± 2	13	± 3
	109	± 4	36	± 2
	112	± 20	33	± 4
	165	± 1	37	± 2
	198	± 18	47	± 2
	215	± 1	57	± 9
304L	20	± 8	14	± 2
	66	± 8	18	± 3
	87	± 15	28	± 3
	94	± 6	19	± 6
	99	± 13	24	± 5
	110	± 7	33	± 2
	143	± 3	31	± 3
	161	± 1	36	± 2
	202	± 13	50	± 5
	278	± 4	63	± 4
	295	± 2	71	± 5
30432B	38	± 1	16	± 2
	53	± 1	15	± 1
	83	± 3	11	± 2
	95	± 1	32	± 2
	199	± 33	39	± 5
	265	± 2	50	± 2
	273	± 2	60	± 4

APPENDIX II

Volume fraction martensite versus temperature curves at a true strain of 0.30 demonstrating evaluation of M_{d30} temperatures for the experimental alloys.

(1) Low Strain Rate % Martensite versus Temperature Curves

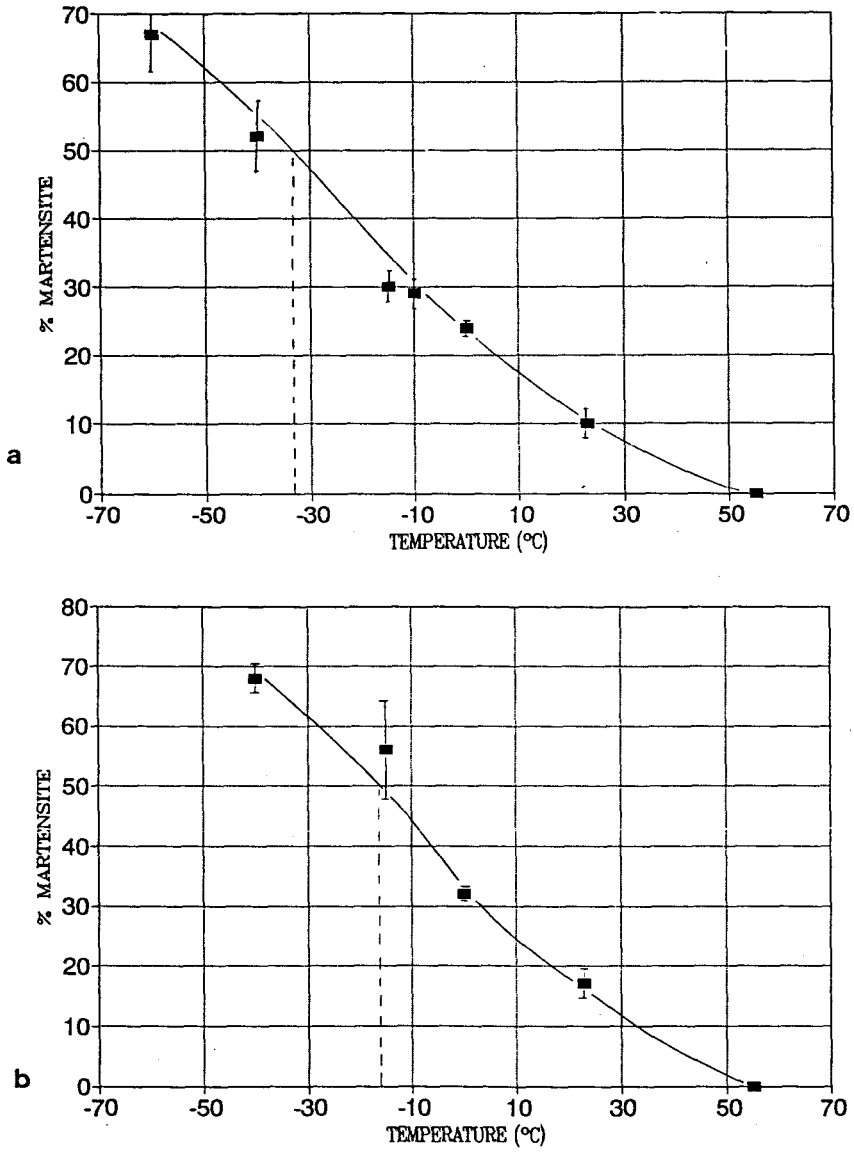

Fig AII:1: Graphs of % martensite versus temperature for alloy: (a) 30422A, (b) 30431A

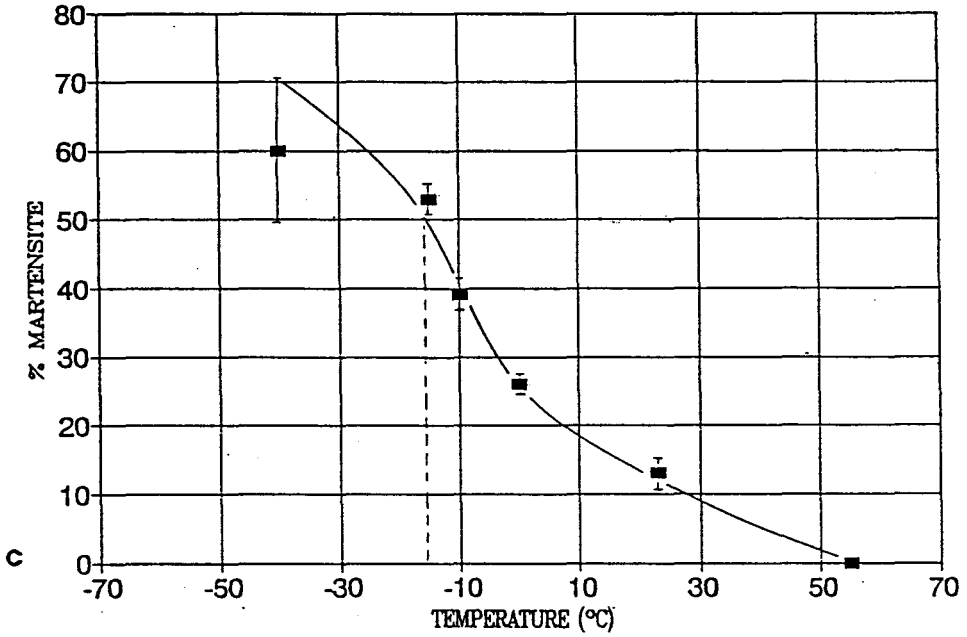

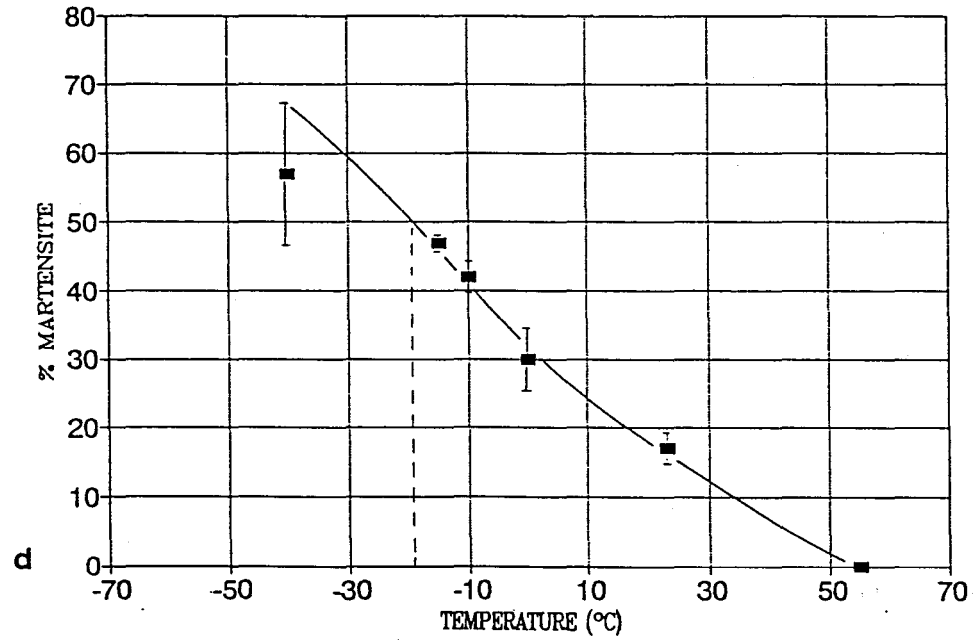

Fig AII:1: Graphs of % martensite versus temperature for alloy: (c) 30432A, (d) 30431B

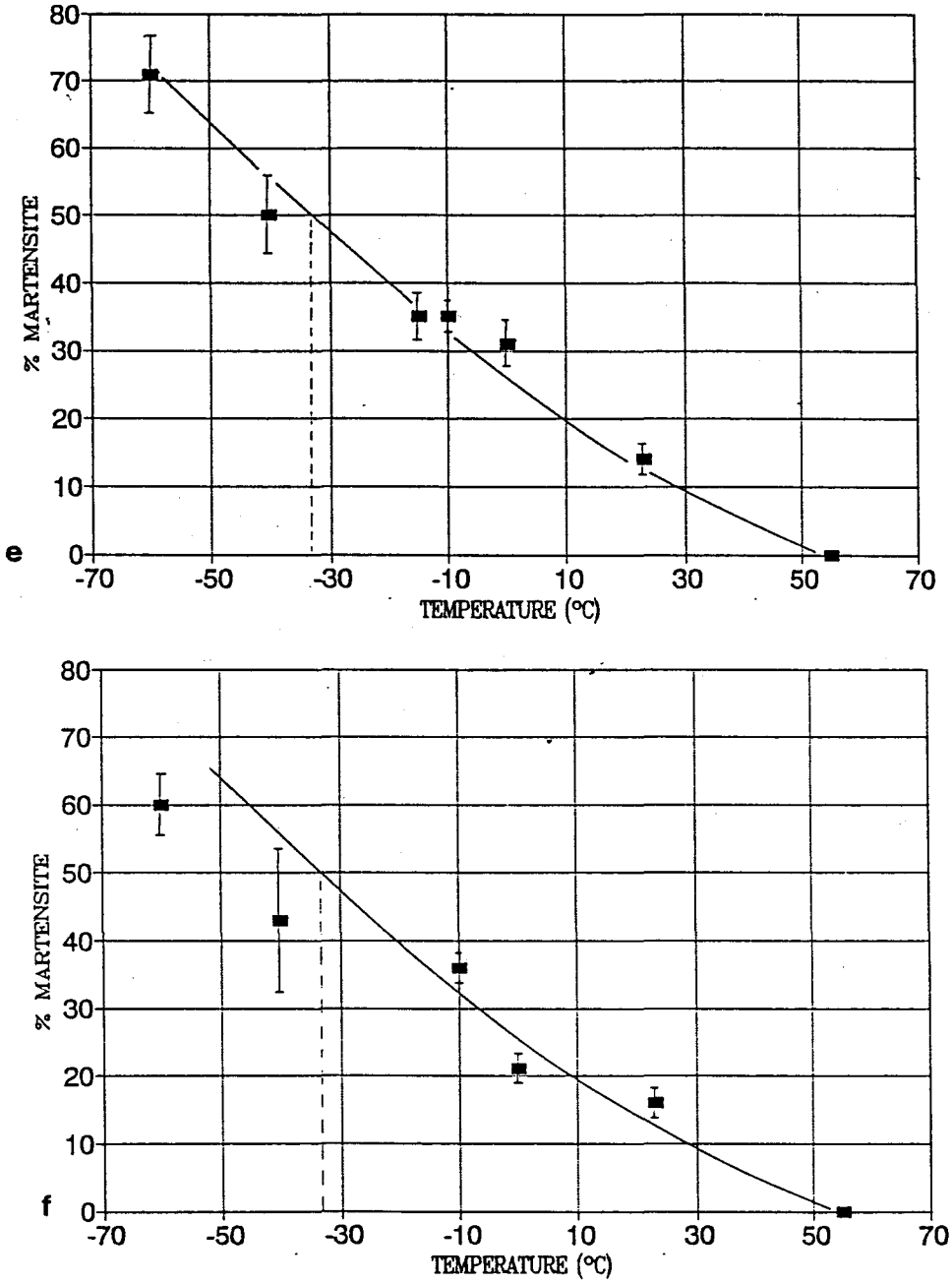

Fig AII:1 : Graphs of % martensite versus temperature for alloy: (e) 304L and (f) 30432B

(2) High Strain Rate % Martensite versus Temperature Curves

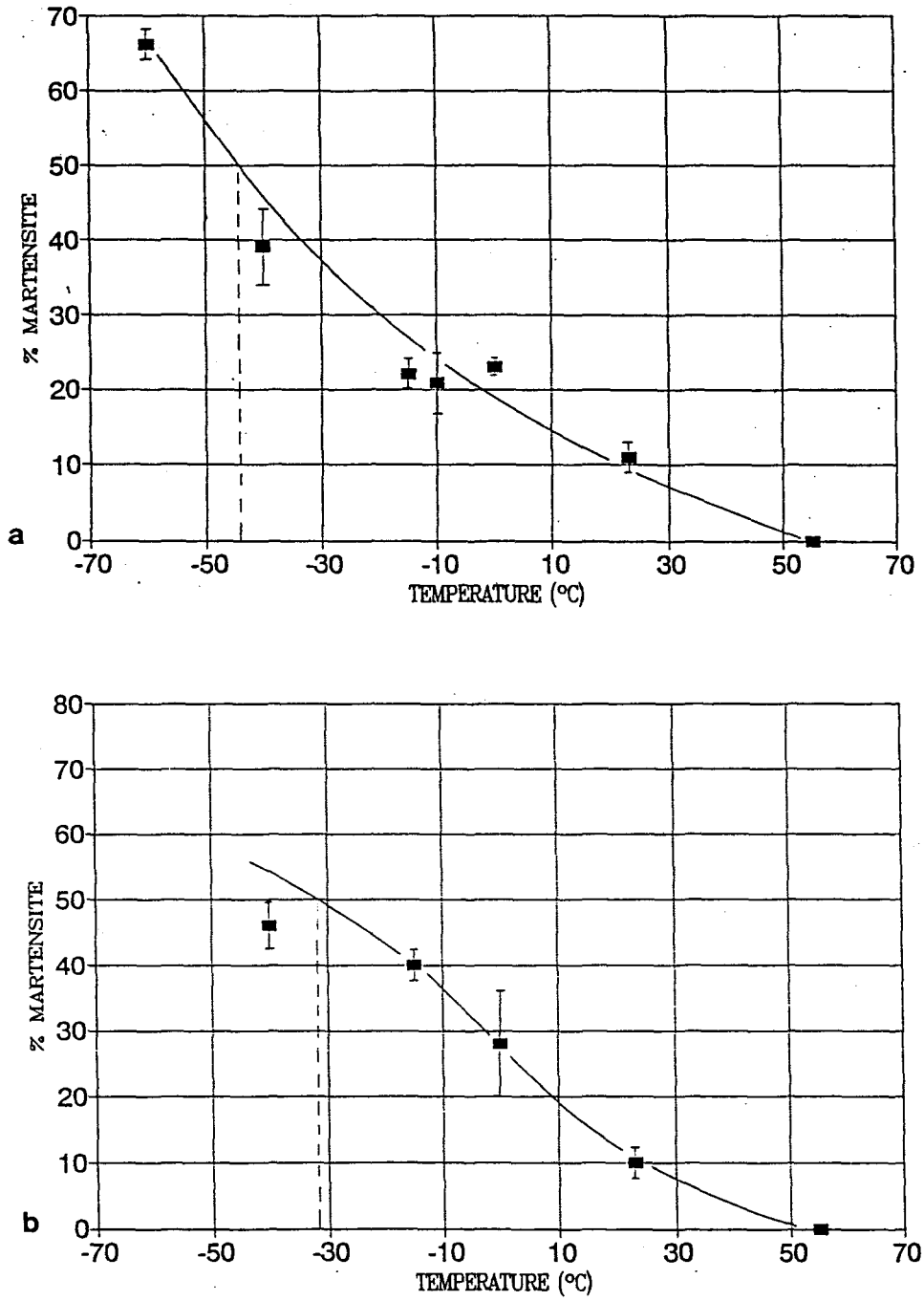

Fig AII:2: Graphs of martensite versus temperature for alloy: (a)30422A and (b)30431A

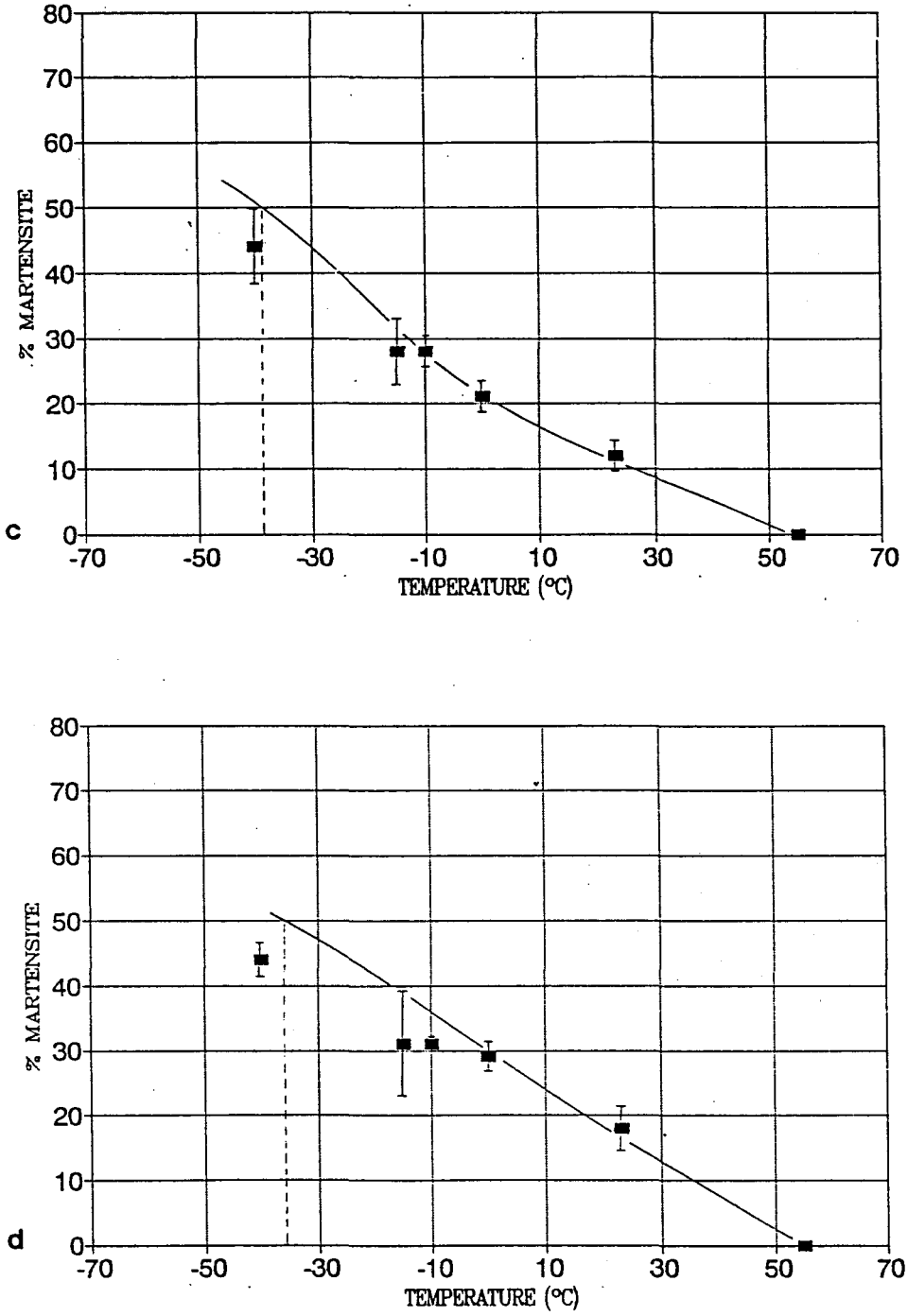

Fig AII:2: Graphs of martensite versus temperature for alloy: (c) 30432A and (d) 30431B

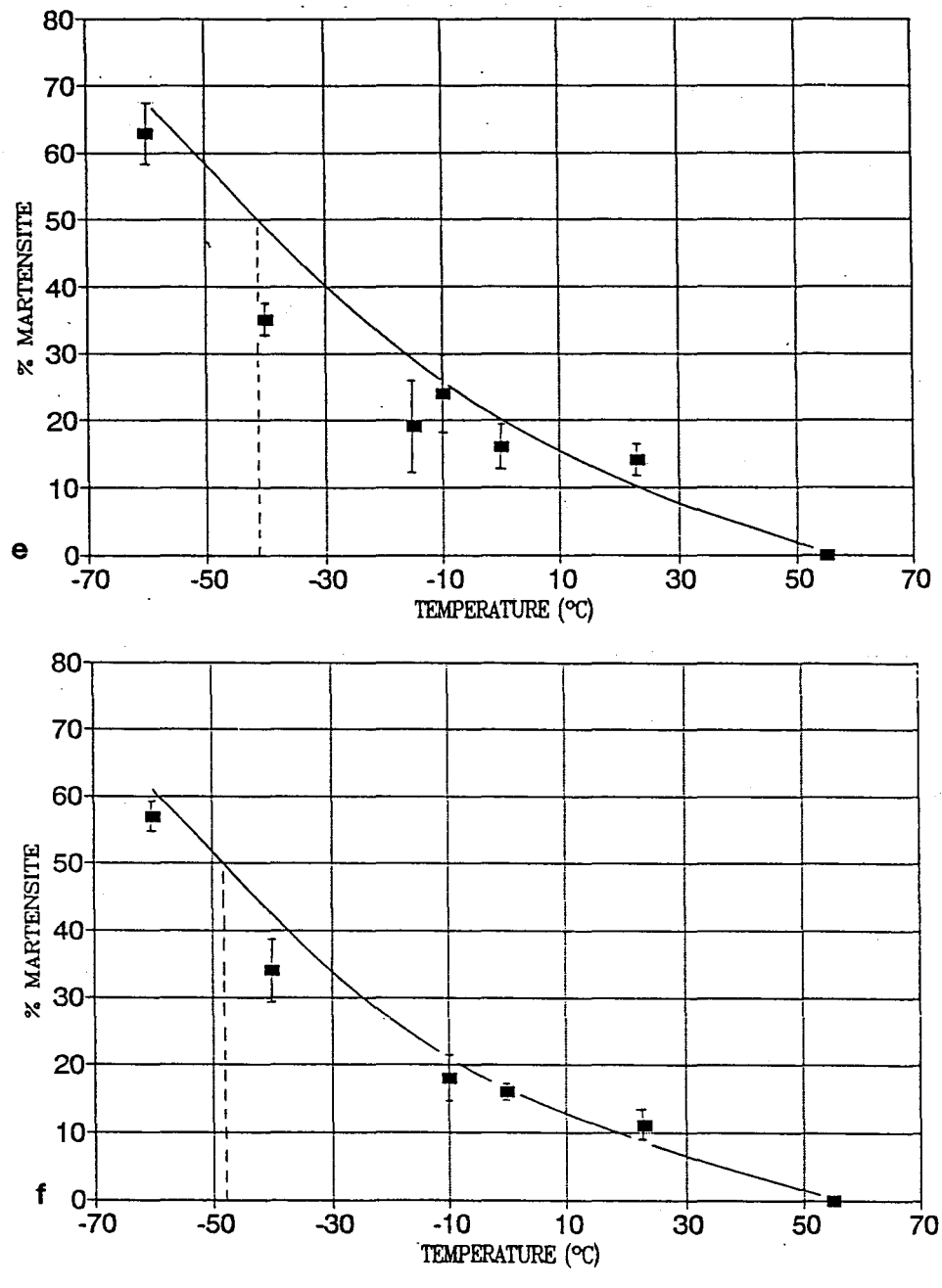

Fig AII:2: Graphs of martensite versus temperature for alloy: (e) 304L and (f) 30432B

APPENDIX III

1. Test Statistics for Empirical M_{d30} Equations According to the Order as Fitted by Angel [12] and Pickering [52]

(i) Low Strain Rate Results (equation 19)

INDEPENDENT VARIABLE	COEFFICIENT	STD. ERROR	P-VALUE
CONSTANT	882.74	216.91	0.05
C + N	-727.98	310.83	0.14
Si	-13.78	25.71	0.62
Mn	-46.67	16.96	0.03
Cr	-32.86	13.71	0.08
Ni	-19.78	9.85	0.18
Mo	-62.76	74.39	0.49
$R^2 = 95.62\%$			

Table AIII:1: Table showing standard error (std.error) and significance levels (p-value) associated with the alloying elements. 95% confidence level was used.

INDEPENDENT VARIABLE	ESTIMATE	STD.ERROR	LOWER LIMIT	UPPER LIMIT
CONSTANT	882.74	216.91	-50.54	1816.02
C + N	-727.98	310.82	-2065.35	609.39
Si	-13.78	25.71	-124.39	96.82
Mn	-46.66	16.96	-119.64	26.31
Cr	-32.86	13.71	-91.86	26.14
Ni	-19.78	9.85	-62.17	22.60
Mo	-62.76	74.39	-382.87	257.34

Table AIII:2: 95% confidence intervals for coefficient estimates.

(ii) High Strain Rate Results (equation 20)

INDEPENDENT. VARIABLE	COEFFICIENT.	STD.ERROR	P-VALUE
CONSTANT	717.52	26.98	0.001
C + N	-307.77	38.67	0.006
Si	4.08	3.19	0.02
Mn	-10.12	2.11	0.002
Cr	-36.51	1.71	0.002
Ni	-6.30	1.23	0.02
Mo	9.27	9.26	0.422
$R^2 = 99.84\%$			

Table AIII:3: Table showing standard error and significance levels associated with the alloying elements. 95% confidence limit was used.

INDEPENDENT VARIABLE	ESTIMATE	STD. ERROR	LOWER LIMIT	UPPER LIMIT
CONSTANT	717.52	26.98	601.42	833.63
C + N	-307.77	38.67	-474.14	-141.39
Si	4.08	3.19	-9.67	17.84
Mn	-10.12	2.11	-19.19	-1.04
Cr	-36.51	1.71	-43.85	-29.17
Ni	-6.30	1.22	-11.58	-1.03
Mo	9.27	9.26	-30.55	49.09

Table AIII:4: 95% confidence intervals for coefficient estimates.

2 Test Statistics for Empirical M_{d30} Equations According to the Order as Fitted by Nohara et al [57]

(i) Low Strain Rate Results (equation 21)

INDEPENDENT VARIABLE	COEFFICIENT	STD.ERROR	P-VALUE
CONSTANT	888.77	40.55	0.03
C + N	-1382.45	107.60	0.05
Si	-15.34	4.62	0.19
Mn	-69.79	4.39	0.04
Cr	-31.57	2.55	0.04
Ni + Cu	-12.64	1.78	0.06
Mo	79.12	24.32	0.13
(GSN - 8.0)	-14.89	2.05	0.09
$R^2 = 99.2\%$			

Table AIII:5: Table showing standard error and significance levels associated with the alloying elements. 95% confidence level was used.

INDEPENDENT VARIABLE	ESTIMATE	STD.ERROR	LOWER LIMIT	UPPER LIMIT
CONSTANT	888.77	40.55	373.57	1403.97
C + N	-1382.45	107.60	-2749.69	-15.21
Si	-15.34	4.62	-74.09	43.41
Mn	-69.79	4.39	-125.59	-14.01
Cr	-31.57	2.55	-63.98	0.84
Ni + Cu	-12.64	1.78	-35.26	9.97
Mo	79.12	24.32	-229.93	388.16
(GSN - 8.0)	-14.89	2.05	-40.99	11.21

Table AIII:6: 95% confidence intervals for coefficients estimates.

(ii) High Strain Rate Results (equation 22)

INDEPENDENT VARIABLE	COEFFICIENT	STANDARD ERROR	SIGNIFICANCE LEVEL
CONSTANT	721.03	26.89	0.02
C + N	-348.36	71.36	0.05
Si	2.93	3.07	0.09
Mn	-11.85	2.91	0.03
Cr	-36.77	1.69	0.03
Ni + Cu	-5.32	1.18	0.09
Mo	17.73	16.13	0.47
(GSN - 8.0)	-0.94	1.36	0.62
$R^2 = 99.92\%$			

Table AIII:7: Table showing standard error and significance levels associated with the alloying elements. 95% confidence limit was used.

INDEPENDENT VARIABLE	ESTIMATE	STD.ERROR	LOWER LIMIT	UPPER LIMIT
CONSTANT	721.03	26.89	379.37	1062.69
C + N	-348.36	71.36	-1255.06	558.33
Si	2.931	3.07	-36.03	41.89
Mn	-11.85	2.913	-48.85	25.15
Cr	-36.77	1.69	-58.26	-15.27
Ni + Cu	-5.32	1.18	-20.31	9.68
Mo	17.73	16.13	-187.22	222.67
(GSN - 8.0)	-0.94	1.36	-18.25	16.37

Table AIII:8: 95% confidence intervals for coefficient estimates.

3 Comparison Between Observed and Calculated Values for the Formulated Equations

ALLOY	M_{d30} (°C)		STRAIN RATE (s^{-1})
	CALCULATED	OBSERVED	
30422A	-32.5	-33	LOW (eqn 19)
30431A	-13.8	-16	
30432A	-16.4	-16	
30431B	-22.2	-19	
304L	-31.1	-33	
30432B	-32.8	-33	
30431C	-22.1	-22	
30422B	-29.0	-28	
30411	-33.1	-33	
30422A	-43.8	-44	HIGH (eqn 20)
30431A	-30.8	-31	
30432A	-39.1	-39	
30431B	-36.1	-36	
304L	-40.6	-41	
30432B	-47.9	-48	
30431C	-39.9	-40	
30422B	-37.1	-37	
30411	-42.2	-42	

Table AIII:13: Comparison between calculated (from equations 19 and 20) and observed M_{d30} values for the low and high strain rate in the order as fitted by Angel [12] and Pickering [52].

ALLOY	M_{d30} (°C)		STRAIN RATE (s^{-1})
	CALCULATED	OBSERVED	
30422A	-32.8	-33	LOW (21)
30431A	-15.9	-16	
30432A	-16.1	-16	
30431B	-18.8	-19	
304L	-32.6	-33	
30432B	-32.9	-33	
30431C	-21.8	-22	
30422B	-28.1	-28	
30411	-33.3	-33	
30422A	-44	-44	HIGH (22)
30431A	-31.1	-31	
30432A	-39.2	-39	
30431B	-36	-36	
304L	-40.9	-41	
30432B	-48	-48	
30431C	-40	-40	
30422B	-37.2	-37	
30411	-42.3	-42	

Table AIII:14: Comparison between calculated (from equations 21 and 22) and observed M_{d30} values for the low and high strain rates in the order as fitted by Nohara et al [57].

APPENDIX IV

Graphs of (-dM/dT) versus temperature comparing the temperature sensitivities of martensite transformation at the low strain rate ($10^{-3}s^{-1}$) and high strain rate ($3 \times 10^{-2}s^{-1}$).

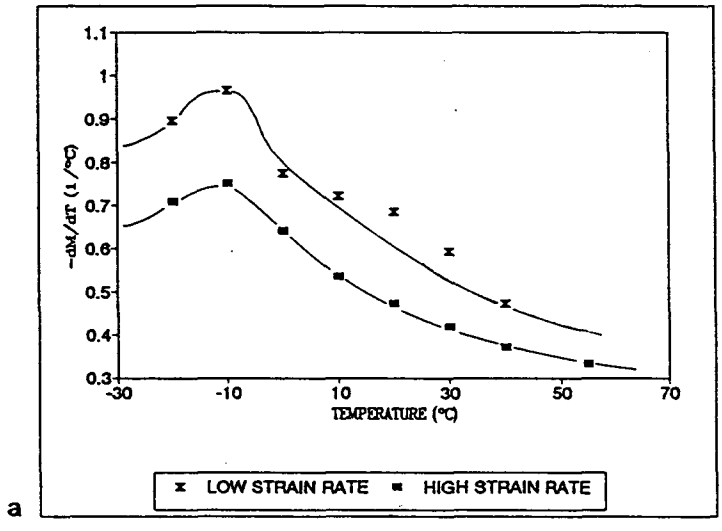

a

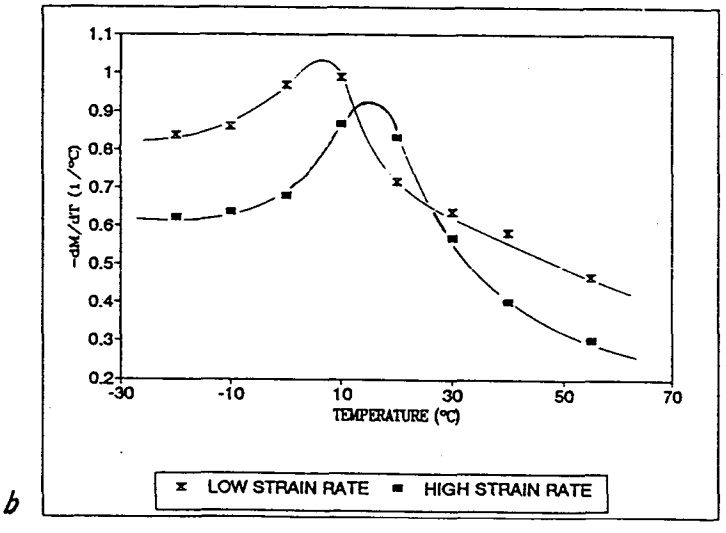

b

Fig AIV.1:Graphs of (-dM/dT) versus temperature at both strain rates for alloy:(a) 30422A and (b) 30431A

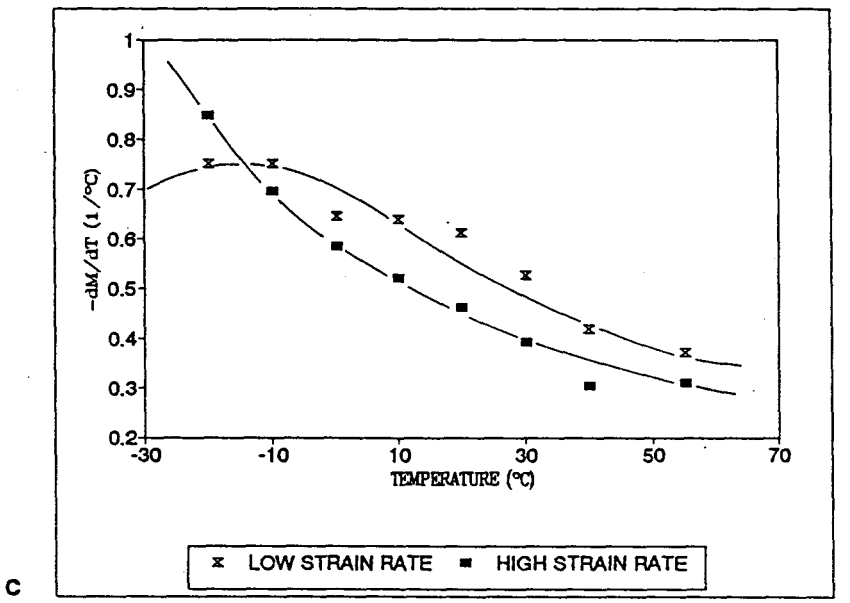

c

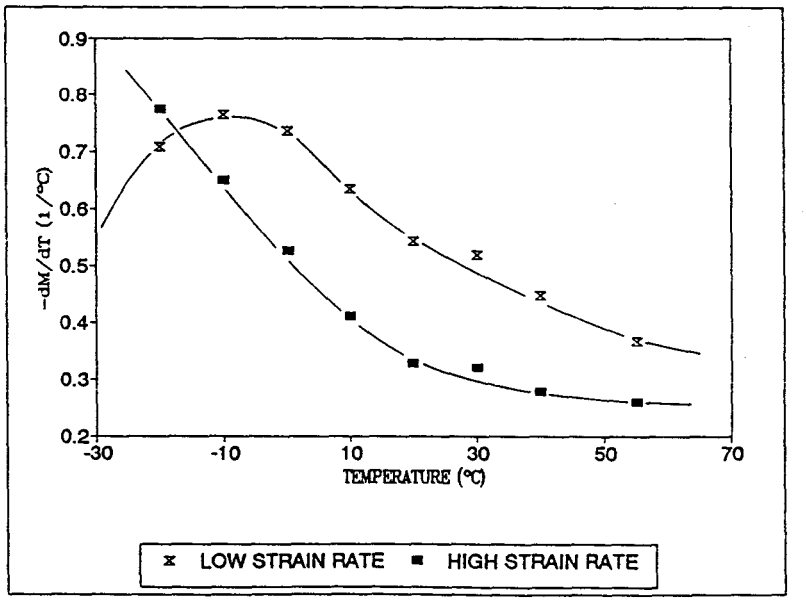

d

Fig AIV.1:Graphs of (dM/dT) versus temperature at both strain rates for alloy: (c) 304L and (d) 30432B